Configuration for Optimal Integration of Hydrogen Fuel for a Medium-Range Airplane

Vishwanath Nagaraj

Delft University of Technology

TU Delft

Configuration for Optimal Integration of Hydrogen Fuel for a Medium-Range Airplane

by

Vishwanath Nagaraj

to obtain the degree of Master of Science
at the Delft University of Technology,
to be defended publicly on Monday August 27, 2025 at 9:00 AM.

Student number:	5978149	
Project Duration:	December, 2024 - August, 2025	
Thesis committee:	Dr. ir. R. Vos,	TU Delft, Supervisor
	Prof. dr. ir. L.L.M. Veldhuis,	TU Delft
	Dr. ir. F.F.J. Schrijer,	TU Delft

Cover:	LH2 Aircraft concepts, Vishwanath Nagaraj
Style:	TU Delft Report Style

An electronic version of this thesis is available at http://repository.tudelft.nl/.

TU Delft

Preface

This report represents the culmination of my work as part of the thesis I conducted at the Delft University of Technology, over the past nine months. The study explores liquid hydrogen aircraft configurations, focusing on tank integration strategies. I hope you enjoy reading it and that it sparks the same sense of appreciation and wonder for the world of conceptual aircraft design that continues to inspire me.

By some stroke of luck in 2023, I ended up at TU Delft for my master's while I was just another student with an inclination for aircraft and aerodynamics. From the very first week of classes, it became clear to me that I was in the right place; with almost each lecture spurring a foundational learning approach and in-depth discussions with professors and friends. The environment fostered here is by far the more valuable thing a student could use. Tons of assignments, courses, and two years later, I find myself at the end of a fantastic journey.

Firstly, I am incredibly thankful to Roelof Vos for giving me the opportunity to conduct this thesis. Every single meeting with him taught me so much, while also leaving me with a sense of direction and energy. His guidance and insights were critical to the thesis, and his support in general was invaluable. I will always look back at this time with great joy.

I am also very grateful to Maurice Hoogreef and Alexander Heidebrecht for our brief meetings during the thesis. Their advice and inputs in the downselection stage were highly appreciated, as well as their help when it came to using the design tool. I would also like to thank Giuseppe Onorato for his support, as the current study stands on the shoulders of his work and research. To every professor or researcher I had the fortune of meeting, I am deeply indebted. Furthermore, I am thankful to all my friends in Delft; especially Surya and Aditya, with whom I spent countless hours working together on numerous subjects and discussing aircraft design.

To my friends back home and around the world, thank you for keeping me going- especially the dosas and the GWBG. Finally, I couldn't have done anything without the constant support and love from my parents, to whom I am forever grateful.

Vishwanath Nagaraj
Delft, August 2025

Summary

The aviation industry's transition to carbon-free fuels is a critical component of meeting global climate objectives, with liquid hydrogen (LH2) emerging as a promising candidate due to its clean combustion and high specific energy. However, LH2's low volumetric energy density and cryogenic storage requirements necessitate large, specialized tanks, which significantly influence aircraft design and performance. This study investigates the question of which aircraft configuration is best suited for hydrogen fuel integration, in the medium-range category. Additionally, the effect of applying operational limits on the design of LH2 aircraft is examined. Numerous configurations are conceptualized and put through a qualitative downselection process to arrive at four configurations of interest: 1) the conventional two-surface aft tank aircraft, 2) the three-surface aft tank aircraft, 3) the top-tank aircraft, and 4) the dual, forward-aft tank aircraft. The selected design tool utilizes analytical, empirical, and numerical methods to size and design CS-25 aircraft; with adaptations implemented to model the new configurations.

The two-surface, aft tank configuration is treated as the baseline aircraft, and several issues that limit the design's performance are identified. The tank's position creates a wide CG range that results in large tail sizes to meet stability and equilibrium requirements- increasing the zero-lift drag. This design also leads to a substantial in-flight CG excursion, which amplifies the average trim drag over a mission. Furthermore, the extreme aft position of the CG causes an undesirable landing gear position relative to the wing; forcing the use of inefficient fuselage-mounted or wing-podded landing gear integration methods. The remaining configurations are optimized and tested in their ability to mitigate or resolve these problems, and improve aircraft performance. The three-surface aircraft is found to reduce structural mass by a sizeable amount through load alleviation of the fuselage, but also carries with it a large induced drag penalty. Even in the optimized state, this configuration's block energy consumption is higher than the baseline's; despite a comparative reduction in weight and zero-lift drag. The forward-aft tank configuration on the other hand, increases in OEM and MTOM compared to the baseline, but improves its aerodynamic performance through better management of the CG variation. However, even the optimized design has only a marginal improvement in block energy consumption.

With the top-tank configuration, the CG range is greatly minimized by placing the fuel's CG closer to the rest of the aircraft's CG, helping reduce trim drag and horizontal tail size. The tank is modelled as a non-integral component supported by struts above and outside the fuselage, with fairings around it to reduce drag. The diameter ratio is found to be a trade between tank gravimetric efficiency and zero-lift drag, with a value of 0.75 providing the best aircraft-level performance. Compared to the baseline aircraft, this configuration provides the most improvement in block energy consumption (-2.4%) while also integrating the landing gear well, and meeting ICAO type-III span limits. In addition to these advantages, this configuration is also deemed to have better crashworthiness and improved safety; making it a strong contender for the optimal hydrogen aircraft.

The effect of activating operational limits with the design of aft tank layouts is studied, and unexpected results are obtained. The use of operational limits is found to improve aircraft performance by much greater amounts than changes in configuration, with reductions in energy consumption of 6-8% being made possible. The simple restriction of the design to only account for the harmonic in-flight CG excursion enables a much smaller tail, with snowball effects that further minimize the weight and drag of the aircraft. Additional benefits are seen in terms of reduced span and improved landing gear integration with the wing. These advancements did, however, come at a cost of heavy ballast requirements for off-design payloads, as well as constraints on ground operations to prevent tip-over.

Ultimately, the study identifies two optimal solutions depending on market requirements. For high-traffic, high-load-factor routes, the two-surface aft tank configuration with operational limits offers the best performance and lowest energy consumption. Conversely, for networks or airlines that demand more payload flexibility and minimal operating restrictions, the top-tank configuration is recommended as the best option.

Contents

List of Figures

List of Tables

Nomenclature

Abbreviations

Abbreviation	Definition
2SA	Two-surface aircraft
3SA	Three-surface aircraft
AC	Aerodynamic center
AFF	Aft tank fuel fraction
ADI	Aircraft Design Initiator
APU	Auxiliary power unit
AR	Aspect Ratio
BWB	Blended-wing body
CG	Center of gravity
FEM	Finite-element method
FOD	Foreign object debris
FM	Fuel mass
FME	Fuselage-mounted engines
FP	Foreplane
FPA	Foreplane area ratio
FPI	Foreplane incidence angle
FwdAft	Forward-aft
GA	General aviation
GH2	Gaseous hydrogen
ICAO	International Civil Aviation Organisation
ISA	International Standard Atmosphere
LG	Landing gear
LH2	Liquid hydrogen
LR	Long range
MAC	Mean aerodynamic chord
MLI	Multi-layer insulation
MLM	maximum landing mass
MTOM	Maximum take-off mass
MZFM	Maximum zero-fuel mass
NLF	Natural laminar flow
NP	Neutral point
OEI	One engine inoperative
OEM	Operative empty mass
OL	Operational limits
SAF	Sustainable aviation fuel
SFC	Specific fuel consumption
SM	Static margin
SMR	Short/medium Range
SOFI	Spray-on foam insulation
TAW	Tube-and-wing
TLAR	Top-level aircraft requirement
TOC	Top-of-climb
TSFC	Thrust specific fuel consumption

Symbols

Symbol	Definition	Unit
b	Wingspan	$[m]$
C_{D_0}	Zero lift drag coefficient	[-]
C_{D_i}	Induced drag coefficient	[-]
C_L	Lift coefficient	[-]
C_{L_α}	Lift slope	[-]
c	Chord length	$[m]$
$\bar{c}$	Mean aerodynamic chord	$[-]$
D	Drag force	$[N]$
D	Diameter	$[m]$
e	Oswald factor	[-]
L	Lift force	$[N]$
l	Distance	$[m]$
m	Mass	$[kg]$
M	Pitching moment	$[Nm]$
P	Pressure	$[kPa]$
R	Radius	$[m]$
r	Radius	$[m]$
S	Reference area	$[m^2]$
S_{wet}	Wetted area	$[m^2]$
S_{H}	Horizontal tail area	$[m^2]$
S_{VT}	Vertical tail area	$[m^2]$
S_{FP}	Foreplane area	$[m^2]$
V	Velocity	$[m/s]$
α	Angle of attack	$[^\circ]$
Δ	Increment	[-]
ϵ	Downwash gradient	[-]
η_{tank}	Tank gravimetric efficiency	[-]
ρ	Density	[kg/m^3]

1

Introduction

This chapter establishes the motivation for the current study and briefly explores the complexity of the problem. The research questions are then set in place, after which the structure of the overall report is explained.

1.1. Motivation

Aviation currently contributes approximately 2% of global carbon dioxide emissions, a figure that is projected to rise significantly as global demand for air travel continues to grow [5]. To combat aviation's growing carbon footprint, substantial and radical changes are required, and need to be developed quickly. The European Union's Clean Sky 2 initiative [16] reiterates the urgency of decarbonizing aviation, and calls for transformative changes in aircraft technology to drastically reduce greenhouse gas emissions. Incremental improvements to current kerosene-based aircraft —such as aerodynamic refinements, material advancements, or more efficient high bypass ratio engines— are unlikely to meet the magnitude of improvement needed to reach these climate targets. Figure 1.1 shows the projected growth of carbon emissions, and it is clear that even with high use of sustainable-aviation fuels (SAF) the industry cannot come close to net-zero emissions. To stay within the 1.5° C warming threshold and ensure long term global sustainability, alternatives to carbon-based fuels must be seriously considered.

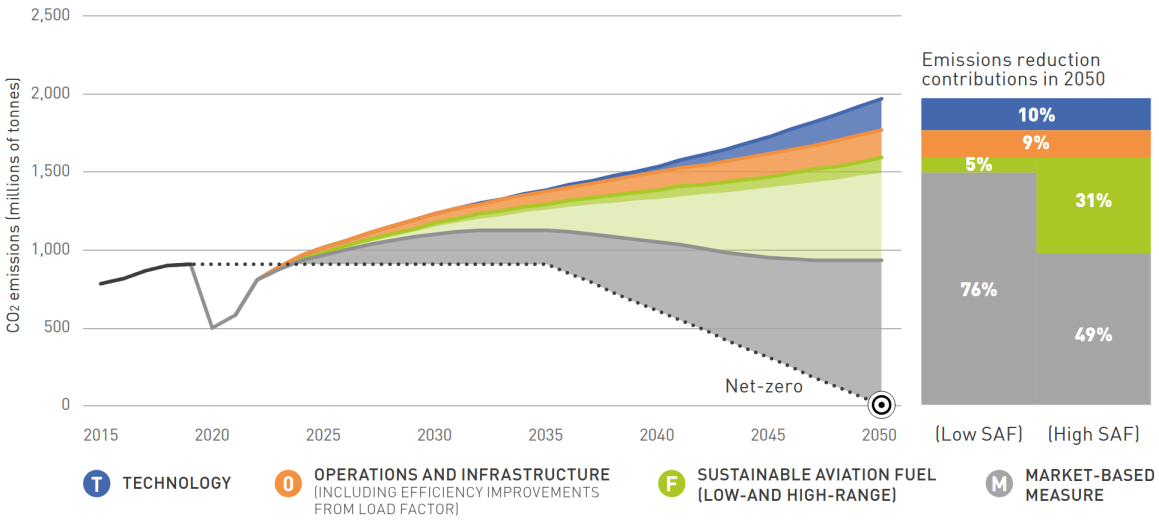

Figure 1.1: Projection of carbon emissions assuming continuation of current trends [5]

Hydrogen is increasingly recognized as a promising solution for zero-carbon aviation. When used in

fuel cells or combusted directly, hydrogen produces no carbon emissions at the point of use. Among its different forms, liquid hydrogen (LH2) offers a high gravimetric energy density- even higher than Jet A fuel- making it an attractive solution for carbon-neutral aviation. However, its low volumetric energy density, handling requirements, and high cost pose challenges for widespread adoption. Furthermore, LH2 must be stored at extremely low temperatures ($\sim$ 20 K) in specialized cryogenic tanks, which introduces complex integration challenges and impacts aircraft design from the conceptual level. Medium-range aircraft are selected due to their large market share, but sustainable solutions would be required for aircraft of other categories as well.

These fundamental differences in the properties of LH2 necessitate a fresh look at aircraft configurations, as conventional fuel-in-wing based storage is no longer feasible. While various designs and integration strategies have been proposed in the literature, there is little consensus on which configuration would be best. The current study aims to explore LH2 aircraft configurations from both a qualitative and a quantitative perspective, and identify the optimal concept. Conceptual design and sizing techniques are applied to create proposals for selected configurations, and a critical analysis of the results is conducted. This research aspires to contribute to the efforts of laying the groundwork of true, large scale sustainable aviation.

1.2. Research Objectives

As stated, there is little agreement or clarity on what configuration is most synergistic with hydrogen as the energy carrier. This is because different studies assume different top-level aircraft requirements, technology levels, or design/sizing techniques. The primary objective of this study is to identify the most optimal configuration for a hydrogen-fueled aircraft in the medium-range category. Various configurations are conceptualized and analysed in terms of potential performance and feasibility, following which a downselection is performed. The selected configurations undergo a comprehensive sizing and design process, including trade studies to obtain the best of each configuration. A critical comparison and analysis of the results is then conducted- taking performance-based, safety-based, and operation considerations- and the overall best configurations are proposed.

For aircraft configurations with an aft tank, the large CG range has proven to be a critical factor in producing large tail areas and degrading cruise performance [33, 27]. A secondary objective is to explore techniques of reducing the in-flight CG excursion through modifications in the design of the aircraft, and examine the effect of design with operationally limited CG ranges; on overall aircraft performance.

1.3. Structure of the Report

The report reviews relevant literature in chapter 2, beginning with studying hydrogen as an energy carrier in aviation and considering tank designs. The focus of the chapter then shift to tank integration solutions and LH2 aircraft designs proposed- looking at a multitude of designs. Chapter 3 then performs a preliminary downselection of aircraft configurations to identify the promising aircraft that can be conceptually designed and sized for the research. Next, chapter 4 explores the methodology employed for design and analyse the selected aircraft, while also giving an overview of the design tool. Chapter 5 then validates the results produced by the tool, comparing them to the reference aircraft as well as selected designs from the literature. The results of the current study's design exploration, and final concept comparison and critical analysis is then performed in chapter 6. Finally, chapter 7 concludes the findings of the research, and provides recommendations for future work.

2

Literature Review

2.1. Introduction to the Chapter

Several studies have been conducted to investigate the various aspects of integrating hydrogen fuel with commercial aircraft, from hydrogen tanks and fuel systems to propulsion systems, and overall aircraft design and performance. This chapter reviews all the relevant aspects of the use of hydrogen fuel, beginning with how its properties affect storage requirements compared to traditional aviation fuels, in section 2.2, and diving deeper into cryogenic tank designs in section 2.3. Finally, the various integration methods of hydrogen storage with aircraft proposed in the literature are reviewed in section 2.4.

2.2. Hydrogen as a Fuel: Aspects Relevant to Aircraft Design

Hydrogen can be stored in multiple forms, but given the sensitivity of aircraft performance to weight, the heavier forms of storing hydrogen, such as in metal hydrides and chemically bound hydrogen are immediately eliminated. Gaseous hydrogen at ambient temperature and pressure has an extremely low volumetric energy density- with an Airbus A320 needing several fuselages' worth of volume to simply store the hydrogen needed for a typical mission. This leaves only liquid hydrogen (LH2) and compressed gaseous hydrogen (GH2) as viable options. The storage temperatures and pressures for each of these types of hydrogen along with Jet A-1 are given in table 2.1, along with their energy properties. Given the extremely low volumetric energy density of GH2, the vast majority of hydrogen aircraft designs outside short-range categories propose LH2 as the form of fuel storage onboard.

Unlike Jet A-1, both GH2 and LH2 need specialized tanks onboard, capable of carrying large volumes and withstanding high pressures or cryogenic temperatures. These additional tank structures and insulation materials increase the weight and decrease the performance of the aircraft, making well-designed tanks important even at the aircraft level. To assess the effectiveness of a tank, a metric called the gravimetric efficiency is introduced,

$$\eta_{\text{tank}} = \frac{M_{H_2}}{M_{H_2} + M_{\text{tank}}} \tag{2.1}$$

where M_{H_2} is the mass of the hydrogen in the tank (liquid or gas), and M_{tank} is the mass of the tank alone.

Property	Jet A-1	LH2	GH2 (350 bar)	GH2 (700 bar)
Energy Density (MJ/kg)	43.2	120	120	120
Volumetric Energy Density (MJ/L)	34.9	8.5	2.9	4.8
Storage Temperature (K)	Ambient	20	Ambient	Ambient
Storage Pressure (bar)	Ambient	∼2	350	700
Typical Tank Gravimetric Efficiency (%)	100	∼30-90	1-15	1-15

Table 2.1: Properties of Jet A-1, LH2 and GH2 [2]

Tank Placement Effects

Aside from the benefit of 100% gravimetric efficiency for Jet A-1, it also boasts another key advantage in being able to be stored inside the wings. This has a load alleviation effect whereby the weight of the fuel acts in close proximity to the center of pressure on the wing, thus reducing the bending stress at the wing root. This results in a lighter wing box and reduced overall structural mass. With hydrogen, storing it within the wings to take advantage of this effect is highly unviable. Firstly, the internal volume within the wing structure is far below initial estimates of the required volume of GH2 or LH2. Furthermore, as GH2 is stored at pressures of upto 700 bar the tanks must be spherical or cylindrical to handle the pressure, making integration with the wing impractical. For LH2 there is an additional consideration: reducing heat leakage from the environment to the tank interior is key to avoiding hydrogen boil-off; and hence tank shapes that have high surface area-to-volume ratios are unfavourable. Such shapes would increase the rate of heat transfer; and thicker, heavier insulation would be needed to counter this- once again reducing the gravimetric efficiency. Hence, alternate tank placement options and aircraft configurations are being actively explored- such as external tank pods, extended fuselages, or BWB-integrated tanks, with some examples shown in figure 2.1. A detailed look at the tank integration effects and proposals is given in 2.4.

(a) TAW tank integration concept examples

(b) BWB tank integration concept examples

Figure 2.1: Some LH2 tank integration options [2]

Boil-off and Venting

While some general-aviation (GA) aircraft and regional aircraft designs propose the use of GH2 [49, 42], it is not considered viable for mid-range aircraft and beyond, due to the increased volume requirements and low gravimetric efficiency of GH2 tanks. Hence, all further information and exploration in this study will assume the use of LH2 as the energy carrier. As mentioned earlier, a key consideration with LH2 tanks is the boil-off effect due to heat leakage into the tank. As the temperature inside the tank rises, the hydrogen that boils off forms the ”ullage”, a portion of GH2 trapped at the top of the tank. The hydrogen expands greatly in this process, continuously increasing the pressure within the tank. To prevent the tank from failing indefinitely, the tank must be continuously cooled, or must be periodically vented. Active cooling systems have been found to be too costly in terms of added mass, complexity, and energy consumption to justify the benefit [28, 14] and hence practically all designs in the literature

employ situational venting. Partial pressure relief is offered by the fuel consumption of the engines, but is insufficient and venting is required; leading to about 0.1% loss of H2 per hour [29]. The exact value depends on the tank shape, insulation, design pressure, and external conditions, but this figure is representative of typical designs with direct venting. Thus, another drawback of using LH2 over Jet A-1 is that a small amount of fuel carried on the mission may simply be vented into the atmosphere, and cannot be utilized. To avoid this wastage, the tank's structure and insulation can be sized to ensure that the internal pressure never reaches the venting pressure on the design mission. Figure 2.2 shows the cryogenic tank proposed for the Airbus ZEROe aircraft, and the detailed design considerations of such tanks are explored further in section 2.3.

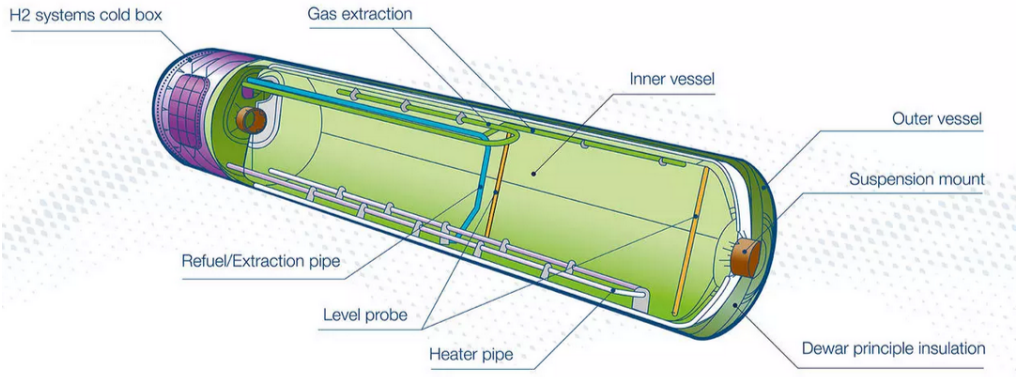

Figure 2.2: LH2 tank used in the Airbus ZEROe concepts [9]

Impact of Operations Design

Boil-off and venting are at their highest when the aircraft is on the ground at a hot location, for an extended period of time. From an operational perspective, there is a case to be made for draining the fuel from the airplanes into a centralized container at the airport, or storing it in separate external GH2 containers, so that the fuel need not be wasted. Here, positive scale effects aid in minimizing the surface area-to-volume ratio of the central store, thus reducing heat loss and cooling power requirements. This practice of draining/refuelling will however induce pressure and thermal stresses on the tank, as well as on balance of plant systems of the tank. These systems- which are the supporting and auxiliary components needed to deliver the energy- also need to be able to handle cryogenic temperatures and be resistant to hydrogen embrittlement, making material selection and tank auxiliary systems design critical. However, these aspects, as well as operations design are outside the scope of the current study.

Propulsion

The use of LH2 instead of Jet A-1 not only has massive implications to the tank designs and aircraft integration, but also to propulsion. There are two primary options with hydrogen: 1) Fuel-cell based propulsion, and 2) hydrogen combustion-based propulsion. The use of fuel cells while often proposed for regional aircraft [49, 4, 36], is an unlikely candidate for heavier, medium-range aircraft. This is due to the low power density of fuel cells and electric motors at the scales required for this application, which is an order of magnitude higher than the most powerful motor currently available [2]. Combined with the thermal management challenges of fuel cells, this type of propulsion system is expected to be much heavier and less aerodynamically efficient for medium-range aircraft.

Hydrogen combustion-based turbofans are often selected as the choice of propulsion for medium-range aircraft and beyond [10, 4, 33, 27, 35]. They are expected to be similar to Jet A-1 based tubrofans except for the combustion stage of the engine, due to the differences in hydrogen's chemical properties. Its wider flammability ranges and the resulting ability to be burned with a leaner equivalence ratio enables a slightly improved thrust-specific fuel consumption [2], along with exhaust-based preheating for the incoming fuel [13]. Figure 2.3 shows hydrogen's combustion range and a schematic of a turbofan engine with a modified combustor stage.

Based on these factors, hydrogen combustion-based turbofans will be assumed as the propulsion unit

for this study. A detailed analysis of the propulsion unit's design is outside the scope of this research, and will remain limited to a basic model to aid in aircraft performance estimation.

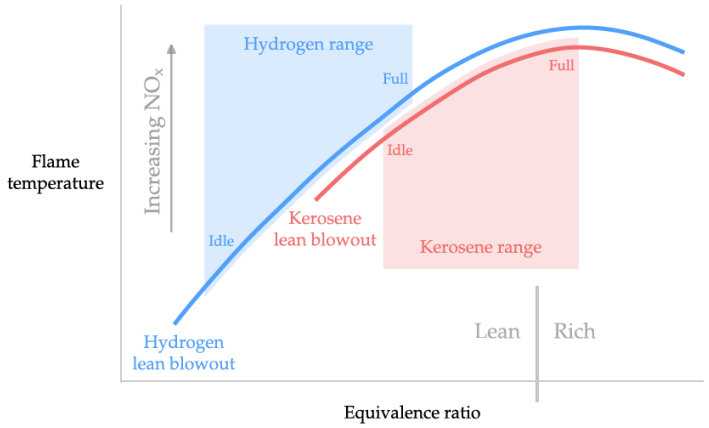

(a) Hydrogen's combustion range compared with Jet A-1 [2]

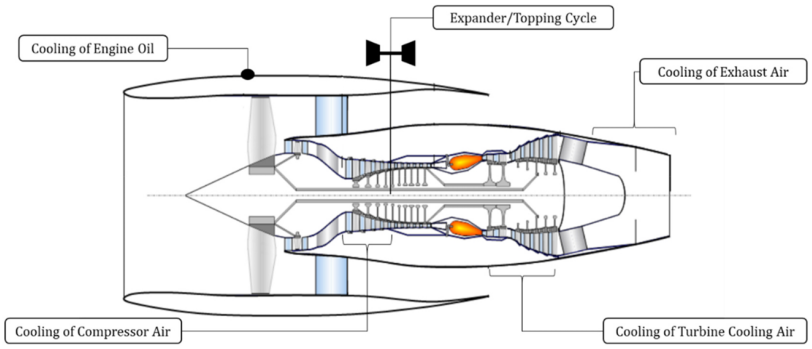

(b) A hydrogen-based turbofan engine and the primary cooling stages [40]

Figure 2.3: Propulsion considerations with hydrogen fuel

2.3. Liquid Hydrogen Tank Design Considerations

Cryogenic tank design for aircraft applications is a nuanced trade-off between weight, aerodynamics, structural efficiency, and insulation. For the purpose of effectively assessing hydrogen aircraft performance, the tank's weight estimation and thermal insulation sizing are key components, involving multiple disciplines. However, in order to estimate these factors, several design choices must be known- such as material selection, tank shape, structural support, and design operating conditions. These aspects are explored in detail below:

- **Wall and Insulation Materials:** Depending on the selected operating conditions, the tank may need to withstand high pressures in addition to cryogenic temperatures, while offering thermal insulation from the environment, to keep the hydrogen below 20K. Spray-on Foam Insulation (SOFI) has been used in aerospace applications and provides a lightweight, yet fairly insulating material that could be applied over a load-bearing tank structure which handles the pressure. However, SOFI is not well equipped to handle thermal cycles and delaminates, losing much of its initial insulation capabilities. Despite this, foam insulation is still proposed by Brewer [14] and Verstraete et al. [45], albeit with some changes to the operation.

  Vacuum-based insulation is heavier but offers much higher thermal insulation and reliability than other alternatives- especially when combined with reflective foils to combat thermal radiation between the wall layers and low-conductivity spacers; known as multi-layer insulation (MLI). This method is expected to vastly outperform SOFI [2][45] in commercial aerospace and hence is often the design choice in many studies. Lower gravimetric efficiencies are expected due to the metallic

tank walls needed to support a vacuum layer, but the superior insulation qualities are often preferred for high dormancy times. The walls themselves are typically chosen as aluminum alloys due to their properties of high strength-to-weight ratio and hydrogen non-permeability. Figure 2.4 shows the two main types of insulation strategies discussed.

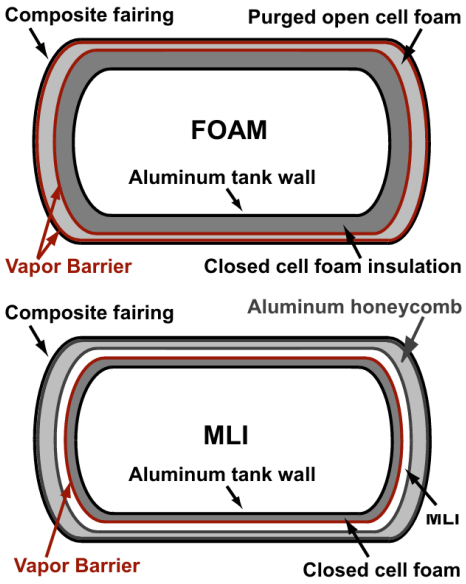

Figure 2.4: LH2 tank concepts shown by Verstraete et al. [45]

- **Tank Structure:** As discussed previously, Jet A-1 based aircraft designs employ fuel tanks embedded within the wing, where the tank itself is a load-bearing part of the wing. Such types of tanks are known as integral tanks, as they are an integral part of the airframe in addition to housing the fuel. Non-integral tanks on the other hand, such as those found in most automobiles, are simply containers of fuel that can be attached somewhere in/on the airframe, with some more flexibility in the design shape. Considering that LH2 tanks are already pressure containers, it is sensible to merge the tank's outer walls with the aircraft fuselage in an integral fashion. This is generally the design choice in studies [11, 33], as it reduces the overall structural weight. However, because the tank walls now need to be stronger (and heavier) to support the airframe, the tank's gravimetric efficiency may be artificially inflated, and it is important to assess the performance accordingly. Another side-effect of using integral tanks is that the flexibility in aerodynamic shaping in the tank region may be further constrained, due to the importance of pressure-efficient tank shaping. Figure 2.5 illustrates the two types of tanks and how they attach to the airframe.

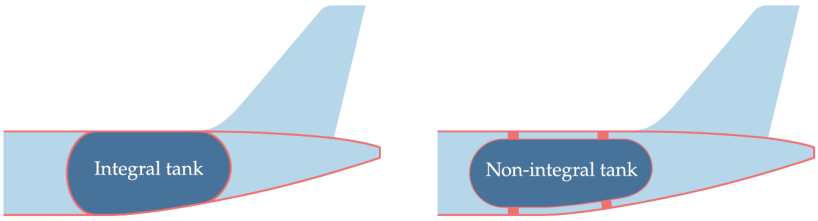

Figure 2.5: Integral vs non-integral tanks in the aft fuselage [2]

The structural sizing of the tank is often carried out using analytical and empirical relations for pressure vessels, in preliminary stages. Dedicated tank design studies have used FEM for a more accurate analysis on stress and mass estimation [22, 31], as well as a more detailed look at the load transfer mechanics between the tank and the fuselage. Montellano et al. [31] analyse the sensitivity of a novel integral tank concept's mass and gravimetric efficiency to primary design

variables such as the maximum operating pressure, insulation thickness, and some geometric factors. The trends established by such studies form a useful tool for tank sizing in conceptual LH2 aircraft designs.

- **Tank Shape:** The shape of the tank is primarily driven by the aerodynamics, the volume constraints in the airframe, the required internal tank volume, and the operating pressure within the tank. If the latter was the only design consideration; the tank would always be a spherical pressure vessel- the lightest structure possible for a given amount of LH2 to be carried, as seen in 2.8. However, spherical tanks are difficult to integrate without adversely affecting the aerodynamics, while maintaining sufficient internal tank volume; and hence are not commonly used. Cylindrical tanks with spherical/elliptical end caps are a popular choice, as they are much easier to integrate with fuselages, while still being quite pressure efficient. Prewitz et al.[34] find that the tank gravimetric efficiency rises with an increasing amount of LH2, creating a positive scale effect that favours one large tank instead of several smaller ones with the same combined volume- a finding supported by basic thermodynamics and geometric scale effects. However, designing one large tank is not always feasible or desirable- as having secondary tanks creates redundancy in case one tank fails. These qualitative considerations will be discussed further in future chapters.

  If the design operating pressure is not very high, then the tanks need not adhere to mechanically efficient shapes, and aerodynamically efficient designs may form the best solution. Such tank shapes are known as conformal tanks, and limit the increase in wetted area or improve the streamwise pressure distribution to reduce drag. Research into conformal LH2 tanks is limited, making preliminary sizing difficult, and leading to aircraft integration studies simply assuming a gravimetric efficiency [1] to estimate aircraft performance. However, initial expectations for the gravimetric efficiency of conformal MLI tanks, shown in figure 2.7 are quite low at 35% based on the COCOLIH2T project [21], compared to cylindrical tanks going up to 60%.

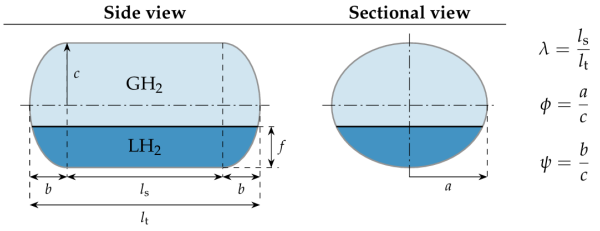

Figure 2.6: Elliptical tank geometry [48]

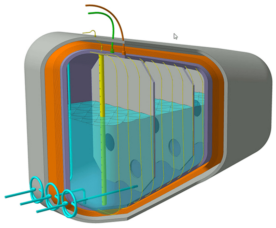

Figure 2.7: A conformal vacuum-insulated cryogenic tank for aircraft applications [21]

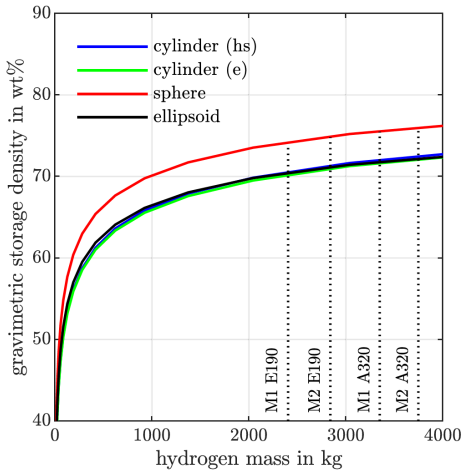

Figure 2.8: Tank gravimetric efficiencies for various shapes end caps [34]

- **Heat Transfer Modelling:** The primary requirement of heat transfer modelling in a conceptual LH2 aircraft study is to estimate the mass of the tank and the boil-off rates. Therefore, even though various levels of fidelity for heat transfer modelling for cryogenic tanks exist, simple analytical models are expected to suffice for this application. Figure 2.6 shows a simplified tank at partial capacity, with the LH2 at the bottom of the tank, and the evaporated GH2 on top; forming the ullage. Thus, the heat transfer between the LH2, GH2, and the inner tank skin occurs in a combination of both conduction and convection; while radiative heat transfer takes place between the layers of the MLI. The concept of electrical resistance for thermal designs is often used [48, 34, 45] for different regions of the tank, and the corresponding Nusselt numbers are estimated using empirical data. An alternative to such low-fidelity thermal modelling techniques would be to use detailed tank designs proposed in the literature directly in the current study, such as by Gomez and Smith [22]. The advantage of this would be that more accurate and reliable tank characteristic data would be fed into the aircraft sizing tool, but with less flexibility on the tank design itself.
- **Operational Design:** From a gravimetric efficiency perspective, the lower the cryogenic tank pressure is, the lighter the tank itself can be. However, it is important from a safety standpoint to maintain the internal pressure well above the gauge pressure; to ensure that during venting or a leak, atmospheric oxygen cannot ingress into the tank and create an explosive mixture. Liquid hydrogen boil-off naturally increases the pressure by expanding and adding to the ullage, but this is a slow process and cannot be relied upon in a situation where the tank's internal pressure needs to be increased due to safety. Specifically for such situations, heaters are proposed within the tank to rapidly boil off the hydrogen to increase the pressure. Careful selection of the venting pressure is necessary to avoid oversizing the tank due to excess venting, or due to minimal venting- potentially leading to severe mass penalties. Figure 2.9 shows the sensitivity of the gravimetric efficiency of the tank to the maximum operating pressure, indicating that lower pressures are favoured.

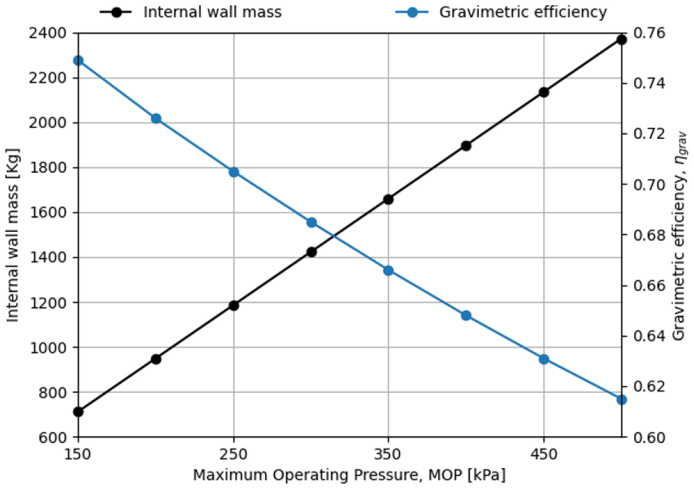

Figure 2.9: Sensitivity of the tank mass and gravimetric efficiency to the maximum operating pressure (MOP) [31]

In addition to estimating the tank and fuel mass, the balance of plant must also be considered, as its weight may cause performance mismatches if not accounted for. Silberhorn et al. [39] identify some of the primary elements and subsystems whose mass needs to be estimated, including components such as the boost pumps, engine fuel delivery lines, drainage lines, venting systems, etc. Given all these design considerations, cryogenic tank design becomes a complex, multidisciplinary process inherently linked to aircraft sizing and performance. This is because of the inter-dependency between the fuel volume requirements, tank insulation and mass effects, aircraft performance, and integration constraints. Onorato [32] provides a detailed workflow to size single-walled tanks that uses a mission-based state evolution method, as described in figure 2.10. The types of tank shapes that can be generated are limited to spherical or cylindrical, but it is deemed a highly valuable methodology nevertheless.

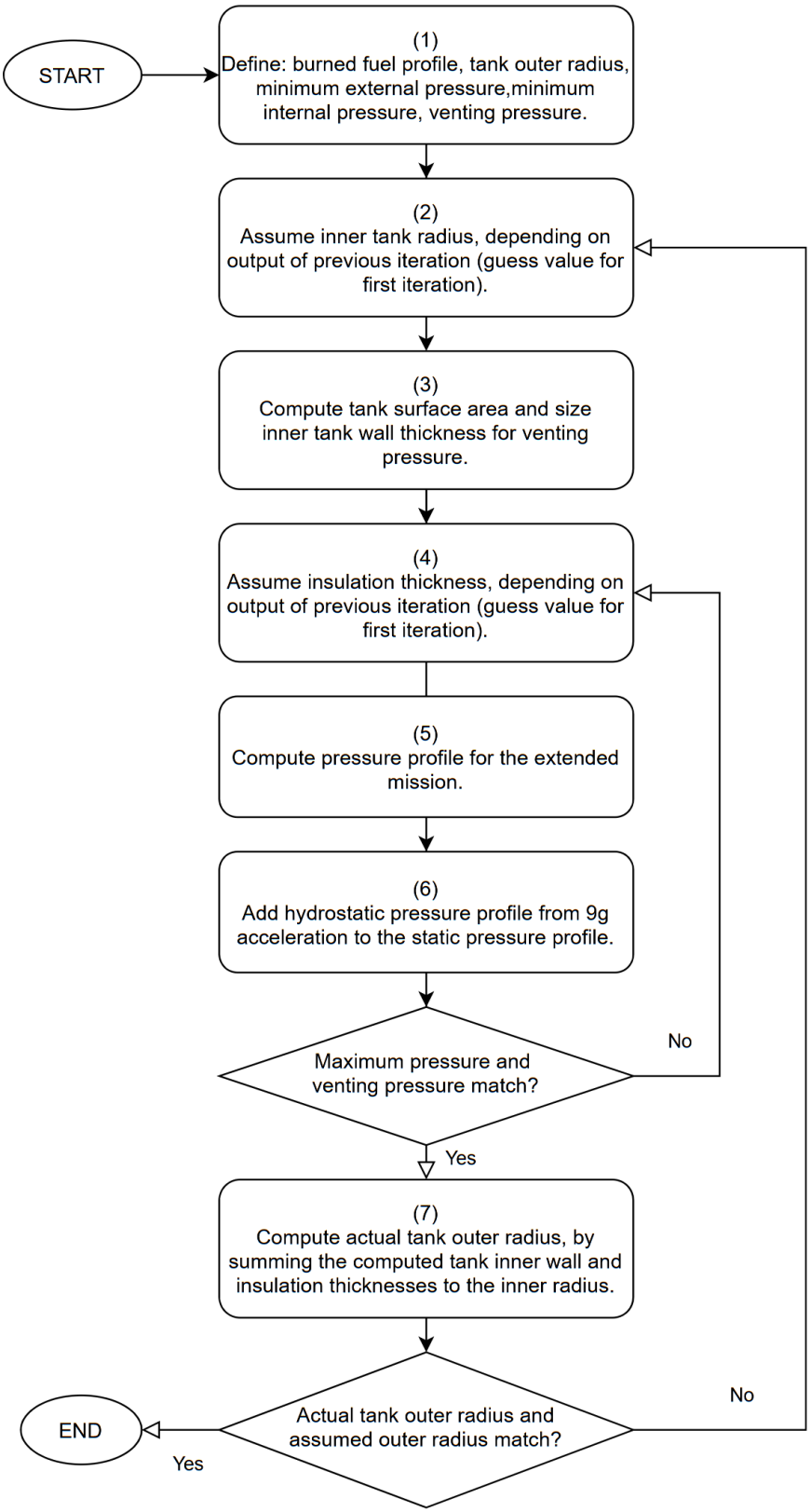

Figure 2.10: The tank sizing procedure used in the Initiator [32]

2.4. LH2 Tank Integration Philosophies

As with the design of any commercial aircraft, considerations of flight performance, profitability, airport compatibility, and safety must be taken. The integration of the large cryogenic fuel tanks presents a very early design decision and has important implications on all the aforementioned factors. Hence, numerous studies have been conducted by industry, governments, and academia to identify the best path of integration for hydrogen fuel.

One of the most well-studied options involves simply extending the fuselage of a TAW aircraft, and placing the tanks in the tailcone of the fuselage, as proposed by Airbus for their ZEROe turbofan [10]. Other concepts such as external fuel pods offer potential mass reductions due to load alleviation, while the BWB concept could suit hydrogen tanks very well with their large internal volume and low wetted area. Each of these tank integration philosophies from the literature will now be critically explored.

2.4.1. TAW Aircraft with Aft Tanks

One of the simplest ways to integrate bulky, cylindrical cryogenic tanks with typical tube-and-wing aircraft is to simply extend the fuselage and place the rear portion of the fuselage behind the cabin, as seen in figure 2.11. This configuration has several immediate advantages. Firstly, there is no major departure from the design of existing and proven kerosene-based TAW airframes of today, minimizing developmental risks. The tank and the fuselage have similar profiles as they are both essentially pressure containers, and integrate well without a major increase in frontal area or pressure drag. While there is an increase in wetted area, it is a smaller increase compared to some other configurations, and the increase in overall drag is further checked by the airflow's shear stress reducing over the length of the fuselage. Hence, compared to an external pod configuration with the same total tank volume, this configuration has lesser pressure drag as well as friction drag.

Figure 2.11: TAW aircraft with a single aft tank [2]

The LH2 tank and the associated fuel piping to the engines are also quite isolated from the passenger cabin, helping minimize the hazards in case of a leak. One of the primary drawbacks of the configuration is the excessive center of gravity (CG) excursion over the course of a flight. With the tank being positioned far away from the airframe's and payload's CG, the aircraft's overall CG position shifts significantly as the fuel is consumed during the flight- requiring considerable trimming from the horizontal tailplane. This CG excursion hence, has an increased trim drag penalty. Another major drag-associated penalty with this configuration is the increased tailplane sizes identified by studies of this configuration [27], [33]. The tailplane is sized to maintain sufficient stability in the most aft CG position, as well as to preserve the capacity to balance the aircraft in the CG's most forward position. While the moment arm of the tail is increased with the presence of the tank, the CG variation effect dominates, and the required tail area is very large compared to the JA1 aircraft. Thus, there is a large drag penalty not only due to the extended fuselage, but also due to the larger empennage.

Furthermore, Manzano [27] and Onorato [32] identify challenges in landing gear integration for aft-mounted LH2 tanks. The aft position of the CG forces the design of the main landing gear further backward than the wing, making folding the gear into the wing infeasible. This necessitates a fuselage-mounted landing gear, which attracts increased weight penalties and drag penalties. Furthermore, it is determined that for LH2 family aircraft the take-off rotation is sometimes the driver for tail sizing, and that changes were needed for the tail volume coefficients during the initial sizing of LH2 aircraft [27]. Figure 2.12 shows the use of scissor plots to portray the CG range and the various flight performance constraints involved. The aircraft concept is based on DLR's D239 [17], which is an interpretation of the Airbus A321neo, but with 2 aft tanks. While merging the two tanks into one large tank would theoretically be more efficient, this may be impossible due to the tailcone preventing a large axisymmetric tank,

necessitating a break-up into two tanks; which is clear in figure 2.13 for the ZEROe turbofan concept. Another effect of the tank placement in this design is the choice of a T-tail instead of the conventional tail because of the internal space constraints. The placement of the auxiliary power unit (APU) may also have to be changed for the same reason in this design. In contrast to this, the ZEROe turbofan concept has a more gradual taper of its tailcone, allowing for a conventional empennage setup.

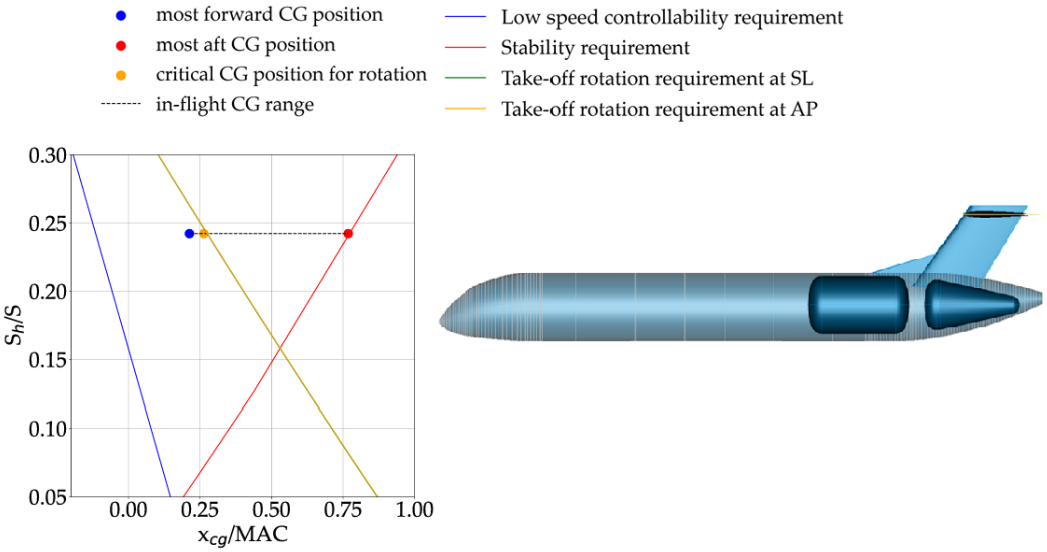

Figure 2.12: Scissor plot-based tail sizing for an LH2 aircraft with aft tanks [27]

Figure 2.13: Airbus ZEROe turbofan with dual aft-mounted tanks [9]

The FlyZero project's [3] research into zero-emission aircraft concepts [4] explores various configurations for LH2-based aircraft for the categories of regional, narrowbody, and midsize aircraft. 27 "scout" configurations were employed to explore the initial design space before the most promising concept was selected for further design. The concept selected for the narrowbody category (with the A320neo as the reference aircraft) was a TAW aircraft with aft-mounted tanks and 3-surface configuration, as seen in figure 2.14. This 3-surface configuration (foreplane, main wing, horizontal tail) may be able to provide some solutions to the challenges faced by the typical 2-surface designs through the addition of the canard.

It has been well understood that at take-off, the aft position of the CG forces the landing gear design position backwards, limiting the lever arm of the tail greatly, and causing large tail sizes in response. The foreplane surface with it's extremely large lever arm to the LG, can easily assist in take-off rotation and general pitch control- thus helping reduce the burden on the horizontal tail- and enabling a smaller tail area. Furthermore, the foreplane allows for the main wing to be positioned further aft alongside the landing gear, which grants the option for folding the landing gear efficiently inside the wing instead of the

fuselage. This is because the foreplane maintains the position of the aerodynamic center (AC) despite the wing being shifted back. These two advantages of smaller tail sizes and landing gear integration offer the potential for considerable drag reduction compared to previous concepts.

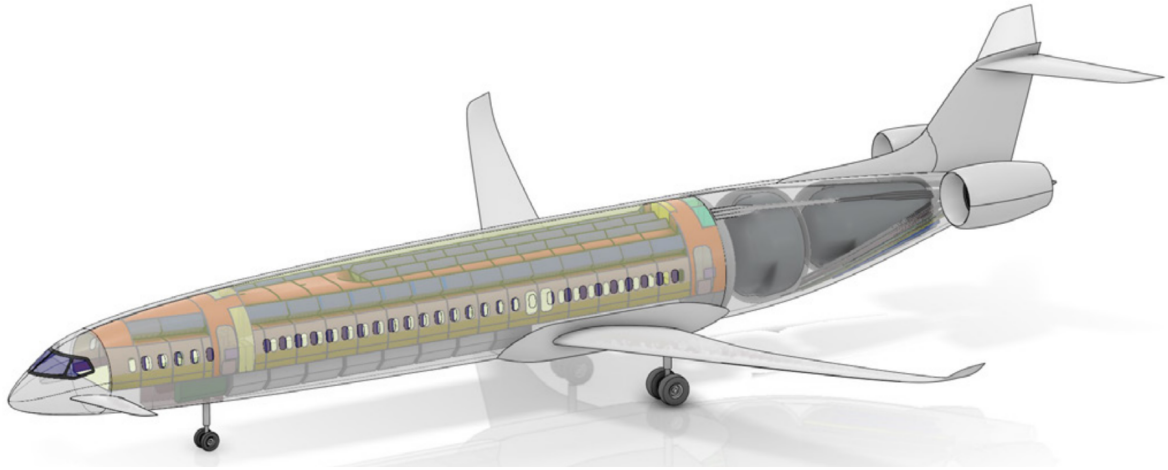

(a) Aircraft configuration

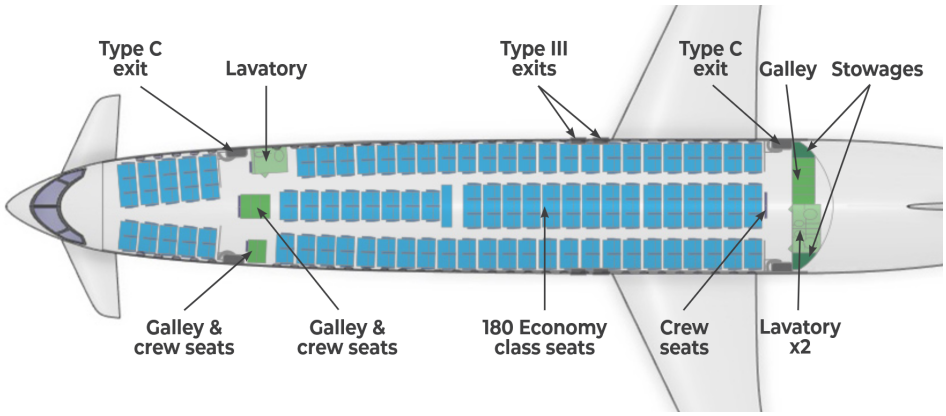

(b) The cabin layout of the FlyZero narrowbody concept

Figure 2.14: The FlyZero narrowbody concept [4]

Another unique design choice made in this concept is the engine placement, which is mounted to the aft part of the fuselage instead of under the wings. There are several advantages and disadvantages to this choice, compared to the standard configuration:

- **Possible Trim Drag Reduction:** With the engines mounted aft, the airframe's CG is shifted back slightly; minimizing the fuel level-induced, in-flight CG excursion. If the design is well optimized for this, it could take advantage of the smaller excursion and reduce the average trim drag over the mission.
- **Possible Shorter Landing Gear:** Depending on the design tip-back angle of the aircraft, positioning the engines on the fuselage may enable shorter, lighter landing gears. The extended fuselage may prevent taking advantage of this, and is yet to be explored further.
- **Cabin Hazard Minimization:** The report highlights that with both the fuel tanks and engines in close proximity, the fuel lines and systems are lighter; and the exposure of fuel to the cabin is greatly minimized, even in case of a leak. Furthermore, the engines' distance from the passengers reduces cabin noise.
- **Heavier Main Wing:** One of the biggest disadvantages of this configuration is that the wing receives no load alleviation from the engines or fuel. The wing structure would have to stronger

and hence heavier, resulting in a performance penalty.

- **Hazard on Vertical and Horizontal Tails:** In case of an engine uncontained blowout, the vertical tail is in a very vulnerable position and yaw control maybe lost- which is a critical function in OEI conditions. The horizontal tail, too, appears within the blade-out envelope and hence endangers pitch authority.
- **Engine Intake Risk:** Given the placement of the engines relative to the landing gear, the engines are now susceptible to damage from foreign object debris (FOD) kicked up by the gear. Even standing water or a tyre blowout poses a direct risk for the engine, making this configuration unfavourable from an operational safety perspective. Previous fuselage-mounted engine designs place the engine closer to the wing but above the debris envelope from the gear. This would not be possible here due to the risk of striking the fuel tanks in a blowout.
- **T-tail Design:** The engine placement forces the use of a T-tail instead of a conventional tail. This introduces challenges in interference effects and a heavier vertical tail structure, but is not expected to be a major concern.

The report does however note that the overall performance of the aircraft between these two engine placements was similar. The design of the fuselage is also a departure from the norm, with its sectional variation to better accommodate the bulky tanks in the rear. With such fuselage shaping, the concept aims to take advantage of natural laminar flow (NLF) and reduce the drag on the fuselage, which accounts for 25% of the total drag of this aircraft. The viability of this goal is, however, far from obvious. The sheer length of the fuselage, combined the the disturbance to the pressure gradients from the foreplane, make it difficult to delay the transition point by any meaningful amount. The non-constant fuselage sections also eliminates the option for an aircraft family due to the lack of commonality; something that is a significant factor for airline manufacturers to reduce cost [27].

The Layout of Passenger Accommodation (LOPA) is also modified to better fit the new fuselage shape. The aft portion of the cabin has 2-3-2 configuration, which transitions to 2-3 configuration near the nose for a 180-seat all economy setup. A constant-section fuselage typically features a 3-3 configuration for narrowbodies or 3-4-3 for widebodies, as they are the most space-efficient.

In order to compare performance, a baseline aircraft based on the Airbus A320neo with technology level assumptions of 2030 was created. In a trend that is practically ubiquitous when comparing LH2 aircraft and their kerosene counterparts, the empty mass is greater for the LH2 aircraft- which is also seen here with the FlyZero concept and the baseline aircraft in table 2.2. This effect is primarily due to the addition of the cryogenic tank and the associated balance of plant components; and the lighter fuel mass of the LH2 concept results in an almost equal MTOM between the two aircraft. Given these parameters, the block energy consumption is expected to be lower for the kerosene aircraft, because it gets lighter and more efficient deeper into the mission. However, the hydrogen aircraft unexpectedly has a 4% reduction in block energy consumption, despite higher average mass over the mission. This result indicates that the three-surface configuration promises good aerodynamic characteristics, enough to offset the higher average mass penalty.

Narrowbody Aircraft Mission Data		Reference A320neo	Baseline A320-2030	Concept FZN-1E
Fuel Type		Jet A-1	SAF	LH2
Payload	No. of Pax @ seat pitch (in.)	180 @ 32”	180 @ 32”	180 @ 32”
	Cargo (kg)	-	-	-
	Total Payload (kg)	19,400	18,795	18,795
Max. Take-Off Weight (MTOW) (t)		79.0	70.6	70.7
Operating Empty Weight (t)		44.9	41.5	48.0
Design Mission	Range (nmi)	2,495	2,400	2,400
	Total Mission Fuel Mass inc. reserves (kg)	14,753	10,312	3,903
	Block Time (hrs)	6.0	5.8	5.8
	Block Fuel Mass (kg)	12,184	8,439	3,283
	Block Fuel Energy (MJ)	523,912	388,194	374,262
	Energy Intensity (MJ/ASNM)	1.13	0.899	0.866
Typical Mission	Range (nmi)	850	850	850
	Total Mission Fuel Mass inc. reserves (kg)	6,638	4,902	1,800
	Block Time (hrs)	2.4	2.4	2.4
	Block Fuel Mass (kg)	4,306	3,187	1,241
	Block Fuel Energy (MJ)	185,158	146,602	141,747
	Energy Intensity (MJ/ASNM)	1.17	0.96	0.92

Table 2.2: FlyZero performance comparison [4]

Numerous other studies also explore the aft-tank configuration, and compare them with other configurations [33, 39, 11], and hence will be explored in the upcoming sections for better clarity.

2.4.2. TAW Aircraft with Fore and Aft Tanks

The primary drawback of the aft-tank configuration was the large CG excursion, and various strategies were seen for dealing with the increased trim drag and other secondary challenges. However, one of the most straightforward solutions is to simply place one tank near the nose, and one tank in the aft fuselage- leaving the cabin in the middle. This immediately resolves the CG excursion problem as the net fuel CG and airframe CG are much closer.

While there is an increase in the total surface area-to-volume ratio for the fuel, this would be true even for dual aft tanks, and does not pose a further insulation penalty. One of the main questions with this design is the cockpit-to-cabin connection, the necessity of which is unclear in the FAR/CS-25 regulations. The fore tank would sever this connection if designed in the same way as the aft tank; leading to some design modifications specifically for the fore-tank to allow for the connection if needed. Figure 2.15 shows two common suggestions for enabling this, each with its own advantages and drawbacks. The CRYOPLANE report’s tentative suggestion maintains a larger volume for the fuel, but will incur a significant weight penalty to maintain complete structural integrity against the stress concentration introduced by the cutout. The option in which the fore tank has a reduced diameter sacrifices a larger amount of fuel volume, but is structurally sound.

Another small structural drawback arises with the aft+fore tank configuration, due to the weight distribution. The lift generated by the wing is transferred to the fuselage near the center, while a considerable portion of the weight of the fuselage is present at the nose and tail region due to the tanks and fuel. This causes an increased bending moment on the fuselage; necessitating a stronger and heavier structure.

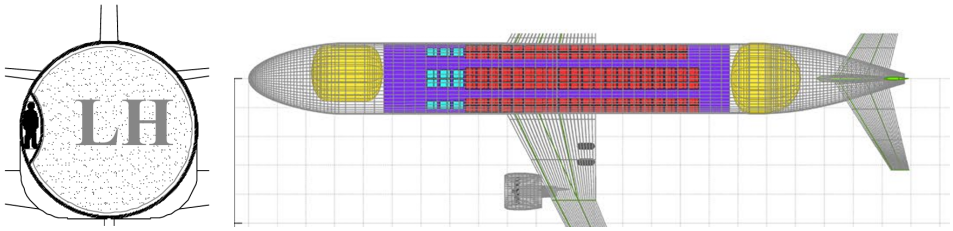

(a) Fore tank cutout [11] **(b)** Reduced fore tank diameter [33]

Figure 2.15: Two common solutions to enable cockpit-cabin connection

Onorato et al. [33] explores integration strategies of LH2 tanks with aircraft in the categories of regional aircraft, short-medium range (SMR) aircraft, and large passenger aircraft. The effects of tank venting pressure, diameter, layout, and structural integration on aircraft performance are studied, as well as their trends across categories. Five LH2 designs are used to study these effects, with their key design differences shown in table 2.3. The assessment is carried out through Aircraft Design Initiator, a design tool under continuous development by researchers in Delft Univeristy of Technology; and employs a combination of empirical, analytical and numerical methods to design and analyse aircraft.

Parameters	SMR-JAI	SMR-LH2-a	SMR-LH2-b	SMR-LH2-c	SMR-LH2-d	SMR-LH2-e
Tank structure	-	Non-integral	Integral	Integral and non-int	Integral and non-int	Integral and non-int
Seats abreast EC	3-3	3-3	3-3	3-3	2-3-2	3-3
Cryotank layout	-	Aft	Aft	Aft and Fwd	Aft and Fwd	Aft and Fwd
P_{vent} (kPa)	-	250	250	250	250	300
Fuel fraction aft	-	1	1	0.6	0.6	0.6
M_{tank} (t) (net)	0	1.73	1.54	1.77	1.81	1.80
η_{grav} (net)	0	0.294	0.268	0.313	0.294	0.321
R_{fuse} (m)	1.99	1.99	1.99	1.99	2.44	1,99
S_{ref} (m^2)	122	130	127	129	140	129
ΔX_{CG}	0.172	0.605	0.565	0.118	0.124	0.117
S_{h}/S	0.260	0.385	0.385	0.193	0.230	0.194
M_{fuse} (t)	10.6	13.7	13.2	14.6	17.7	14.5
M_{wing} (t)	9.99	10.4	10.0	10.2	11.4	10.2
C_{D_0} (counts)	212	234	233	225	225	224
L/D (mid-cruise)	17.4	16.4	16.4	17.0	16.9	17.0
FM (t)	15.1	5.88 (-60.9%)	5.73 (-61.9%)	5.63 (-62.7%)	6.14 (-59.2%)	5.62 (-62.7%)
OEM (t)	44.8	51.4 (+14.8%)	49.8 (+11.1%)	51.0 (+13.9%)	56.9 (+27.1%)	50.9 (+13.7%)
MTOM (t)	79.1	76.6 (-3.2%)	74.8 (5.5%)	75.9 (-4.1%)	82.4 (+4.1%)	75.9 (-4.2%)
SEC (kJ/pax/m)	0.778	0.842 (+8.2%)	0.821 (+5.5%)	0.806 (+3.7%)	0.878 (+13%)	0.804 (+3.3%)

Table 2.3: Design differences effects on SMR aircraft studied by Onorato et al. [33][1]

The kerosene version of the SMR aircraft is validated against the Airbus A320-200, while the LH2 version with only an integral aft tank is compared with the equivalent from Silberhorn [39], both of which base their top-level requirements similar to the A320. The LH2 tanks in this study are sized based on the harmonic mission rather than an intermediate design mission to maximise efficiency for the representative missions and improve gravimetric efficiency. All cases with the dual tanks utilize a non-integral fore tank due to the reduced diameter with respect to the fuselage; as well as a 60-40 fuel fraction split between the aft and fore tanks.

[1]The symbol η_{grav} shown in the table is the gravimetric index and not gravimetric efficiency.

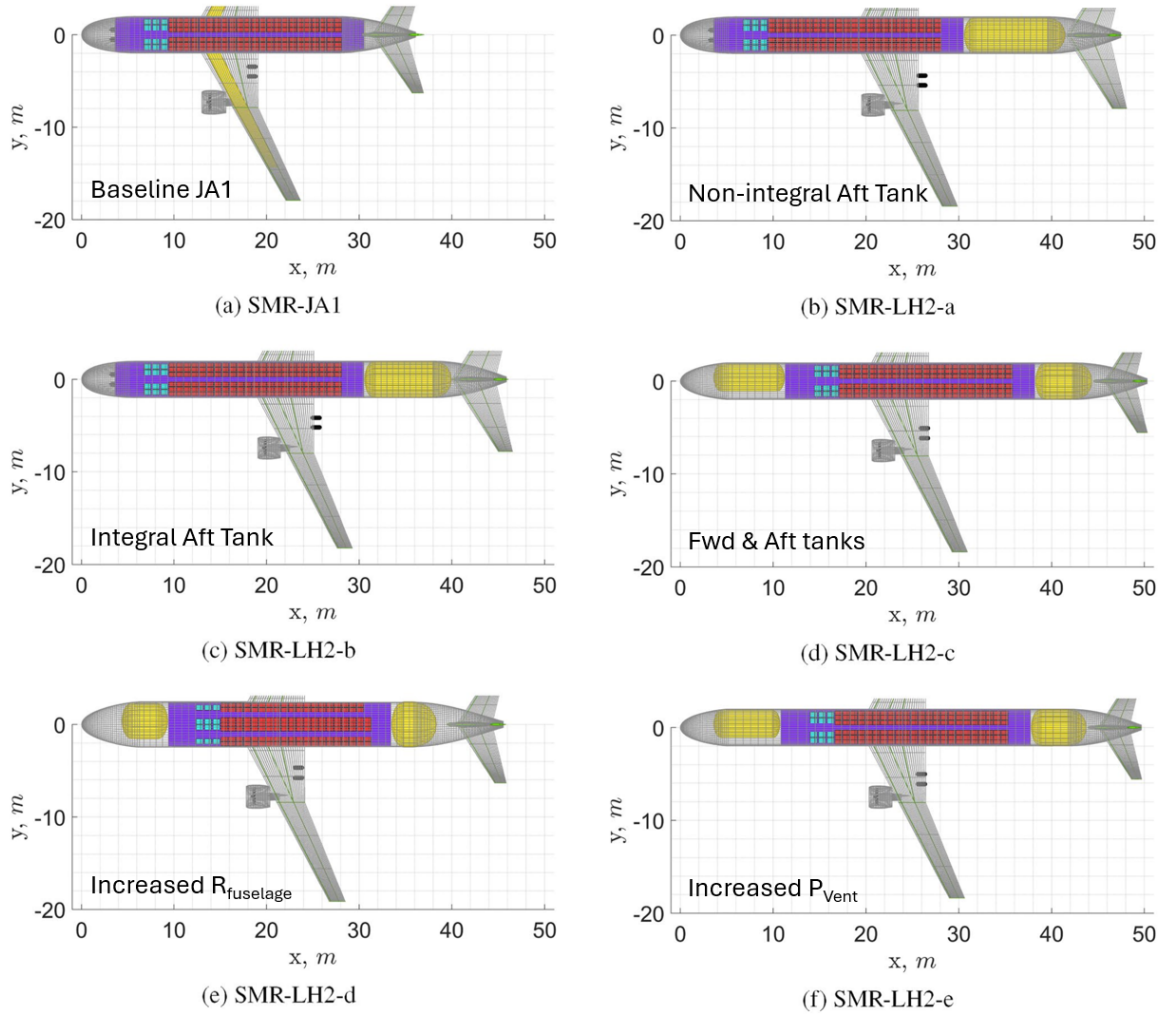

(a) SMR-JA1 (b) SMR-LH2-a

(c) SMR-LH2-b (d) SMR-LH2-c

(e) SMR-LH2-d (f) SMR-LH2-e

Figure 2.16: SMR aircraft top views [33], with their primary design characteristics on the bottom right corner of each variant

Comparing the SMR-LH2-a and -b designs from table 2.3, it is once again confirmed that an integral tank offers better gravimetric efficiency, operating empty mass, and specific energy consumption. Considering the SMR-LH2-c variant, it can be seen that there is a significant decrease in the CG excursion due to the tank placement, bringing it below even the Jet A-1 version (SMR-JA1). This results in a much smaller horizontal tail, reduced drag, fuel mass, and specific energy consumption. As expected, the tank gravimetric efficiency decreases due to the split tanks needing additional walls and necessitating thicker insulation to limit the heat leak.

The effect of increasing the fuselage diameter to better accommodate the tanks is examined by the SMR-LH2-d configuration. The seating arrangement has to be shifted to 2-3-2 instead of 3-3, and the addition of the second aisle appears to be detrimental to overall aircraft performance due to lower packing efficiency. As such, a comparatively large increase in the diameter allows for only a small decrease in fuselage length. Thus, while the insulation thickness and gravimetric efficiency improves; there is a larger penalty from the increased fuselage mass and required fuel mass, resulting in significantly higher energy consumption.

Finally, the effect of the venting pressure is investigated through comparing the SMR-LH2-c and -e variants, which have 250kPa and 300kPa as the venting pressures respectively. The overall performance shows a marginal improvement, as a small reduction in fuel mass and fuselage length (driven by insulation thickness here) is traded for a slight increase in tank mass. The specific energy consumption comes down as a result of the lower MTOM and OEM, but it is uncertain as to what limit increasing the venting pressure remians beneficial. It is expected that if it is kept increasing, at some point the

gravimetric efficiency penalty would overtake the fuelsage length shortening benefit, and the overall performance would suffer. Nonetheless, this study provides very valuable data and trends that can inform future trade studies.

Troeltsch et al [41] study the application of this tank configuration for an aircraft in the long-range category, with the reference aircraft taken as an A330 with 2040 technology level assumptions. While the current study focuses on medium-range aircraft, there are some design decisions taken by Troeltsch that may be of interest for more than just long range aircraft. A major decision is made to reduce the cruise Mach number from 0.82 to 0.7 for emission and energy use reduction purposes, which presents the opportunity to attempt to integrate some other attractive technologies. Since the wing remains dry (no fuel storage) and has a lower Mach number, the study proposes removing the wing sweep and increasing the aspect ratio to take advantage of natural laminar flow (NLF). Furthermore, it suggests abandoning elliptic lift distribution, and targeting a bell-shaped lift distribution on the wing instead. This newer type of distribution reduces the load near the tips, and the overall root bending moment- which is important for saving weight in a high aspect ratio design such as this. Figure 2.17 shows the aircraft concept and illustrates the lift distribution change.

The study illustrates that in the search for the optimal integration of cryogenic tanks with aircraft, it is also important to consider synergistic technologies that would benefit overall aircraft performance, which are only made viable through a tank integration design choice.

(a) The optimized lift distribution

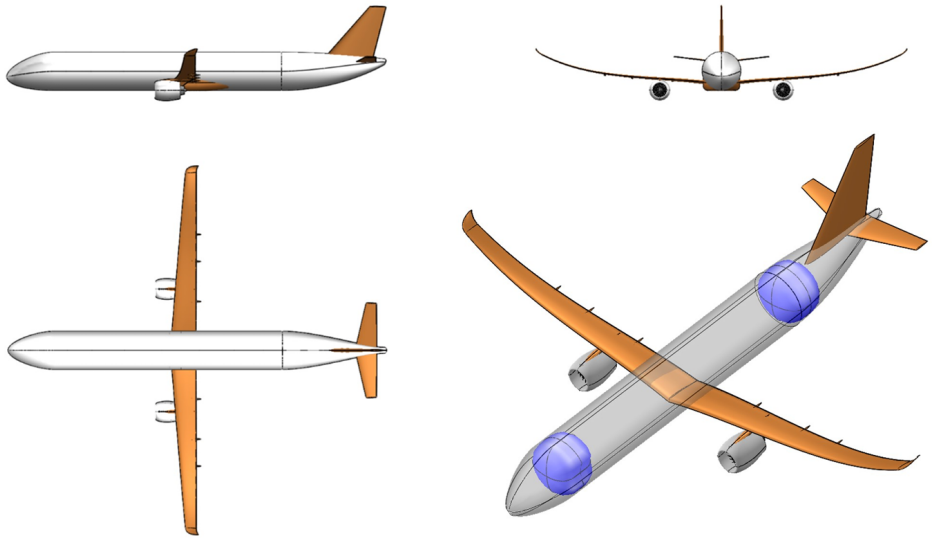

(b) The aircraft geometry

Figure 2.17: Bauhaus Lufthart Hyliner 2.0 [41]

The assessment also includes a trade study for the tank integration, between the current fore + aft tank design and another over-cabin design. The over-cabin configuration will be explored in further detail in the next section, but will be briefly looked at here. A ”volume split factor” is introduced to distribute fuel between the fore/aft tanks and the over-cabin tank; and the block fuel consumption is monitored

while this split factor is varied. Figure 2.18 shows the results of this trade study, which shows the pure fore/aft tank configuration having the least fuel consumption overall. However, this may not be true in all categories and designs, as will be studied in the next section.

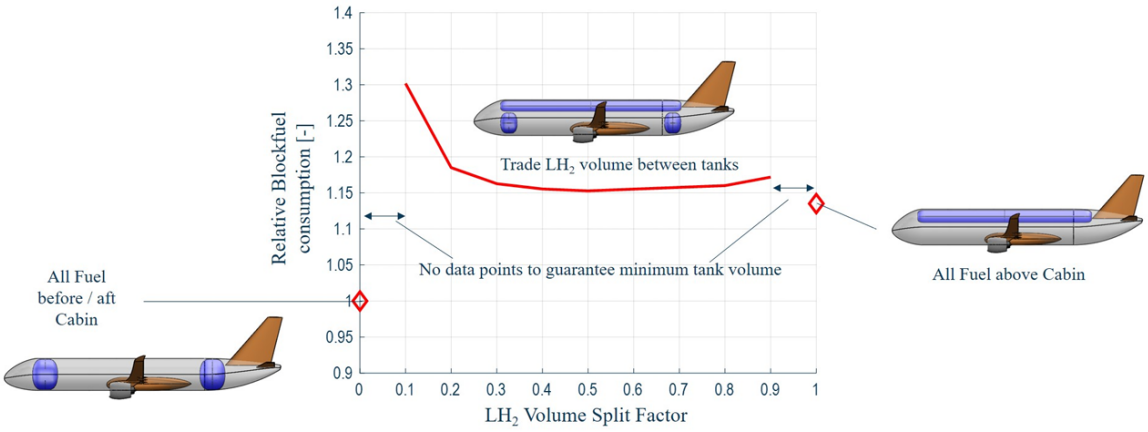

Figure 2.18: Block fuel consumption as a function of the volume split factor [41]

2.4.3. TAW Aircraft with Top Tanks

To combat the problems faced by the CG-excursion of the aft-tank configuration, the dual fore+aft tank configuration was introduced and found to perform significantly better. However, as found by Onorato [33], the fuselage length increased compared to the single aft tank case, and consequently, the mass as well. A contribution to the increase in mass is likely due to the increased bending moment by the tank positions compared to the lift transferred by the wings, which are close to the center of the fuselage. With this type of over-cabin configuration illustrated in figure 2.19, the design aims to reduce the fuselage weight, and de-link the tank diameter with the fuselage diameter- enabling high gravimetric efficiencies while maintaining suitable cabin configurations.

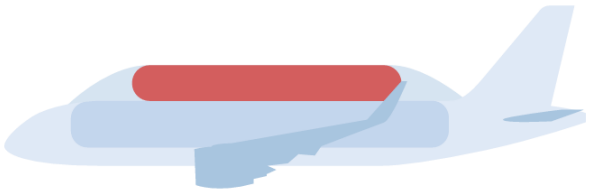

Figure 2.19: Over-cabin tank configuration [2]

There are however, some considerable drawbacks with this design that may render this configuration with low performance. There is a major aerodynamic penalty that arises from the tank's position and a resulting increase in wetted area. Potential blockage effects may result in an increased vertical tail size as well. Furthermore, long slender tanks are typically used in this case to limit the aerodynamic impact, but this necessitates thicker walls and insulation for the same pressure and boil-off limits. Although it may be possible to design an integral tank that assists in the bending loads experienced by the fuselage, it is unclear how much mass could be saved; as the fuselage structure still has to be sized for pressurization loads at the least- which cannot be shared with the tank.

Despite all these drawbacks, this configuration has drawn interest because of its potential safety advantages. Mounting the tank over the cabin protects it from debris and damage in the event of a belly landing, and reduces the risk of tank rupture. Furthermore, it's placement ensures that even in case of a leak, the interaction with the cabin is minimal as the buoyant GH2 will tend to rise upwards.

The CRYOPLANE Project [11] investigates hybrid tank integration methods, including over-cabin tanks as seen in figure 2.20 for short/medium range transport aircraft. The initial concept suggested the use of inboard wing tanks in addition to the over-cabin and aft tanks, but the drag penalty from thickening the wing was considered too large. The revised configuration used a larger tailcone to store aft tanks with 3, smaller over-cabin tanks. The empty mass fraction (OEM/MTOW) was found to be 0.7 and the specific energy consumption increased by 10% compared to the Jet A-1 equivalent aircraft; a trend that holds for most recent studies as well. The report does, however, indicate that the pure fore-aft tank configuration would be the most efficient if feasible.

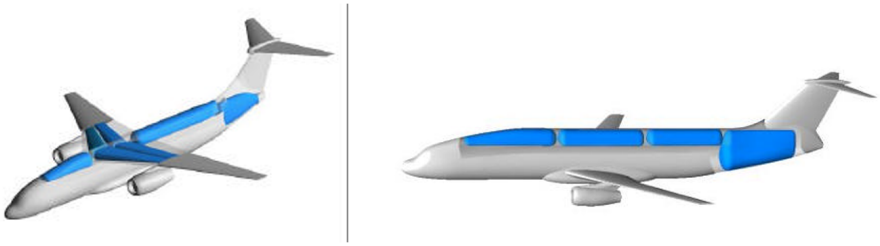

Figure 2.20: CRYOPLANE SMR concepts; initial proposal (left) and the revised configuration (right) [11]

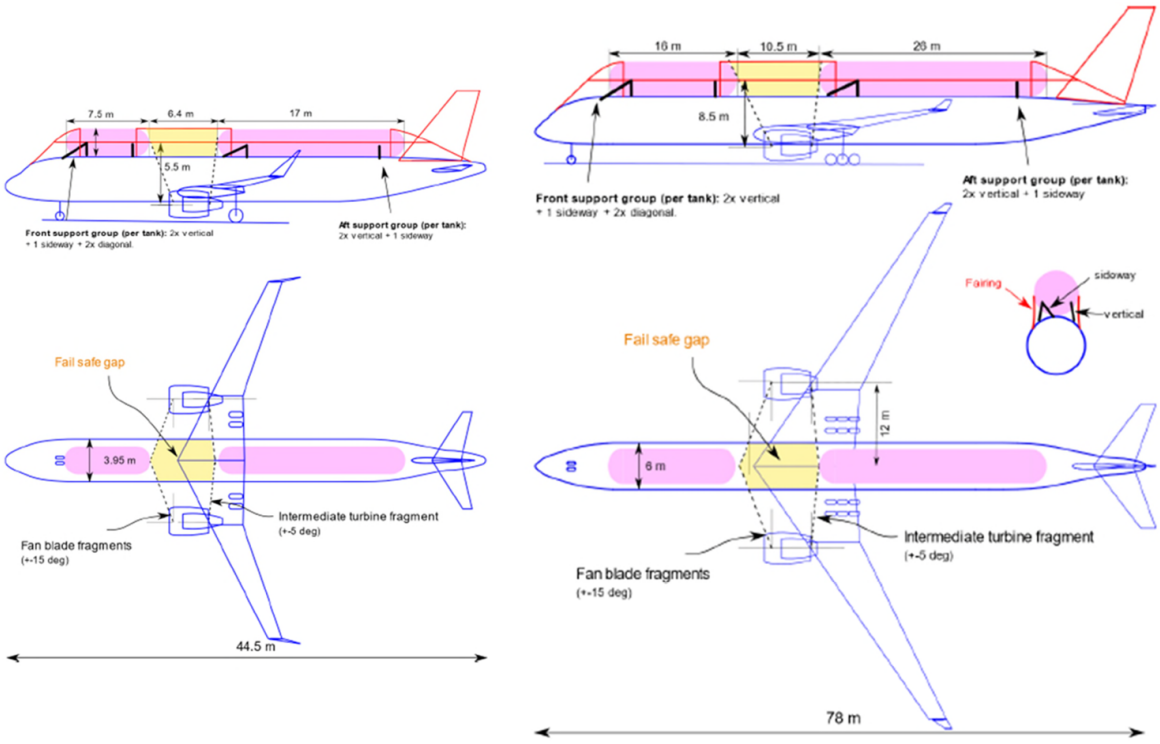

Figure 2.21: ENABLEH2 Low Risk SMR concept (left) and LR concept (right) [37]

More recently, the ENABLEH2 project concluded its studies on the use of hydrogen in aviation. This includes LH2-based SMR and LR aircraft concepts, for two categories each: 1) a conservative, ”Low Risk” design and 2) a more aggressive ”Max Synergy” design which assumes the use of more advanced technologies ready by the year 2050. The ”Max Synergy” concept will be discussed in a later section due to its novel configuration, but the low-risk concept will be explored here. The concept, proposed by Chalmers University, uses non-integral cylindrical tanks mounted by struts above the pressurized fuselage. A fairing connects the tanks and fuselage to reduce interference drag, and to cover the gap between the tanks. The gap is designed to reduce the risk of tank damage in case of an engine blowout, illustrated in figure 2.21. The tank utilized is a rigid closed-cell type and allows for 2% boil-off over the

course of the design mission, but few other details are given, such as the gravimetric efficiency or the weight breakdown of this configuration. The block energy consumption is unfortunately 20% higher than the Jet A-1 baseline aircraft of 2050 assumed in the study. Considering this is higher than the predicted increase for other LH2 configurations in previous studies, the drag and weight penalties of the top tank layout appear to dominate over its quantitative benefits. Qualitatively, the configuration retains advantages in terms of crashworthiness and operational ease at airports.

Waddington et al. [46] study this configuration on a single-aisle transport aircraft with top-level aircraft requirements based on the Boeing 737-800, assuming a 2050 entry into service. This concept differs from most aircraft in that it utilises fuel-cell based propulsion instead of turbofans, leading to 9 electric motors present on the aircraft. Three are placed on each inboard wing root and three are placed on top of the tailcone, between the V-tail. The centerbody contains 8 LH2 tanks as well as some electrical systems in an unpressurized environment, and forms a lifting body unlike previous concepts discussed. The aircraft is shown in figure 2.22. It is not clearly stated why the decision was made to have 8 separate LH2 tanks despite the drawbacks arising from increasing the surface-area to volume ratio of the fuel in this manner. While regulations stipulate that a separate fuel supply is needed for each propulsor, this could also be satisfied by having fewer, larger tanks with internal dividers. It is speculated that a combination of safety, design for redundancy, and aerodynamic shaping of the centerbody was considered more important and hence lead to this tank configuration. The study does confirm that the reason for offseting the tanks laterally is to ensure that no fuel lines crossed the cabin, and path directly to the neighbouring fuel cells to ensure safety.

The wings are mounted on the same elevation as the centerbody, and the thermal management system interlinks the fuel cell cooling with the LH2 feed line to the fuel cells for improved efficiency. The wings also feature folding wingtips to meet the same gate requirements as the reference aircraft, and the landing gear is integrated with the fuselage due to the high-wing configuration. From a performance prediction perspective, there are several noteworthy decisions made in the study. Firstly, even though the EIS is set to 2050, no advancements in material weights are assumed; and the potential positive effects of boundary-layer ingestion (BLI) on the aft fans is disregarded completely. Secondly, the study concedes that a battery will be needed to assist the fuel cells in peak-power conditions, but does not allocate any weight for it due to the lack of knowledge on the transient loads. The airframe weight estimation on the other hand, takes the average of two separate empirical methods to consider a wider range of designs, but increases the uncertainty of the results simultaneously. These factors indicate that further research is required into this configuration to draw conclusions on its performance relative to the reference aircraft.

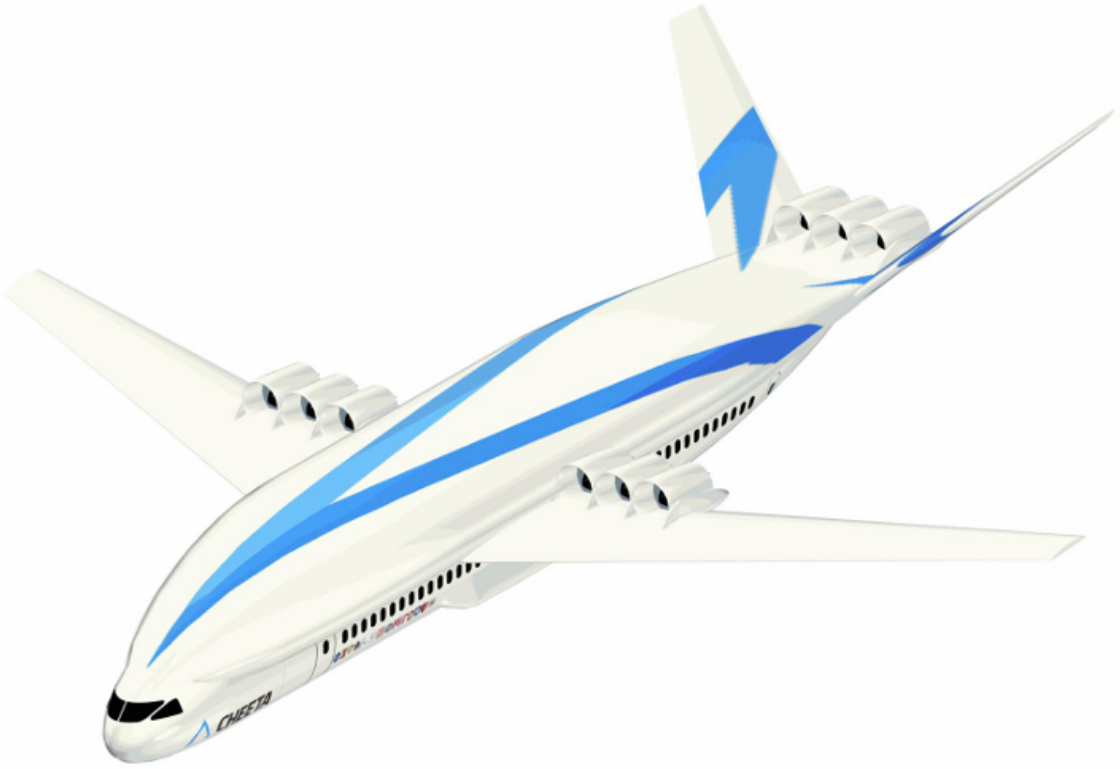

(a) The aircraft geometry, isometric view

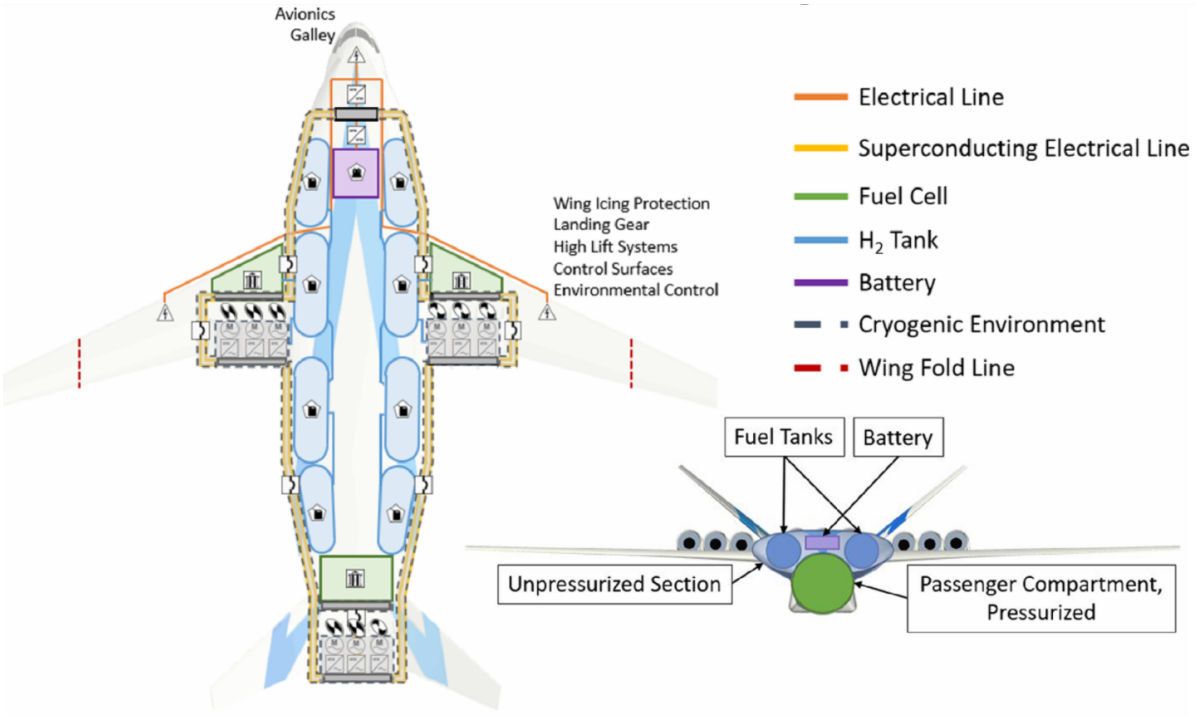

(b) The layout of systems on the aircraft

Figure 2.22: UIUC CHEETA aircraft [46]

Silberhorn et al. [39] examine and compare the integration of hydrogen tanks with SMR aircraft in a detailed and fundamental manner. The EIS is set to 2045, and several technology factors are applied

to the A320neo to make it a representative baseline Jet A-1 aircraft of the year. The integration of cryogenic tanks is carried out through 3 different configurations: 1) Aft tanks, 2) Over-cabin tanks, and 3) External wing-mounted podded tanks. There is a physics-based model created for the thermodynamic time evolution of the hydrogen in the tank and linked with the mission profile, making for a higher-fidelity analysis than most previous studies. The tank operating pressure is set to 1.5 bar, and the insulation method is selected as closed-cell foam for its low weight and cost.

The study also considered the effect of thrust-to-weight ratio on the block energy consumption, as the use of hydrogen over kerosene results in a higher thrust requirement at the top of climb (TOC). This changes the engine sizing and hence the overall drag and aircraft performance over the mission. For each of the three concepts, a sensitivity analysis is carried out on the effect of varying tank geometry and insulation thickness on block energy of the aircraft. This is a very important step to ensure that the best of each concept is extracted, enabling a fair comparison between the concepts.

The investigation into the aft-tanks concept found that a thrust-to-weight ratio of 0.3 and insulation thickness of 7cm was the right balance between managing boil-off and weight, leading to the best possible block energy. The airframe mass increased due to fuselage extension to support the integral tanks, and the landing gear size also had to be increased to maintain the same tip-back angle; leading to a 11% increase in OEM. It appears that the tail sizing did not take into account the changes to the CG-excursion and stability requirements, so the actual performance might be slightly worse than predicted by the study. The geometry of the tank integration can be seen in figure 2.24a, where the bottom image shows the aircraft without the fuselage skin.

Parameter	*Rear*	*Top*	*Pod*	*Unit*
MTOM	67819	66045	64584	kg
OEM	44334	42605	41084	kg
MZFM	64334	62605	61084	kg
MLM	65069	63331	61823	kg
Design block-energy	533.0	530.3	535.6	GJ
Thrust to weight	0.300	0.310	0.319	-
Wing loading (TO)	620.4	620.7	621.8	kg/m^2
Aspect ratio	11.9	12.2	12.5	-
Insulation thickness	7	10	9	cm
Fuel system mass	781	627	630	kg
Fuel containment mass*	1651	2429	2190	kg
Rel. trip boil-off	1.9	2.5	2.0	%

*including the additional masses such as support structure, safety features or pylons

(a) Parameters of the 3 concepts

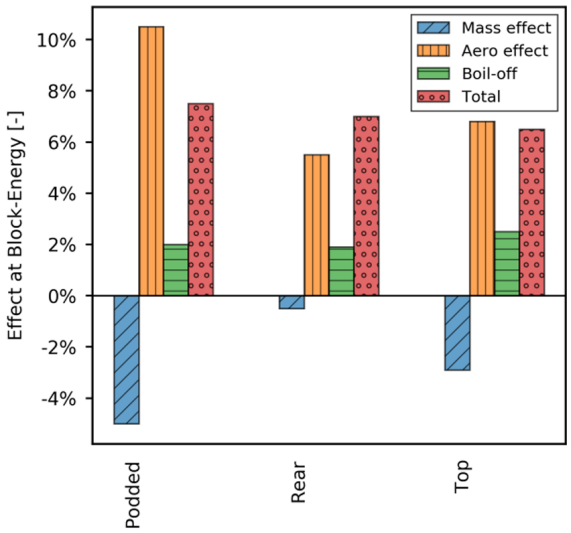

(b) Effect of integration on block energy usage

Figure 2.23: LH2 aircraft configuration performance comparison [39]

With the over-cabin tank integration, the tank shape was seen as a key control factor over performance, where the optimal ratio of radii between the two circumferences of the tank were targeted. Similar to previous studies, the tank appears to be attached in a non-integral, with a fairing over both tanks to reduce drag, as seen in figure 2.24b. The podded tank concept also requires an increased landing gear length, and maintaing sufficient side clearance angles and high lift performance poses a challenge. This concept does however offer wing bending relief unlike any previous LH2 integration strategies, at a significant aerodynamic cost. It is also attractive from a safety perspective in that it maximises the distance from the cabin to the tanks greatly, but it must be kept in mind that the fuel lines will have to cross the fuselage to access the opposite engine.

Figure 2.23 compares all three configurations from a block energy perspective and aircraft parameter breakdown based on key variables. The podded concept does have the most positive mass effect on block energy, and has the lowest MTOM and OEM of all three concepts. As expected however, it has

the greatest aerodynamic penalty and appears to outweigh the mass benefits, and leaves it with the highest block energy consumption of the three configurations.

The aft-mounted tank configuration, conversely, is found to have the smallest aerodynamic penalty and is the heaviest of the three configurations. This is a very interesting result, as the integral nature of the aft-mounted tanks typically leads to a weight reduction over other concepts but is not the case here. Finally, the top mounted configuration is reported to balance the aerodynamic and mass penalties better and have the best block energy consumption of the three configurations. This too is unexpected, as the integration of the tanks in this manner has previously been found to lead to overall heavier OEMs than integral tanks. Given its increased surface area, it also necessitated the highest amount of insulation.

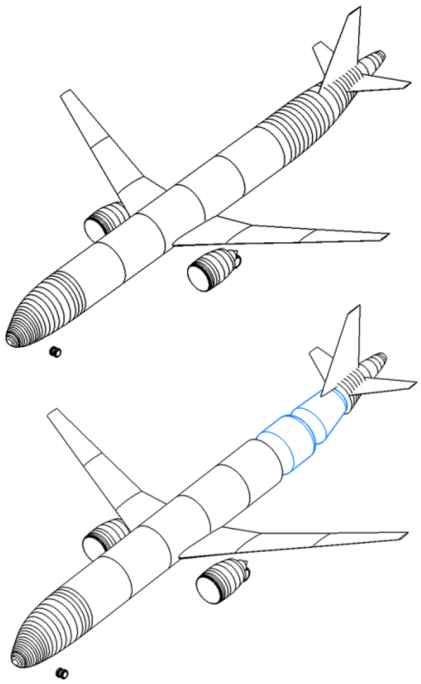

(a) Aft tank configuration. The lower image shows the aircraft without tank fairings

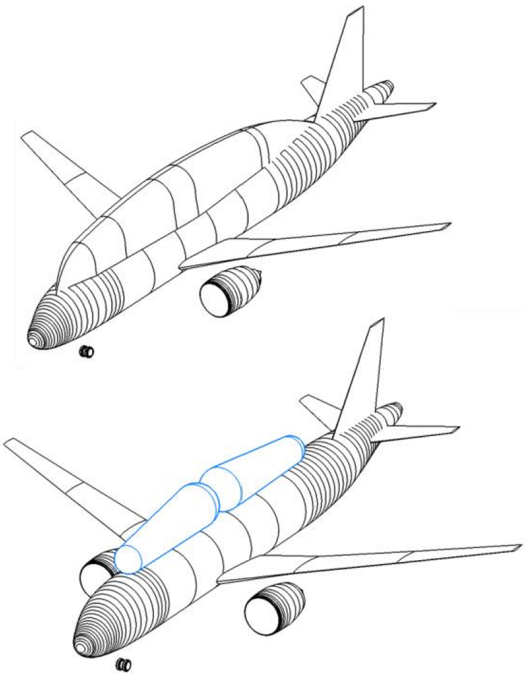

(b) Over-cabin tank configuration. The lower image shows the aircraft without tank fairings

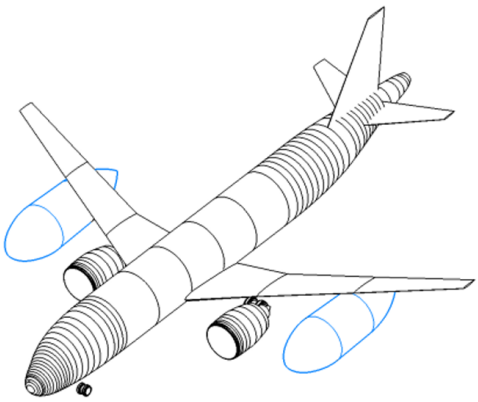

(c) Podded tank configuration

Figure 2.24: LH2 aircraft configurations [39]

2.4.4. BWB Aircraft

Given the bulky nature of cryogenic tanks and all the constraints involved in trying to integrate them with conventional tube-and-wing aircraft, blended-wing-bodies (BWBs) may provide the ideal solution for hydrogen-powered aircraft. BWBs differ from TAW aircraft in that their fuselages are typically oval instead of cylindrical, and have much smaller wetted area for a given wing reference area. This leads to reduced drag and improved performance. However, non-cylindrical fuselages pose the main challenge for BWBs due to their difficulty in designing and manufacturing; and has been touted as the main reason why BWB aircraft have not seen any entry into service or even full scale experimental aircraft. This has not stopped research into this configuration, and has only increased since the idea of hydrogen-powered aviation has gained momentum in recent years, notably Airbus' ZEROe LH2 BWB concept, and JetZero's collaboration with NASA. Figure 2.25 shows these two aircraft, with further details on performance and layout limited in the public domain.

(a) Airbus ZEROe BWB concept [10] **(b)** JetZero BWB concept [24]

Figure 2.25: Recent BWB aircraft concepts

Adler and Martins [1] study the BWB configuration as well as the TAW configuration, for both kerosene and LH2 fuel. The reference aircraft chosen is a Boeing 787-9 like aircraft and is the basis for the mission requirements as well as the geometry of the TAW aircraft. The hydrogen tanks are integrated in a fore-aft configuration for the TAW aircraft, and it is attempted to be integrated in the blending wing region of the BWB. Initial attempts to put cylindrical LH2 tanks in this region are found to be very challenging and the required fuel could not be carried without disturbing the outer mould line or reducing packing efficiency significantly. A significant decision is made to switch to conformal tanks for the BWB because of this, even though the technology for this is still at its infancy, and the feasiblity is unkown. Despite this, the study assumes a gravimetric efficiency of 60%, same as the TAW concept, and proceeds with the study- giving what may be an upper bound performance estimate. Whether or not there is a change in tank operating pressure for conformal tanks is not addressed.

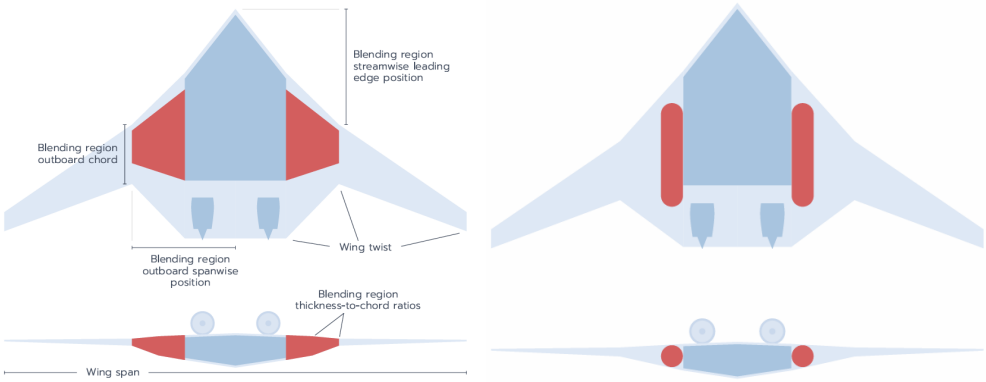

(a) Conformal tanks on the BWB blending region **(b)** Cylindrical tanks on the BWB

Figure 2.26: LH2 versions of the BWB studied in [1]

For both the TAW and BWB LH2 aircraft, compared to their kerosene-based equivalent aircraft; the MTOM is smaller and the OEM is larger. This is due to the lighter hydrogen leading to smaller fuel mass but the integration effects leading to a higher empty weight, a trend seen also in previous TAW concepts. The effect on energy usage is that both LH2 versions use more energy than their kerosene counterparts (5.1% more for the TAW and 3.8% more for the BWB). The study is however, very reluctant to directly compare the BWB and TAW concepts, due to the difference in weight estimation of the two configurations; and a true comparison is left wanting.

Sensitivity analyses are carried out to gain further knowledge on the difference between the characteristics of the TAW and BWB. The LH2 TAW is found to be more sensitive to tank gravimetric efficiency than the LH2 BWB, especially at low efficiencies; where its energy consumption is significantly higher. The LH2 BWB concept is also a lot less sensitive than the LH2 TAW to the OEM and aircraft drag compared to their respective kerosene counterparts. This is primarily due to the BWB having a better lift to drag ratio, so a smaller increase in thrust is required for a given penalty in weight or drag, compared to the TAW. The study concludes that, given the challenges in tank integration even with the BWB, this concept may not be the silver bullet some may have considered, but that BWBs are still worth investigating regardless of the fuel type due to potential efficiency increases.

Karpuk at al. [25] investigate the design of hydrogen combustion based BWBs. One of the primary challenges in the conceptual design of BWBs is the constraint based modelling needed to ensure that the cabin and other internal components fit inside the outer mould of the aircraft. The cabin is sized first in this study, using a pentagonal parametric model shown in figure 2.27a, with six different passenger bays linked to the leading edge sweep. The lower part of the centerbody is allocated for cargo space, and the tanks are placed outboard of the centerbody. Due to the decreasing airfoil thickness moving away from the center, the outer tanks had to have smaller radii, decreasing storage efficiency.

Aside from the structural challenge of pressurizing such a cabin efficiently and safely, this design also raises potential difficulties with its wing structure. The front spar is shaped in a typical manner similar to TAW aircraft, but the rear spar has a severe kink inboard to accommodate the LH2 tanks. This is likely to introduce increased stress, and require a heavier structure to support it. A possible solution might involve integrating the tanks with the spars and wing box to create a much lighter structure, but the feasibility of this solution has not been explored.

The study concludes that compared to the kerosene BWB, the LH2 BWB had to be much longer to accommodate the required fuel, and this impacted the optimal cabin layout as well; which in turn affected the overall wetted area of the aircraft. The block energy consumption was 26% higher than the kerosene version, but 36% lower that the TAW reference aircraft; keeping in mind that the uncertainty in these results is generally greater than that of TAW aircraft performance estimations.

The ENABLEH2 project [37] also proposed an LH2 BWB for zero carbin emission long range aircraft. The geometry is based on NASA's N2-X aircraft, but scaled to meet the necessary internal volume requirements. The aircraft concept is show in figure 2.28. In an unconventional step, they choose to place 6 tanks in the belly of the BWB instead of the inboard wing region, as is common. The tanks are cylindrical with hemispherical caps, and feature an innovative system in which a combination of LH2 and GH2 from the tanks are fed to the engine to better control the pressure in the tanks. The outboard tanks are the smallest but have been designed for long term storage; as they are meant for reserve fuel only. This means that for the majority of missions, and if no special modifications were made they would simply boil off and have to be refilled often. This solution has the potential to avoid that and enable more efficient operations, but the impact on aircraft performance is not discussed.

Another unorthodox tank integration strategy is explored by Versprille [44], seen in figure 2.29, where the LH2 tank is placed aft of the cabin in the BWB. This improves the surface area-to-volume ratio of the fuel, and it appears that an integral tank would be feasible in this design; making for a potentially much lighter tank. The tank shape is highly elliptic instead of cylindrical, similar to the cabin in this design. One disadvantage with this concept is that the problem of the CG-excursion returns, although it is reduced compared to the TAW due to the shorter centerbodies.

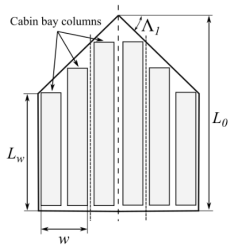

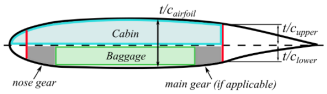

(a) BWB cross section showing the cabin layout and cargo hold

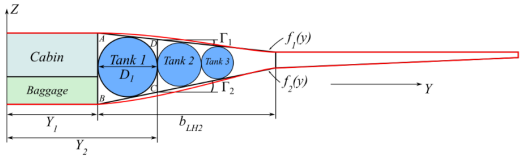

(b) BWB front view

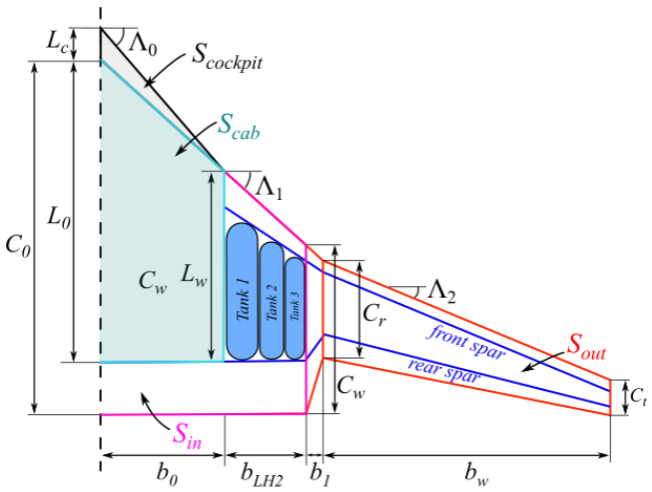

(c) Tank Integration

Figure 2.27: LH2 BWB aircraft configuration presented by karpuk et al.[25]

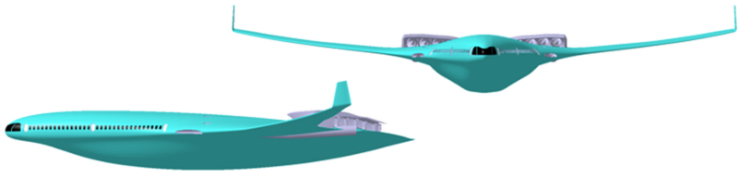

Figure 2.28: ENABLEH2 BWB concept [37], with tanks placed in the underbelly

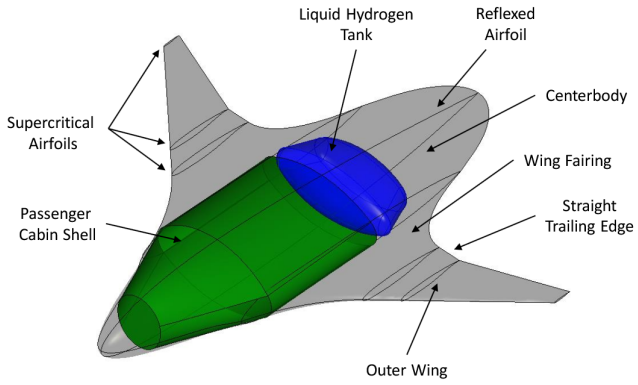

Figure 2.29: LH2 BWB proposed by Wilod Versprille [44]

3

Configuration Downselection

3.1. Introduction to the Chapter

Numerous concepts and configurations were introduced in the previous chapter. This chapter will perform a downselection to arrive at specific configurations of interest, based on viability, potential performance, safety, or simply as a good point of comparison. The selected configurations will then be appropriately sized, designed, and compared in future chapters. The figures shown here are purely for illustrative purposes.

3.2. The Candidates

3.2.1. Standard Aft Tank Aircraft

As one of the most common configurations, the aft tank design presents itself as a good baseline aircraft for LH2 aircraft studies. Among all concepts, this deviates the least from the conventional jetliners of today, and offers a relatively straightforward method of integration. Furthermore, its inclusion in Airbus' ZEROe project has motivated the decision to shortlist it for the current study.

Slight variations to the design will also be included, such as engine placement and tail configuration. Fuselage-mounted engines with a T-tail could reduce the CG excursion compared to conventional wing-mounted engines, but the effect on overall aircraft performance is unknown. For the sake of improved gravimetric efficiency, a single aft integral tank with an internal separator is chosen. The separator is required as regulations stipulate that each engine is connected with an independent fuel system. A notional design of the configuration is shown in figure 3.1, with the tank represented in pink at the aft part of the fuselage.

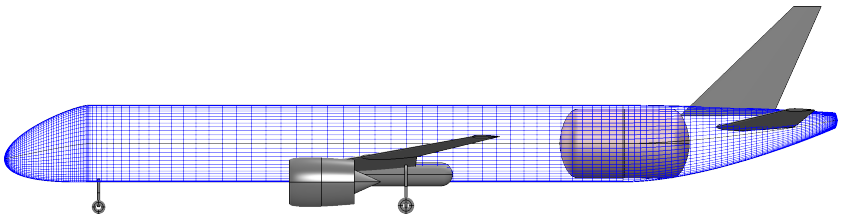

Figure 3.1: Standard aft tank configuration

3.2.2. Dual Forward-Aft Tank Aircraft

Given the problems and challenges posed by the previous configuration, the dual forward-aft tank layout presents a conceptually simple solution for resolving the large CG excursion. Through this fuel split, the need for an oversized horizontal tail can be eliminated, and the integration of the landing gear is also likely to be much simpler. While the previous and current configurations have been introduced by Onorato et al. [33] in the same tool as this study, they remain of interest for further exploration and

simply as points of comparison.

The primary performance-based drawback would be that a) the fuselage would become even longer and heavier as a result, even to carry the same total fuel volume, and b) the peak stresses experienced by the fuselage would be higher due to the load distribution. In most studies of this configuration, the forward tank is made non-integral to enable a cabin-cockpit connection for the crew. As a consequence, the external environment for the tank is the same as the cabin environment, which is undesirable from a safety perspective. Now, in case of a leak, there will be an explosive mixture formed either inside the tank or inside the cabin, depending on the pressurization of the tank. Nonetheless, this configuration is of interest and will be included in the study as an additional point of comparison. Figure 3.2 shows a notional design, with the reduced diameter forward tank, to accommodate a walkway on one side.

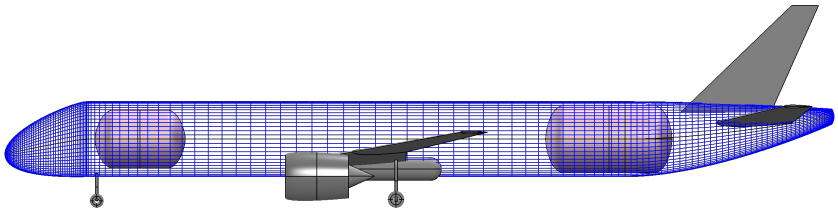

Figure 3.2: Dual forward-aft tank configuration

3.2.3. Mid-Tank Aircraft

An even simpler solution is sought for the issues arising from the large CG excursion of the aft tank layout- what if the fuel tank is just placed at the center of the fuselage? It is conceptualized that the tank could take the full radius of the fuselage, as the cockpit is now attached to the front of the cabin. The rear cabin, behind the tank, would be completely separated- having its own cabin crew, exits, lavatories, etc.

Compared to the forward-aft tank configuration, the mid-tank solution should result in a shorter, lighter fuselage, with better load distribution, and better tank gravimetric efficiency. The tank could be efficiently placed right above the central wing box, potentially enhancing its crashworthiness. However, with this position of the tank, a pass-through wing is no longer possible, and the wing is attached below the fuselage, similar to business jets. As a result, the nose landing gear needs to be longer as shown in figure 3.3, but the rest of the components remain largely the same.

On paper, this concept is quite promising, until the practicality is considered further. Separating the cabin requires the doubling of numerous systems and resources, and an increase in crew would incur higher operational costs. Airport gate compatibility would be another challenge, as the ingress and egress of the rear cabin necessitates a second bridge or staircase- posing further operational restraints. Given these issues, the configuration is not considered further in this study.

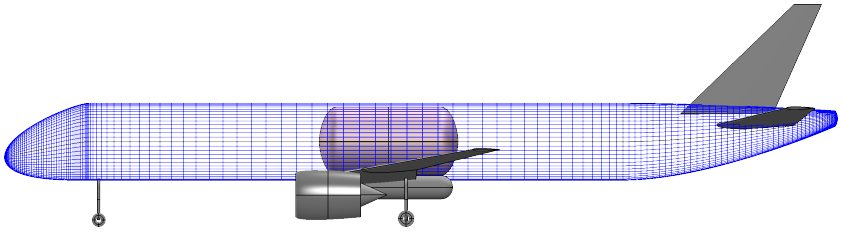

Figure 3.3: Mid-tank configuration

3.2.4. Three-surface Aircraft

The three-surface aircraft (3SA) with the aft tank layout appears to be a synergistic combination of decisions; leading to improved aerodynamic performance and simpler landing gear integration. The design proposed in the FlyZero project [4] shows promising results, and the design is adapted here. As discussed earlier, the viability of maintaining laminar flow over any meaningful part of the fuselage is

unclear, and the importance of having an aircraft family option is too high; hence, the current concept utilizes a conventional constant-section fuselage, as shown in figure 3.4

Key design parameters such as the foreplane's vertical location, engine placement, and tail configuration will be studied to identify the best trade-off. The correct placement of these parts is assumed to be especially important in this configuration to avoid interference penalties. While an all-moving foreplane with control authority would be beneficial in further reducing the size of the horizontal tail, it is presumed that this mechanism would be too heavy and bulky for integration in the nose region. Hence, a simple foreplane with a flap is selected, where the activation of the flaps is linked with the flaps on the main wing- removing any additional complexity for the pilot. In this setup, the change in pitching moment as flaps are deployed is also similar to that of conventional aircraft.

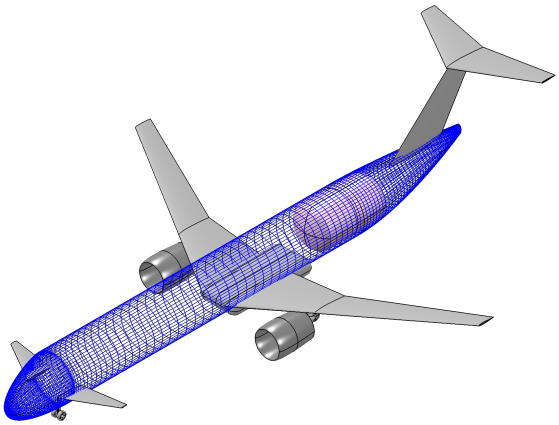

Figure 3.4: Three-surface aircraft configuration

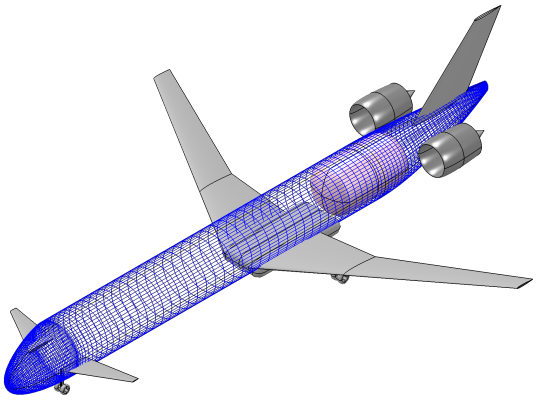

Figure 3.5: Canard configuration

3.2.5. Canard Aircraft

This configuration builds on the advantages of the 3SA by eliminating the horizontal tail altogether, and using the canard as a control surface. Given it's position at the front of the aircraft and its large moment arm, it is hypothesised that the canard would be much better suited for aft tank layouts than traditional tails. A concession would have to be made in that the wing would be placed further aft than usual, to ensure a sufficient stability margin, but the reduction in zero-lift drag might be worth this change. Figure 3.5 shows the aircraft configuration, with fuselage mounted engines to further reduce the CG excursion. As this concept has not seen much research for LH2 transport aircraft, it is certainly worth exploring further.

Unfortunately, the selected design tool does not support the canard configuration; and the adaptations needed to enable support would have a large time cost. Hence, in the interest of studying a larger number of configurations, the LH2 canard aircraft is not considered further in this research.

3.2.6. Top Tank Aircraft

Another popular configuration in the literature, this design resolves the large CG excursion by placing the tank above the fuselage. The design of the fuselage itself remains largely the same as it is still a pressure vessel, but now with some mounting points for the tank above. A fairing, purely for aerodynamic purposes, would be placed around the region between the tank and the fuselage, as shown in blue in figure 3.6. A H-tail is initially proposed to avoid the wake of the tank and maintain sufficient directional stability.

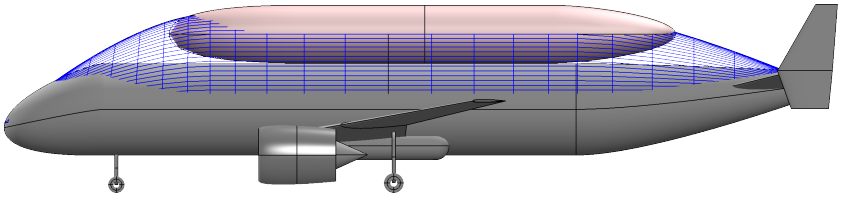

Figure 3.6: Top tank configuration

Despite the drawbacks of an effectively reduced slenderness ratio for the fuselage and reduced tank gravimetric efficiency, this configuration has promising levels of performance and safety; based on the literature. Variations of this configuration were also considered, including a double-bubble fuselage and multi-tank layouts; but the original design was finally presumed to hold the best compromise in weight and drag; and was selected for further study.

Chapter 4 details the exact modelling techniques and design decisions made with this configuration- covering the aerodynamics, stability, weights, and load paths.

3.2.7. BWB Aircraft

Blended-wing body (BWB) aircraft have been hypothesised to be better than tube & wing aircraft for carrying hydrogen fuel, due to their large internal volume. Several tank layouts were envisioned and modelled, with the aim of best utilizing the available space; behind and around the cabin. However, it was quickly found that despite the large available volume, the shape constraints discouraged the use of few, high-diameter tanks, and favoured multiple, slender tanks. Despite this, concepts prioritizing high gravimetric efficiency were conceived and qualitatively analysed. Some examples are shown in 3.7: ranging from spar-integrated shoulder tanks to low dormancy conformal tanks.

The required fuel volume was assumed to be equal to TAW aircraft at this stage, but lower fuel requirements may have unlocked other, more efficient tank layouts. Unfortunately due to the limited time available, and the large amount of work needed to enable BWB design on the selected tool- these concepts were not considered further.

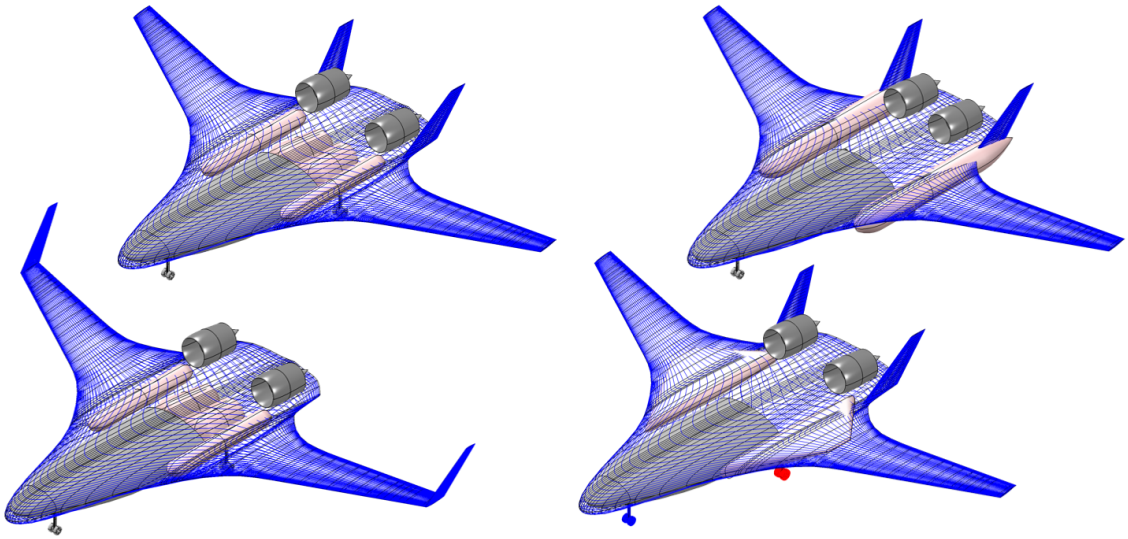

Figure 3.7: Some BWB configurations considered

3.3. Selected Configurations

The qualitative downselection conducted involved in-depth considerations into a variety of safety and operational factors. This included scrutiny on hazard in case of tyre blowouts, tail stikes, belly landings

and roll-over tip trikes. Emergency exit placement and operation in water landings was also studied for each configuration, and was found to be one of the main concerns with BWB designs. Engine placement was also found to be a key variable in preventing a cascading critical failure, while also minimizing fuel proximity to the cabin. These factors, when combined with presumed performance trends from literature, forms basis for an initial concept ranking. Next, based on the time available for the study, four configurations are selected for a more detailed design exploration as explained in the individual configuration sections. Finally, the following configurations are selected for further study:

- Standard aft tank aircraft (2SA-LH2-Aft)
- Dual forward-aft tank aircraft (2SA-LH2-FwdAft)
- Three surface aircraft with an aft tank (3SA-LH2-Aft)
- Top tank aircraft (2SA-LH2-Top)

4

Methodology

4.1. Introduction to the Chapter

This chapter conducts an in-depth explanation of the methodology used for the design of aircraft in this study. Firstly, the main tool- Aircraft Design Initiator, and its workings are introduced in section 4.2. Next, the modifications made to design and analyze new aircraft configurations are explored in sections 4.3 and 4.4. Specifically, the three-surface configuration and top-tank configuration require special attention in terms of aerodynamic and structural modelling. Finally, the implementation of operational limits is discussed in section 4.5, considering the effect of tail sizing, landing gear integration, and ground operations.

4.2. Aircraft Design Tool

The conceptual design and sizing tool selected for this study is the Aircraft Design Initiator, referred to simply as the Initiator from now. It is a MATLAB-based program capable of synthesizing CS-25/FAR-25 compliant transport aircraft, using a combination of empirical, analytical, and numerical methods in an efficient framework.

Conceived in 2012 by Elmendorp et al. [18][19], Initiator showed great versatility with its ability to design conventional as well as unconventional aircraft, while maintaining a high level of accuracy. Since then, many improvements have been made to expand its capabilities in a wider range of configurations and architectures; and it remains under continuous development in the Faculty of Aerospace Engineering at TU Delft. In the early stages of the current study, various other design/analysis tools were considered, such as the Future Aircraft Sizing Tool (FAST) [30], SUAVE [26], and other design codes- but the Initiator was selected specifically for its flexibility, modularity, and high level of fidelity. Considering the nuanced ways in which some configurations of interest differ from each other, this last quality was deemed important in order to better study designs.

The Initiator employs an object-oriented programming architecture, wherein a ”controller” object is instantiated at the start of the design process. An aircraft input file containing the top-level aircraft requirements (TLARs) and configuration parameters, combined with settings files containing regulatory constraints, airport requirements, and other restraints forms the basis for the design. The controller reads and stores all the appropriate data from these files and begins the design convergence process to arrive at a feasible design that meets all the input requirements. The convergence process itself is composed of 3 partially nested loops, with each proceeding loop increasing the level of fidelity and complexity in an efficient manner. Each loop employs various modules from a multitude of disciplines to size, design, and analyze the aircraft as it evolves through every iteration.

4.2.1. Initiator Modules

Sizing modules are used to perform the initial sizing of the aircraft at the start of each iteration. Data from the previous iteration, as well as TLAR/configuration data, is first used to create a wing & thrust

loading constraint diagram, as well as a class-I weight estimation of the aircraft. The results from these modules are then used by the GeometryEstimation module to execute a new definition of all primary parts of the aircraft (wings, empennage, engines, etc.); with the exception of the fuselage, which is configured by its own module.

Analysis modules are utilized to build up various aspects of the aircraft's performance, and are an integral part of the convergence process. A dedicated drag module exists to create drag maps for different flight conditions; which is heavily relied on by the Mission Analysis module. In this module, a time-step based simulation is carried out to track various parameters through every stage of every mission- offering excellent results for a design tool. Weight estimation modules are also present here, providing a detailed breakdown of component-level masses for the aircraft, which are drawn upon for other analyses such as FEM-based wing sizing, and mission analysis.

Design modules work with the limits imposed by the previous two types of modules and physics-based models, to generate an efficient design of a specific component. Examples include the stabilizing surface module, which identifies the design corresponding to the smallest horizontal tail; and the landing gear module, which finds the shortest (and hence lightest) feasible landing gear design.

4.2.2. Convergence

The design convergence workflow efficiently places said modules in an efficient framework, constructing a tool that converts a set of TLARs and configuration parameters to a complete, feasible aircraft design. As discussed earlier, the Initiator uses three partially nested loops to accomplish this task, which can be seen in figure 4.1.

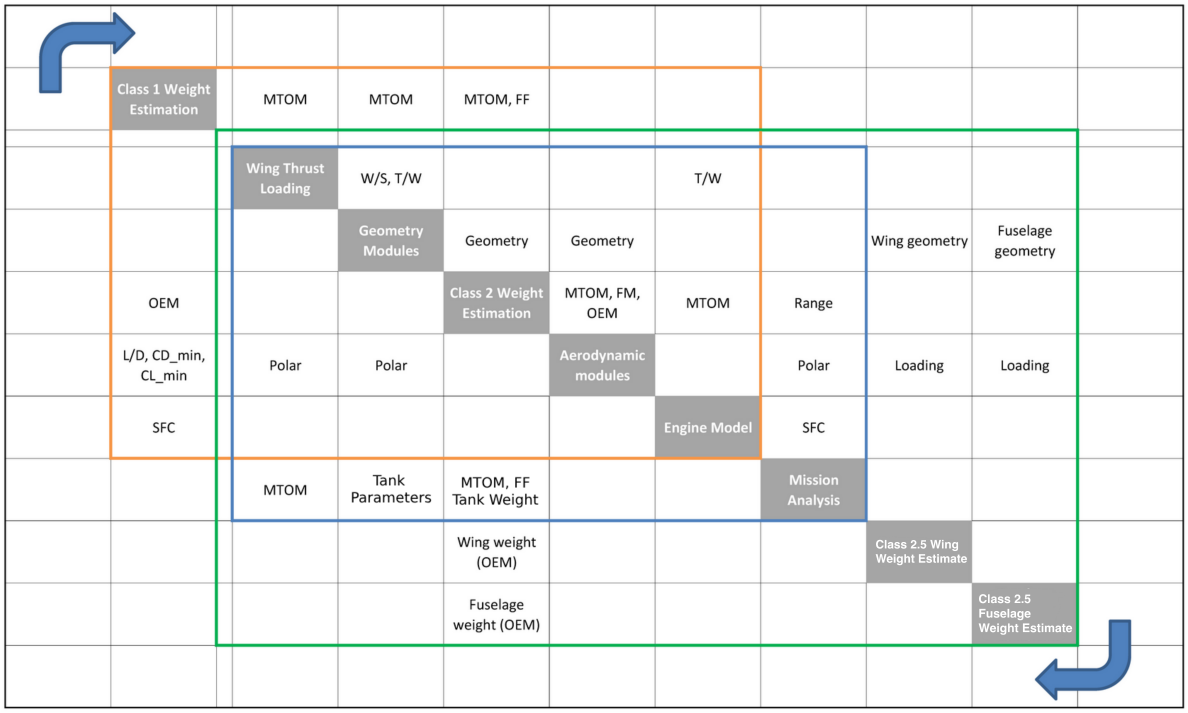

Figure 4.1: The N2 diagram of the Initiator. The class-I loop is represented in orange, the class-II loop is represented in blue, and the class-II.5 loop is represented in green. [12]

The first loop, traced in orange, uses class-I weight estimation techniques and simplified analytical drag models to predict the aircraft's performance. This means that the results are not very sensitive to configuration variations and do not offer accuracy; but form an ideal starting point for the next loop. This loop, traced in blue, now takes the weight results from the previous loop and uses more advanced methods to obtain a more accurate design for the aircraft. Class-II methods replace the basic fuel-fraction based methods for mass estimation, while drag is now predicted through higher fidelity. Zero-

lift drag is now truly sensitive to the geometry, induced drag is numerically found using AVL, and even wave drag is accounted for. Furthermore, the mission analysis module is also activated; thus providing much-needed accuracy of aircraft performance through various mission stages (take-off, climb, cruise, etc.). The importance of accounting for CG-excursions in LH2 aircraft was previously highlighted, and the detail of this module enables the inclusion of it within the design/analysis process. The second loop is terminated when consecutive results fall below a certain tolerance.

After the class-II loop has converged, the final loop is triggered. At this stage, empirical relations for wing and fuselage weights are replaced by physics-based FEM models, known as class-II.5 methods. The wing structure is set to handle the critical 2.5g pull-up manoeuvre, and the fuselage structure is sized to take on the combination of loads produced by the maximum longitudinal bending moment and the pressure differential. The resulting masses of these structures are passed on to form a new OEM estimate, and the remainder of the final loop works exactly as the class-II loop for other disciplines. Once the class-II.5 loop also converges, the design of the aircraft is complete.

4.2.3. Cryogenic Tank Modelling and Sizing

This study utilizes the cylindrical tank model created by Onorato [32] for the same design tool. The tank consists of a single structural wall, externally covered with thermal insulation. The structural sizing follows the relations for thin-walled pressure vessels (eqn 4.1), which means it is not designed to also take on bending loads that could be transferred from the fuselage. In that sense, it is not a completely integral tank; relying on stringers of the fuselage to bear bending loads. However, unlike the non-integral tank case, the fuselage frames can be eliminated in the region of the fuselage containing the tank to save weight; as the region outside the tank is not pressurized. In both cases, the fuselage skin is still present over the tank for aerodynamic purposes.

$$t_{\text{shell}} = \frac{(P_{\text{vent}} - P_{\text{amb}}) \cdot r_{\text{shell}}}{\sigma \cdot e_w} \tag{4.1}$$

The tank mounting structure is conceptualized based on Brewer [14], where four support points on the sides of the tank connect to the fuselage stringers. This setup allows for thermal expansion/contraction without causing mechanical stress, and does not transfer the stringers' bending loads to the tank. The insulation is sized to ensure that the GH2 within the tank reaches the venting pressure only at the end of the extended design mission. The outer diameter is constrained by the fuselage diameter, and the inner radius is primarily driven by the insulation thickness. Thus, the length of the tank is the main variable used to ensure sufficient internal volume for the fuel. Figure 2.10 illustrates the workflow used for the overall tank sizing- including the geometry, insulation, and structure. This module is called at the end of every mission analysis run, and uses the relevant atmospheric temperature and pressure profiles, block times, and total fuel requirements as inputs. A notional aft tank schematic is shown in figure 4.2, and the pressure evolution for an extended mission is shown in figure 4.3.

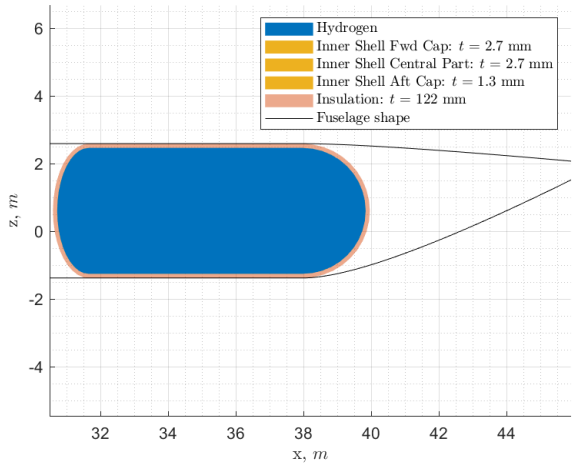

Figure 4.2: Simplified sectional view of an aft tank

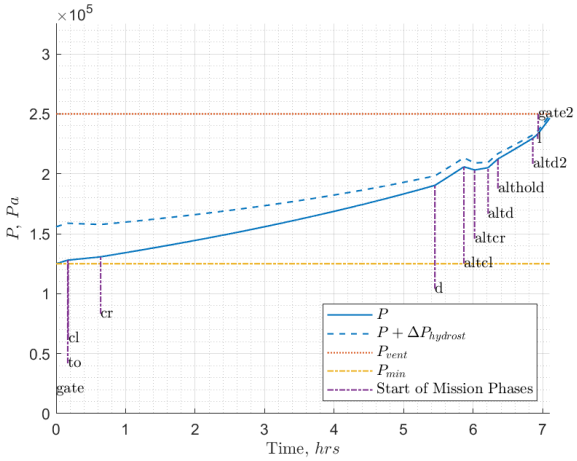

Figure 4.3: Tank pressure evolution example

4.3. Three-Surface Configuration

The type of foreplane deemed viable for this application is the loosely coupled, lifting foreplane. A closely coupled foreplane would not be beneficial here as the interaction effects would reduce the net lift efficiency of the aircraft, and the high angle-of-attack manoeuvrability is not a major concern for modern transport aircraft. A loosely coupled setup allows the foreplane to be positioned as forward as possible, enabling the main wing to be placed further back- while maintaining the same aerodynamic center. As highlighted earlier, this could provide a solution for better main landing gear integration with the wing, while also reducing the CG excursion by pushing the OEM CG closer to the fuel's CG.

Through the input file, the user to provides a fixed volume coefficient or a fixed area ratio of the foreplane, with respect to the main wing. The default position of the foreplane is set directly behind the cockpit, close to the top of the fuselage. This is done to minimize wake interaction with the main wing, which is in the conventional low-wing configuration. Once the aircraft mass is estimated and the constraint diagram provides the wing loading, the total reference area of the aircraft is determined. This area is then split between the main wing and the foreplane during the geometry estimation phase of the iteration. Other geometrical parameters such as the sweep, aspect ratio, incidence, taper ratio, etc., use presets to begin with but may be optimized through other modules.

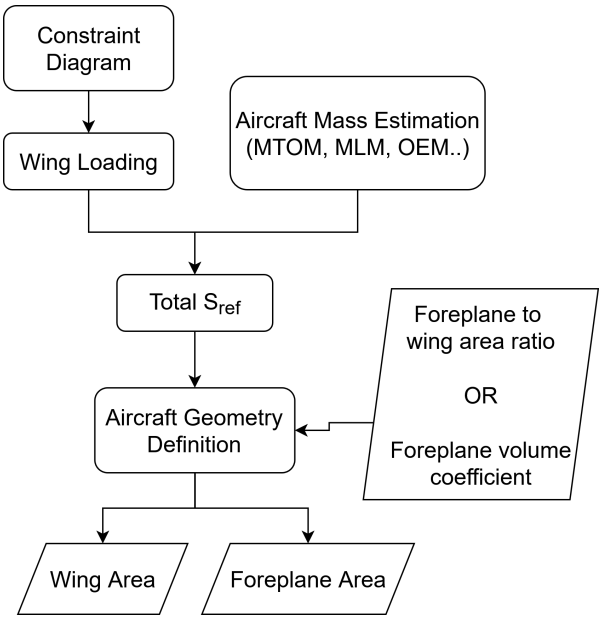

Figure 4.4: The process to define the respective reference areas of the wing and foreplane

4.3.1. Stability and Control

With the addition of the foreplane, the longitudinal stability and control characteristics of the aircraft are greatly altered. Stability refers to the characteristic of the aircraft to produce a pitching moment opposite to the perturbation in angle of attack, helping maintain stable flight. Controllability refers to the ability to impose a certain pitching moment on the aircraft.

The aircraft must be designed for stability and control at their respective critical flight conditions. The stability of the aircraft is most vulnerable at the extreme aft position of the CG, where the contribution of the main wing towards stability is least. The presence of the foreplane at the front of the aircraft decreases the stability, affecting the sizing of the tail. Conversely, at the extreme forward position of the CG; there is a large pitch down moment that the tail needs to be able to match. The situation is exacerbated during landing by flap deflections on the main wing, further adding to the pitch down moment. In this scenario however, the presence of the foreplane is beneficial: offering a pitch-up moment due to its position at the front of the aircraft. Hence, the foreplane is detrimental for longitudinal stability and advantageous for the controllability of the aircraft. Figure 4.5 illustrates the forces and moments on a three-surface aircraft, from which the stability and control limit equations can be derived.

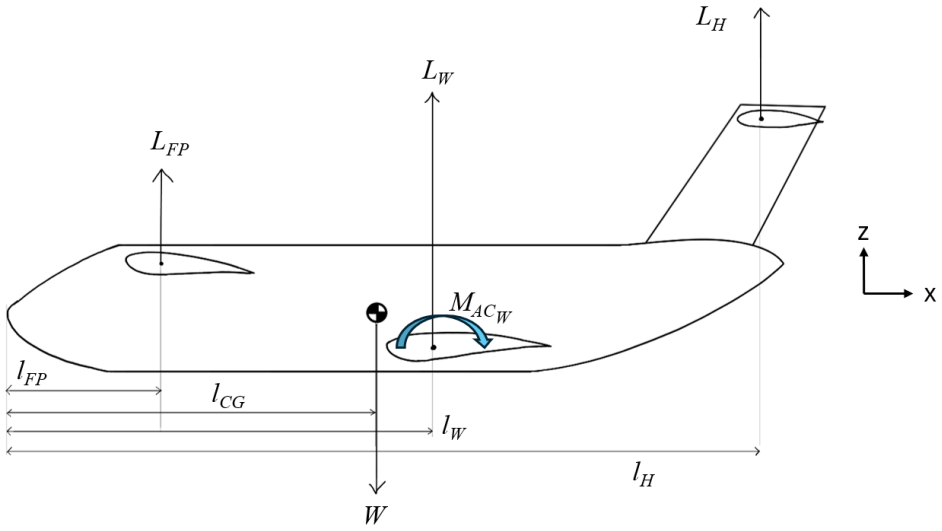

Figure 4.5: 3SA simplified schematic, indicating the primary forces, moments, and lengths

L_{FP}, L_W, and L_H are the lift forces present on the aerodynamic centers of the foreplane, wing, and horizontal tail, respectively. l_{FP}, l_W, and l_H are the horizontal distances from the reference point to the aerodynamic centers of each lifting surface, while l_{CG} is the distance to the center of gravity of the aircraft. M_{AC_W} is the aerodynamic moment about the wing, defined positive in the pitch-up direction. The moments of the foreplane and tail about their aerodynamic centers are traditionally neglected because of their small magnitude.

Balancing the longitudinal moment equation of the aircraft and differentiating with respect to the angle of attack leads to the pitching moment derivate about the CG. The neutral point is defined as the point about which the aircraft is neutrally stable; and by shifting the CG to this location in the equation, rearranging the terms, and adding the static margin (SM), equation 4.2 is obtained. This relation defines the aft limit of the CG, for a given set of aircraft parameters. The reference area and mean aerodynamic chord of the aircraft are denoted by S and $\bar{c}$, while the subscript designates the relevant lifting surface. The wing's large circulation produces downwash at the tail (ϵ_H) and upwash at the foreplane (ϵ_{FP}), changing the local angles of attack, which are estimated through AVL and used in the equation. The lift curves for all three surfaces are estimated through empirical relations provided in the DATCOM database [20], with a slight modification made for the foreplane. Since the foreplane is relatively small and partially buried in the fuselage, a decision was made to use a reduced effective aspect ratio; intended to provide a more realistic lift curve for the foreplane. Moreover, the high incidence of the foreplane is intended to allow for a mild slope to improve stability.

$$\left(\frac{x_{CG}}{\bar{c}}\right)_{aft} = SM + \frac{l_{\mathsf{W}}}{\bar{c}} - \frac{1}{C_{L_\alpha}}\left[\frac{dC_{L_{\mathsf{FP}}}}{d\alpha_{\mathsf{FP}}}\left(1+\frac{d\epsilon_{\mathsf{FP}}}{d\alpha}\right)\left(\frac{V_{\mathsf{FP}}}{V_\infty}\right)^2 \frac{S_{\mathsf{FP}}(l_{\mathsf{W}}-l_{\mathsf{FP}})}{S\bar{c}}\right.$$
$$\left. - \frac{dC_{L_{\mathsf{H}}}}{d\alpha_{\mathsf{H}}}\left(1-\frac{d\epsilon_{\mathsf{H}}}{d\alpha}\right)\left(\frac{V_{\mathsf{H}}}{V_\infty}\right)^2 \frac{S_{\mathsf{H}}(l_{\mathsf{H}}-l_{\mathsf{W}})}{S\bar{c}}\right] \tag{4.2}$$

The forward limit of the CG is typically reached during approach and landing, where fully extended flaps cause a large pitch-down moment on the aircraft. Equation 4.3 is obtained by performing the moment balance about the CG, and shows how the lift of the foreplane and the downforce of the tail work together to combat the pitch down moment represented in $C_{M_{AC_W}}$. The maximum lift coefficient of the flapped foreplane ($C_{L_{\mathsf{FP}}}$) is conservatively estimated to equal to 1.0, and the airspeed ratio is similarly set to unity. A more comprehensive study would also consider the take-off rotation pitching requirements in the tail sizing process, but the Initiator currently does not have a stable computational for this phase,

which needs to account for the ground effect. Hence, only the low speed trim/controllability requirement is analysed for the forward CG limit.

$$\left(\frac{x_{CG}}{\bar{c}}\right)_{fwd} = \frac{l_{\mathsf{W}}}{\bar{c}} - \frac{C_{M_{AC_{\mathsf{W}}}}}{C_{L_{\max}}} - \frac{C_{L_{\mathsf{FP}}}}{C_{L_{\max}}}\left(\frac{V_{\mathsf{FP}}}{V_\infty}\right)^2 \frac{S_{\mathsf{FP}}(l_{\mathsf{W}} - l_{\mathsf{FP}})}{S\bar{c}} + \frac{C_{L_H}}{C_{L_{\max}}}\left(\frac{V_H}{V_\infty}\right)^2 \frac{S_H(l_{\mathsf{H}} - l_{\mathsf{W}})}{S\bar{c}} \tag{4.3}$$

In order to ensure stability, the foreplane is set to stall before the wing. This can be achieved through designing it with low sweep; high incidence angle; or low aspect ratio. The first two options are typically employed, as they can offer the desired lift slope without greatly compromising the maximum lift coefficient or drag. Sensitivity analyses are conducted in later chapters to obtain the optimal foreplane design. With the area ratio of the foreplane already dictated by the user, the primary control parameter remaining in equations 4.3 and 4.2 is the horizontal tail's area ratio. A very large tail will ensure that the aircraft is stable and controllable in all scenarios, but will draw a large drag penalty. Hence, the next section addresses how the best tail size can be obtained while satisfying all requirements.

4.3.2. Tail Sizing

As previously stated, the objective of the tail sizing module is to find the smallest possible horizontal tail that satisfies all stability and control requirements. Furthermore, this module also finds the optimal wing position (in x) that corresponds to the smallest tail. The wing position on the fuselage influences the CG excursion, which in turn influences the tail area ratio.

Taking data from the class-II weight estimation, weight distribution, the wing group and the rest of the aircraft is virtually unlinked. The wing position is varied from 10% to 90% of the fuselage length. Combining this with data from mission analysis, a curve fit is created that produces the CG excursion corresponding to every wing position. The red and blue curves in figure 4.6 represent the forward and aft limits for any given wing position on the 2nd y-axis. As the wing is placed further aft, the OEM CG gets closer to the fuel CG, reducing the overall excursion, but pushing the overall aircraft CG further aft as well.

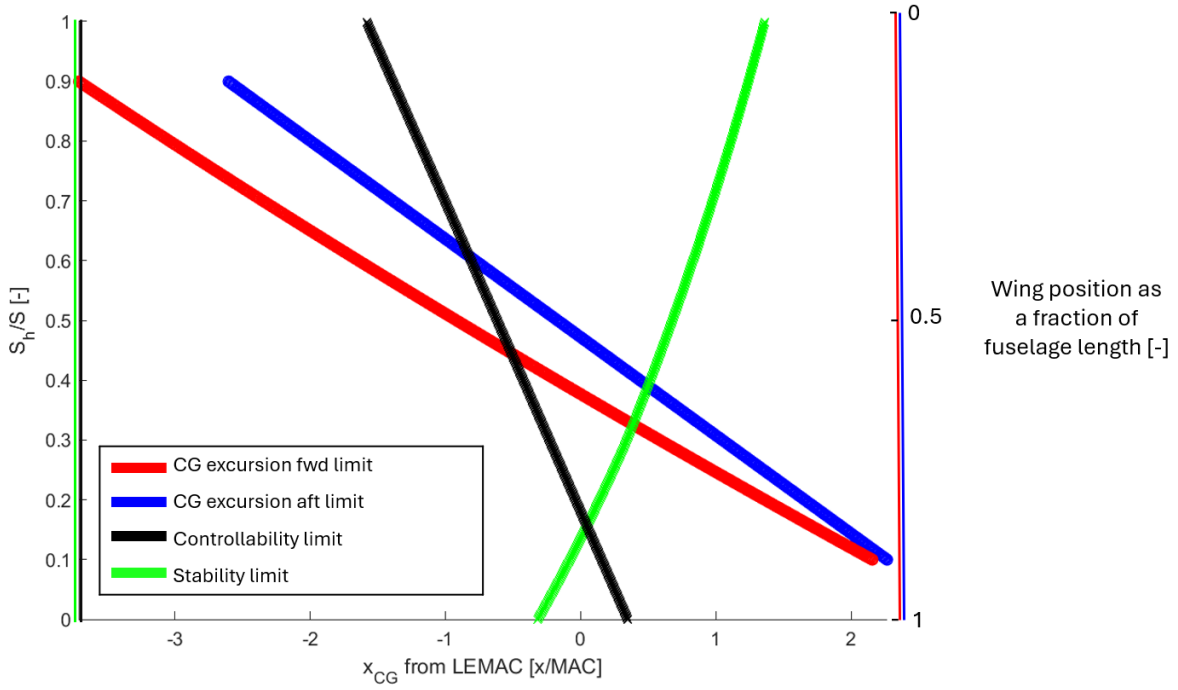

Figure 4.6: Plot matching technique

The CG limits imposed by the stability and controllability requirements are represented by the green and black curves, respectively. These correspond to the tail area ratio (S_h/S), given on the 1st y-axis.

As it can be seen, a large tail area ratio allows for a larger CG range on the x-axis. Another inference made is that any tail ratio smaller than 0.18 (the point of intersection of green and black curves) will not meet the stability or controllability requirements, regardless of where the CG is placed.

The process taken to identify the smallest tail is known as plot matching, and involves analysing the two pairs of curves discussed here. For any given wing position, there is a CG excursion range formed by the red and blue curves. Tail areas are then iterated on until they produce enough allowance to accommodate the CG range needed, and this value is stored in an array. This process is repeated for every wing position, creating an array of minimum tail area ratios for each case. The smallest value from this array and the corresponding wing position is the selected design case- and the entire process is repeated until the tail area ratio converges- within each outer loop of the Initiator's workflow. Figure 4.7 shows a converged scissor plot for a 3SA aircraft. The final stability limit is formed by the critical case of stability in takeoff, cruise, and landing.

Since the effect of the foreplane is to pull the stability and control limits further forward, the main wing is essentially pushed back relative to this- bringing it closer to the main landing gear. This is what helps the 3SA configuration obtain simpler landing gear integration with the wing.

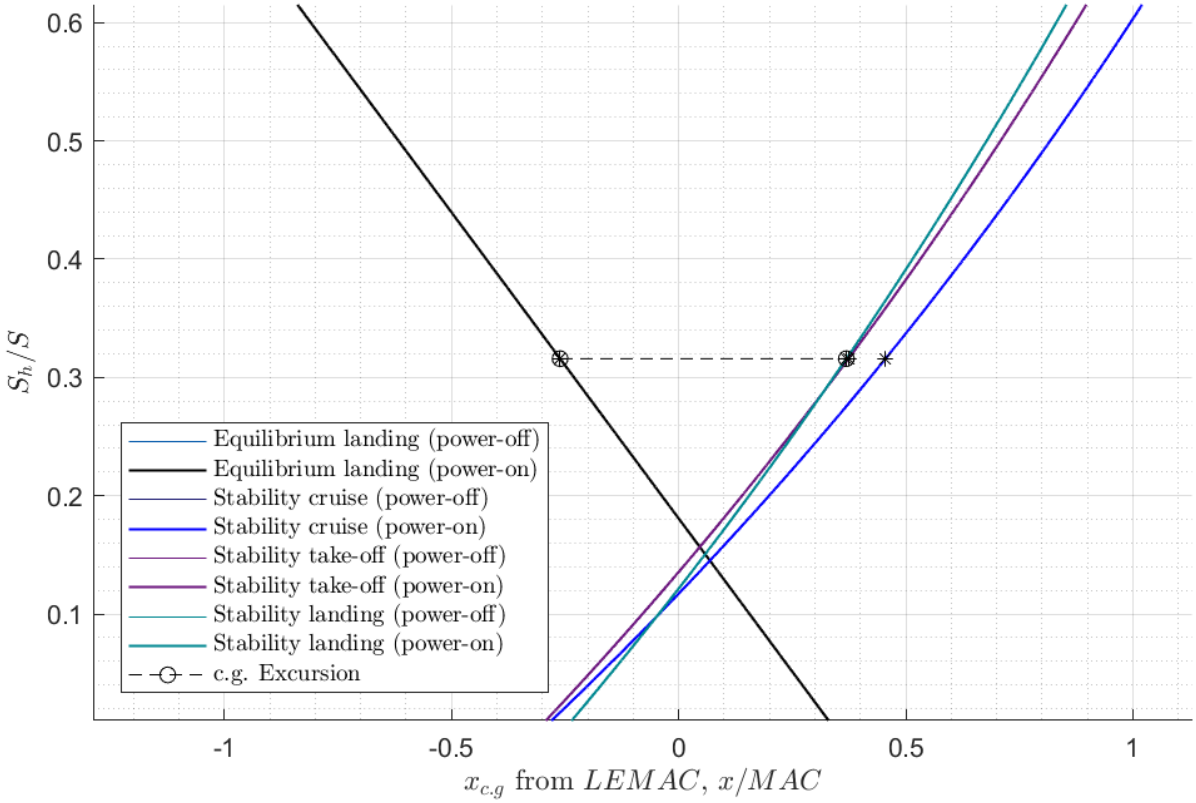

Figure 4.7: Final scissor plot, showing the CG excursion and the smallest corresponding tail size

4.3.3. Drag Considerations

Although the plot matching technique ensures that the smallest possible tail can be designed and used, it is important to consider the effect of this on overall aircraft performance. The smallest horizontal tail would indeed minimize the zero-lift drag (C_{D_0}), which is desirable. However, the corresponding wing position on the fuselage may not be ideally placed with respect to the CG; creating the need for some persistent corrective pitching moment- leading to a trim drag penalty.

Without taking this into account during the design phase, the aircraft might perform poorly in the mission analysis, despite potential improvements in its zero-lift drag. The target scenario in design cruise would be one in which the lift from the foreplane and wing maintains level flight while also producing zero net pitching moment. Hence, the tail would not need to produce any lift or downforce; eliminating

unnecessary induced drag and trim drag. Of course, this cannot be maintained throughout cruise, as the fuel is consumed and the CG continuously shifts- necessitating trim from the tail. This fact notwithstanding, reaching the target scenario at some point between top-of-climb and mid-cruise is expected to result in lower block fuel consumption, and a more efficient aircraft overall.

In order to balance the aircraft without the tail, there are several design variables that could be used- mainly controlling the moment arm or lift of the foreplane or wing. A selection must be made on how to best tackle the issue in the most efficient way.

- **Wing Position:**
  By shifting the location of the main wing, the moment arm of the wing's lift could be tailored to produce a net zero pitching moment. However, the wing is already positioned for the smallest tail, and any deviation from this position would necessitate a larger tail- making this an undesirable option.
- **Wing Airfoil:**
  As seen in flying wings and BWBs, the airfoil could be shaped to produce the required pitching moment and trim the aircraft at a chosen design point. Here too, however, the airfoil is already selected for optimal L/D; and changing it would be an ill-advised compromise.
- **Foreplane Position:**
  The foreplane's position is effectively linked to its moment arm with respect to the aircraft's CG, and hence could be used to trim the aircraft. The disadvantage here is that bringing the foreplane closer to the wing increases the interaction effects, reducing combined lift efficiency. Further, the aircraft's nose presents an upper limit for the arm length, restricting the trimming capabilities of this technique.
- **Foreplane Size:**
  Even though the foreplane area ratio is currently prescribed by the user, it could conceivably be modified to provide the amount of lift needed to trim the aircraft. Since the foreplane size could influence the wing sizing process and have far reaching implications on aircraft performance, a separate sensitivity analysis will be conducted to study this variable.
- **Foreplane Incidence Angle:**
  Similar to the previous case, this too effectively dictates the lift of the foreplane, and could be tuned to meet the pitching moment requirements at the design point. Compared to all other options, the incidence angle was deemed the most appropriate design variable to help reduce the trim drag of the aircraft.

A foreplane optimization module is created and activated after each tail sizing exercise in the Initiator. This module utilizes AVL to perform a sweep of foreplane incidence angles, runs the complete aircraft in cruise conditions, and selects the case resulting in the least amount of total induced drag. The results of this configuration also have the least magnitude of downforce produced by the tail- consistent with the hypothesis presented earlier.

While this workflow identifies the best foreplane incidence angle from an aerodynamic perspective, it ignores the structural implications. The lift produced by the foreplane influences the stresses in the fuselage; thus affecting its structural sizing- and impacting the weight of the aircraft. Thus, in order to truly capture the effect of the foreplane incidence on aircraft performance, another sensitivity analysis is carried out and presented in chapter 6.

The final aspect of drag prediction to be addressed is the calculation of the zero-lift drag itself. The Initiator employs empirical relations to estimate the zero-lift drag of individual (external) parts of the aircraft. The wetted area of these components is used in these empirical relations, and the overall aircraft drag is built up through these component-wise estimations. However, for the wing and foreplane; a non-negligible portion of their wetted area is actually buried within the fuselage. Therefore, for these two components specifically- a modified wetted area calculation is made to capture only what is exposed, as illustrated in figure 4.8. Of course, this also applies to the wing of other configurations.

In calculations involving lift and induced drag however, the planform areas of these surfaces include the embedded regions as well. This is standard practice, and in line with the conventions regardless of the

configuration at hand. Thus, a realistic estimate for the parasitic drag is obtained without compromising the overall aerodynamic performance estimations.

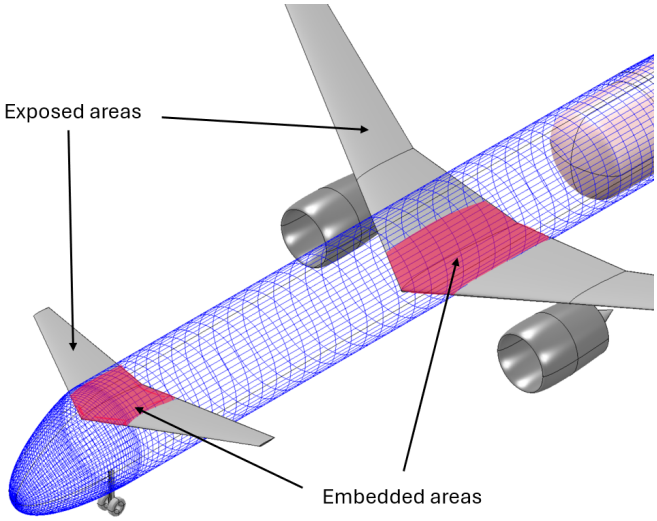

Figure 4.8: Illustration of wetted area modification for the foreplane and wing

4.4. Top Tank Configuration

As previously explained in chapter 3, the top tank configuration places the cryogenic tank outside and above the fuselage of the aircraft. With this design, several changes are made with regard to the drag model, structural sizing routines, and vertical tail sizing.

4.4.1. Tank and Fuselage Design

The tank model itself remains virtually unchanged in this configuration. It is positioned right above the middle of the cabin, with no gap between the bottom of the tank and the top of the fuselage. Two pairs of support struts are conceptualized to either side of the contact line near the front and back of the tank. Through this design, the tank can be isolated from the longitudinal bending strains of the fuselage, while still allowing for linear loads to be transferred. Thus, the tank sizing is still carried out while only considering hydrostatic and pressure loads, and does not need to handle bending loads transferred from the fuselage.

For the structural sizing of the fuselage, the tank is accounted for in the mass distribution, which allows for the additional loads to be captured in the 2.5g pull-up manoeuvre analysis. The fuselage structure will then be appropriately strengthened to manage the additional mass above it. The mass of the support struts and tank fairings are not explicitly calculated due to the lack of data and hence is estimated based on Brewer's findings [14]. The total support and fairing mass is added as 2% of the tank + fuel mass, which implicitly assumes a linear relation between the tank mass and the support mass. Despite the non-integral nature of the current configuration, the position of the tank close to the wing may result in an efficient and lightweight fuselage structure, and will be investigated in chapter 6.

4.4.2. Drag modelling

The placement of the tank outside the fuselage greatly impacts the overall drag of the aircraft. In order to minimize base drag, interference drag, and friction drag, a fairing is added in the regions between the tank and the fuselage. The additional drag due to the tank/fairings are calculated and added in the fuselage drag module, for bookkeeping purposes. In order to reduce complexity, the fairing is not explicitly modelled as a geometry component but rather, its effect is taken into account in the wetted area calculation.

A simple, yet robust geometry based approach is adopted to calculated the net additional wetted area of the fuselage. For the entire length of the tank, the fairing is assumed to be a rectangle tangential

to both the tank and the fuselage, and present on either side of the aircraft, as shown in figure 4.10. The exposed part of the tank above the fairings is also accounted for, while the surface of the fuselage now covered by the tank and fairing, is subtracted. This is because it no longer contributes to the outer wetted area, which is what is relevant for zero-lift drag calculations. Figure 4.9 shows the cross-sectional view of the areas in question.

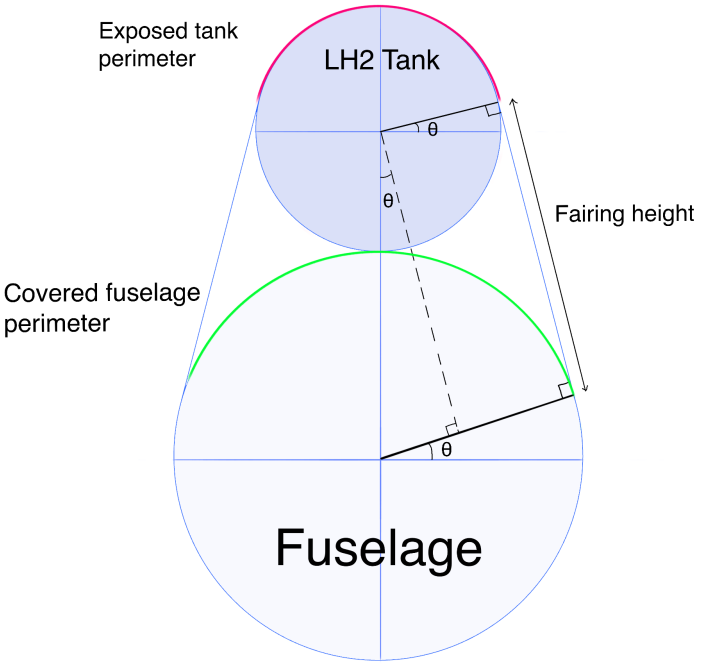

Figure 4.9: Illustration of the cross-sectional view of the tank and fuselage

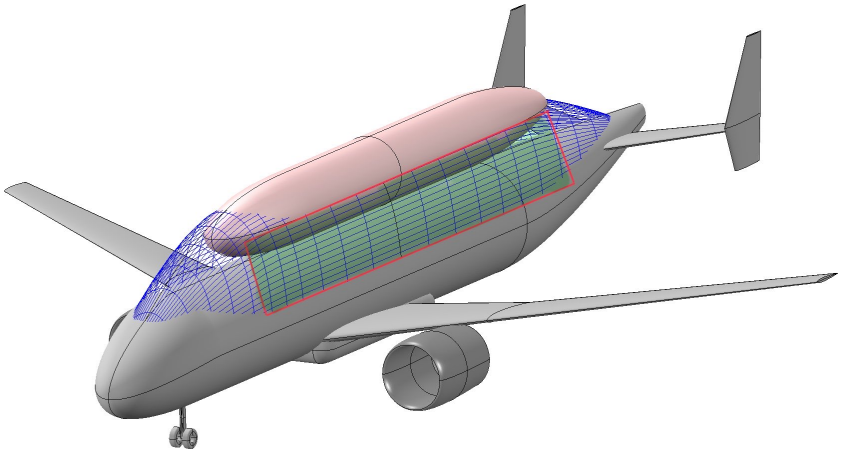

Figure 4.10: The fairing envisioned in blue around the tank. The rectangular section of the fairing on the sides of the tank is highlighted in green.

The front and rear parts of the fairing are complex, three-dimensional surfaces. Given the difficulty in calculating the exact wetted area contributions of these sections, the increase in each end due to these parts is approximated as two times the frontal area of the tank ($S_{\text{faring, end}}$). Equation 4.7 summarizes the wetted area calculation employed for this configuration, while equations 4.4, 4.5 and 4.6 provide relations for the terms used in the main equation.

$$h_{fairing} = \sqrt{(R_{\text{fuse}} + R_{\text{tank}})^2 - (R_{\text{fuse}} - R_{\text{tank}})^2} \tag{4.4}$$

$$\theta = \arcsin(\frac{R_{\text{fuse}} - R_{\text{tank}}}{R_{\text{fuse}} + R_{\text{tank}}}) \tag{4.5}$$

$$\epsilon = \frac{\pi - 2\theta}{2\pi} \tag{4.6}$$

$$S_{\text{wet, total}} = S_{\text{wet, fuse}} + 2\pi R_{\text{tank}} \epsilon l_{\text{tank}} + 2h_{\text{fairing}} l_{\text{tank}} - 2\pi R_{\text{fuse}} \epsilon l_{\text{tank}} + 2S_{\text{faring, end}} \tag{4.7}$$

The new wetted area of the ”reshaped” fuselage is given by $S_{\text{wet, total}}$ while the outer radius and length of the tank are represented by R_{tank} and l_{tank} respectively. The height of the fairing (from figure 4.9 is denoted by h_{fairing}, and θ is its tilt angle. Through this, the perimeter split ratio, ϵ is found. Finally, the term $S_{\text{wet, fuse}}$ is the wetted area of the isolated fuselage, which is computed through its mesh in the Initiator.

In addition to modifying the wetted area of the fuselage, another effect must be taken into account within the fuselage drag module. The effective fineness ratio of the fuselage is impacted by the bulky tank above it- a factor that plays a role in base drag, fuselage lift-induced drag, and zero lift drag. A new equivalent diameter of the fuselage is calculated from a circle of the same area as the total frontal area of the cross section from figure 4.8. This equivalent diameter divided by the length of the fuselage yields the fineness ratio. No special considerations are taken for the non-circularity of the current fuselage, and it is assumed that the same empirical relations with modified input values will produce sufficient accuracy in all drag calculations.

While the top tank configuration greatly reduces the longitudinal CG excursion over a mission, the vertical CG excursion increases due to the tank’s position. However, this effect is not expected to alter the dynamic trim requirements or mission performance significantly; and is not taken into account by the Initiator.

4.4.3. Vertical Tail Sizing

The presence of the bulky tank above the fuselage has another major impact on the design of the aircraft. The increased ”side” area of the aircraft necessitates a larger vertical tail to ensure sufficient directional stability and control. The aerodynamic center of the fuselage is typically forward of the CG, and the large side area produces a proportionally large side force that the vertical tail needs to contend with.

The Initiator does not have a stable directional stability module available, and hence it is decided to adopt a direct empirical approach. The Airbus BelugaXL has a similarly large fuselage for oversized cargo, and was based on the Airbus A330-200. In the conversion process, the vertical tail was heavily modified due to the larger fuselage; and this data is used to develop the vertical tail sizing process for the top tank configuration.

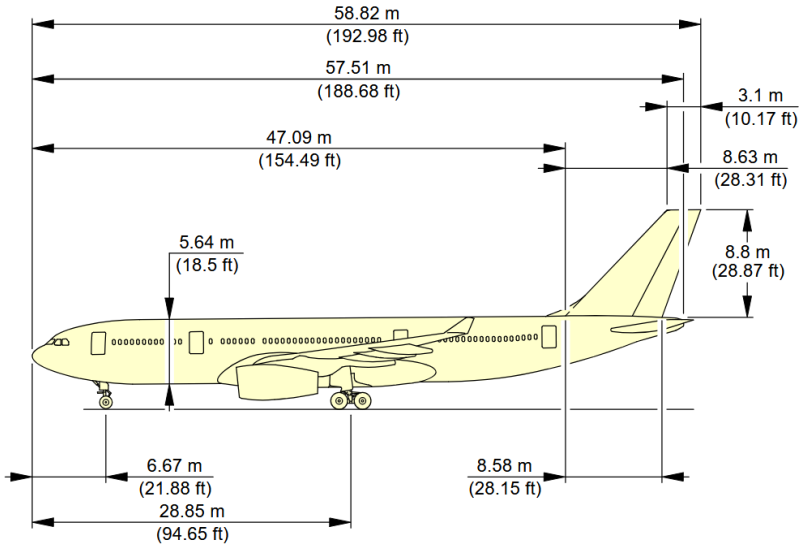

Figure 4.11: A330-200 aircraft dimensions [8]

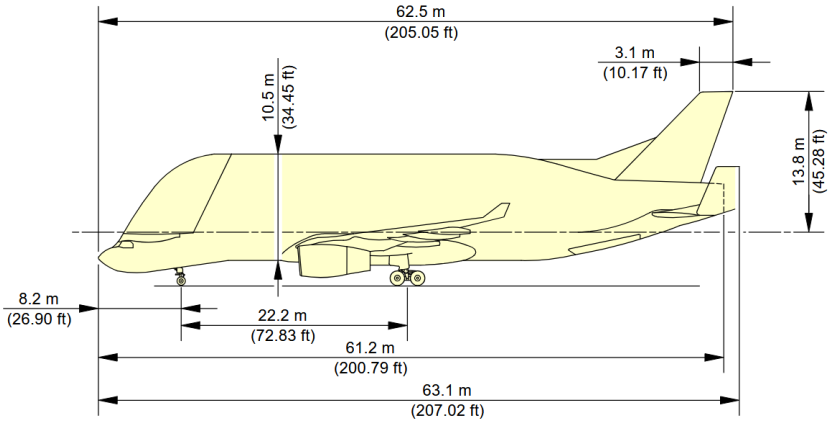

Figure 4.12: BelugaXL aircraft dimensions [7]

While the initial concept for the current configuration used an H-tail, concerns with roll clearance at high angles of attack swayed the decision to use a triple tail, as with the BelugaXL. This tail layout has a primary vertical tail with two additional secondary vertical tails attached to the ends of the horizontal tail. This attachment method has the potential to design a smaller horizontal tail due to the endplate effect, but is neglected in this study to maintain a conservative approach.

For both the BelugaXL and A330-200, the projected side area of the fuselage is estimated based on the provided dimensions. The tailcone is excluded from the area. Similarly, the total vertical tail planform is calculated for both aircraft. The proposed methodology for sizing the top tank aircraft's vertical tail is to use a relative increase in the total vertical tail size, based on the relative increase in fuselage side area, from the addition of the tank and fairing. Equation 4.8 represents this mathematically, where the constant (0.1304) is derived by taking the ratio of the difference in tail size to the difference in fuselage side area from the conversion.

$$S_{\text{VT, TT}} = 0.1304 \times (S_{\text{fuse, tank}} - S_{\text{fuse, notank}}) + S_{\text{VT, original}} \tag{4.8}$$

The terms $S_{\text{VT, TT}}$ and $S_{\text{fuse, tank}}$ are the total vertical tail area and fuselage side area, respectively, of the aircraft with the tank; while $S_{\text{fuse, notank}}$ and $S_{\text{VT, original}}$ are the respective areas for the aircraft without a

tank or triple tail. The new total vertical tail area, $S_{\text{VT, TT}}$, is then distributed between the three fins in the same ratio as the BelugaXL does with its tail. Thus, all primary concerns and modelling aspects of the top tank configuration are addressed. Figure 4.13 shows a top tank configuration designed through the Initiator, with all methods implemented as discussed.

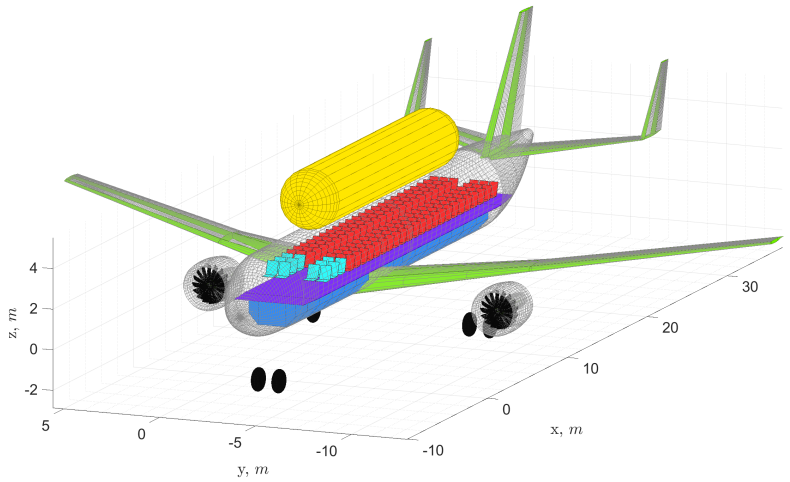

Figure 4.13: Top tank configuration from the Initiator

4.5. Operational Limits

The large CG excursion with aft tank layouts and the performance penalties arising from this have been well established at this point. An alternative solution to tackling this problem can be found through imposing operational limits on the aircraft, and integrating these limits into the design process. Figure 4.14 shows the loading diagram, or the CG-shift diagram of an aircraft without operational limits. The x-axis represents the relative position of the CG, and the y-axis shows the overall aircraft mass. Beginning at the bottom of the graph, the red curves snaking upwards denotes the passenger loading, up till 67.5t. Since there are two ways of loading passengers for each column (back to front or front to back), two curves are drawn on the graph, both leading to the same final CG location. Similarly, from 67.5t to 75t the cargo loading is show. Finally, the fuel loading on the aircraft pushes the total mass to 81t, and shifts the overall CG aft due to the location of the fuel relative to the rest of the aircraft. The complete red path represents the harmonic mission scenario.

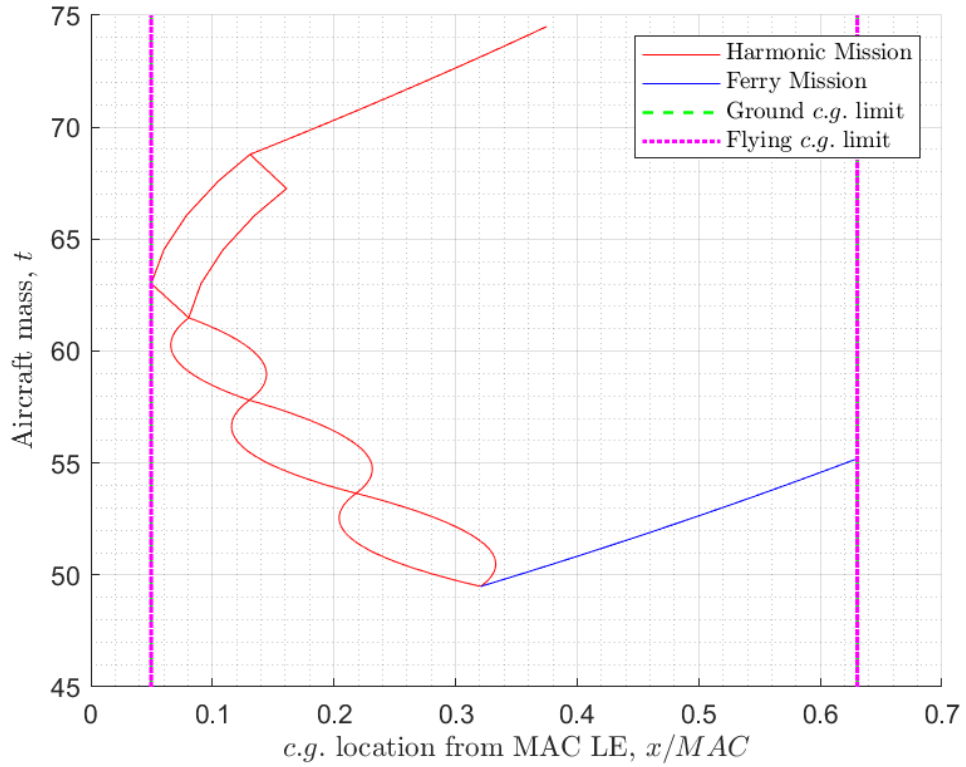

Figure 4.14: Loading diagram with no operational limits. The overall CG excursion here is 58% of the MAC

The blue line on the other hand, represents the ferry mission- where the aircraft carries no payload and only fuel. In this configuration, the CG of the aircraft is extremely aft as no payload exists to balance the fuel's mass at the back of the aircraft. The extreme forward and aft limits taken from both these missions forms the CG limits that the aircraft is designed to satisfy. Recalling the impact of the CG limits on horizontal tail sizing from section 4.3, it is clear that meeting ferry flight requirements oversizes the tail for the harmonic mission. Figure 4.15 shows the loading diagram of an aircraft designed with operational limits activated.

4.5.1. Impact on Off-Design Missions

By imposing operational limits on the CG shift used in tail sizing, a much smaller tail could be designed while still retaining sufficient stability and controllability for the harmonic mission. For ferry missions and off-design payload conditions however, the operational strategy in the air and on the ground, would have to change.

Any CG position within the flying CG limits would allow safe flight and operations on the ground without problems. If an off-design payload mission is going to be flown, performance calculations have to be made to ensure that the position of the cargo and/or passengers is such that the aircraft's CG remains within limits. For the ferry mission, ballast would have to be placed in the front of the aircraft, keeping it within the flying limits. This would, of course, impact the range of the ferry mission; but is often not a major concern for airlines. The range for off-design payload missions would also be impacted, but to a lesser extent.

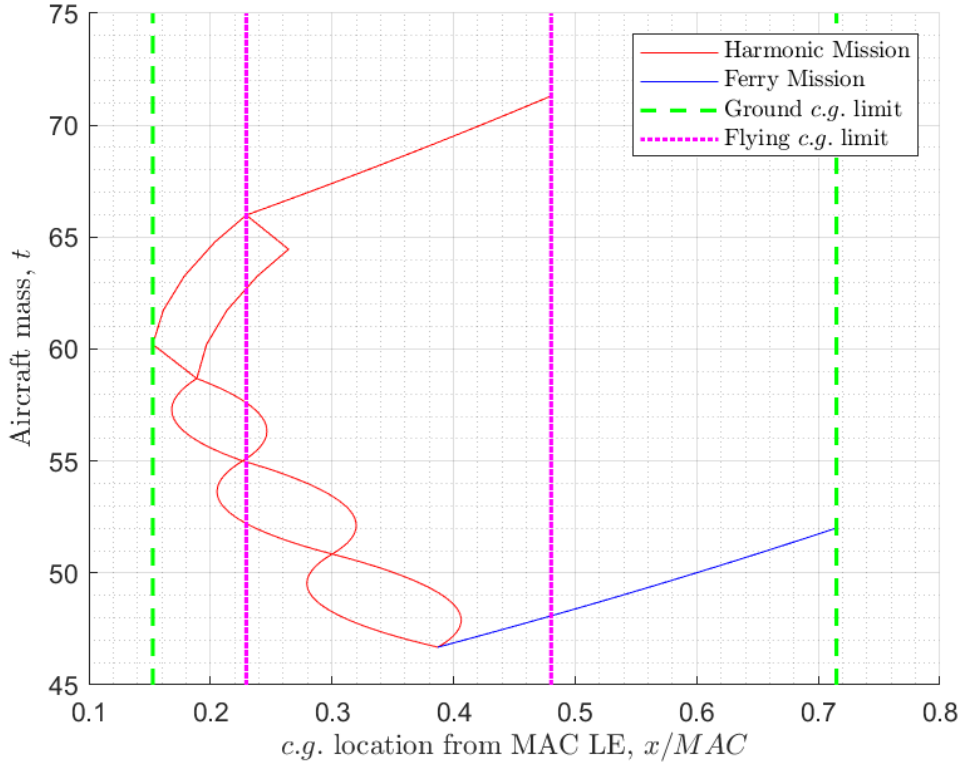

Figure 4.15: Loading diagram with operational limits, resulting in flying CG excursion of 25% of the MAC, which is less than half of the original excursion.

To quantify the degree of operational modifications needed, a simplified analysis is carried out on the ferry mission, which faces the largest change. In order to push the aircraft's CG back within the flying limits at the start of the ferry mission, it is found that a 3t ballast mass (placed at the front of the cabin) would be needed. This ballast would also push the empty aircraft's CG in front of the forward limit imposed by the tail- endangering the end of the ferry mission. In order to prevent this, 1.5t out of the 6t of the fuel must remain in the tank to ensure the CG stays within safe limits. This, combined with the ballast mass, would reduce the actual range of the ferry mission but is not explicitly calculated in this study. For off-design payloads, the required ballast and fuel restrictions reduce as the CG excursion naturally shifts to a favourable window. Furthermore, the placement of cargo could be strategically done to reduce the required ballast by a larger extent.

The ballast itself could presumably be served by a pair of large water tanks placed at the front of the cabin and hold, taking up $3m^3$ of space to keep sufficient volume. This could replace typical water tanks on aircraft kept in the cargo deck, with a capacity of 200kg of water. On design missions, these tanks could be filled only to the required level (200kg), while ferry missions would utilize the full capacity of 3 tons. This could have a small impact on turnaround times when swapping between ferry and design missions, as a large amount of water would have to be filled or drained by ground tankers. However, this is not expected to be a major concern as larger volumes of fuel are routinely filled within limited time-frames. Assuming these two processing can be carried out in parallel, there would be no penalty on the turnaround time.

Alternatively, a ballast mass of 2.6t could be placed on either side of the nose landing gear, as lead blocks occupying a combined volume of $0.2m^3$, and connecting to the front bulkhead for load transfer. This option occupies less space and is more structurally efficient than the water tank option, but increases complexity in installing/removing it, based on the mission to be flown. Due to these reasons, this option is not preferred and the water tank method is chosen.

4.5.2. Ground Operations

So far, the discussion has covered the changes needed to safely fly an aircraft designed with operational limits. However, even ground manoeuvring and other ground operations requires attention, depending on the design input for the landing gear. For example, if the landing gear design uses the same CG limits as the in-flight limits, the loading procedures must ensure that at no point does the CG breach the aft limit, and tip the aircraft back. If loading procedures cannot ensure this due to scheduling constraints with fuel/cargo/passengers, a tail support strut could be used to prevent ground tip-over, as seen in figure 4.16. Of course, the CG must be returned to safe limits before the tail support strut can be removed and taxiing can begin- which may necessitate the use of ballast again- for off design missions.

Alternatively, if the landing gear is designed for the complete CG range, the aircraft would have more ground operational flexibility, but a special landing gear configuration would almost certainly be necessary. Fuselage-mounted landing gears (figure 4.17) or wing-podded landing landing gears (figure 4.18) are potential solutions, but each of them have drawbacks in terms of inefficient load paths or reduced max lift coefficients. In either case, the drag significantly increases even when the landing gear is fully retracted. Hence, when operational limits are activated in the Initiator, the landing gear design uses the same CG limits as those used in tail-sizing, potentially improving landing gear integration, while sacrificing some operational flexibility. It is important to note that the Initiator does not actually model the landing gear mechanism or fairings, but simply provides the position of the wheels; informing the designer of possible integration and impact.

Figure 4.16: Tail support jack for flexible loading procedures [47]

Figure 4.17: Boeing C-17, showing the large fairings needed to house the main landing gears [43]

Figure 4.18: Tupolov 104, designed with podded wing-mounted landing gears [38]

5

Validation

5.1. Introduction to the Chapter

This chapter conducts an exercise in validating the aircraft design tool and verifying its results. Section 5.2 contrasts the baseline kerosene aircraft with the selected reference aircraft, and analyses the degree of similarity and differences. The calibration process is briefly explained, and some key performance metrics are discussed. Then, section 5.3 briefly compares LH2 aircraft configurations from the current study with similar proposals from the literature.

5.2. Comparison with Reference Kerosene Aircraft

In order to ensure the results and findings of the study holds value, the design tool must be appropriately verified. To accomplish this, the Initiator is used to size and design an aircraft based on the reference aircraft, whose results will then be compared with the real-life aircraft's performance metrics. The reference aircraft selected here is the Airbus A320neo, weight version 55 (WV0055) with a single auxiliary center tank.

Top-level aircraft requirements from this aircraft, along with basic performance parameters were used to create an input file in the Initiator. A 2-class, 150 passenger cabin configuration is selected, while the harmonic payload, range, and other parameters are obtained through the A320 airport planning manual [6]. In order to expand the overall design space knowledge, most parameters are kept consistent with the study conducted by Onorato et al. [33], which uses the same design tool. The primary inputs are summarized in table 5.1, and a complete input file example is provided in appendix A.

As previously explained, the final convergence loop of the Initiator utilizes an FEM-based weight estimation for the fuselage and main wing. A correction factor is used in the input to better match the predicted aircraft weights to reality, and this is then kept fixed when transitioning to LH2 configurations. The cruise TSFC is given a similar treatment, but is reduced by a factor of 2.80 for LH2 aircraft to account for the change in energy density. This implicitly assumes that the engine efficiency is identical between JA1 and LH2 fuels, in terms of energy consumption per unit thrust.

Parameter	Value
Harmonic payload (t)	19.3
Number of passengers	150 (2 classes)
Mass per passenger (kg)	80
Harmonic Range (km)	4560
Cruise Mach number	0.78
Cruise altitude (m)	11278
Take-off distance (m)	2040
Approach speed (m/s)	67.7
$C_{L_{\text{max}}}$ take-off	2.45
$C_{L_{\text{max}}}$ landing	2.95
Wing aspect ratio	10.5
Diversion range (km)	370
Loiter endurance (min)	30
TSFC (kg/Ns)	1.388e-5

Table 5.1: Top-level aircraft requirements and performance parameters used as inputs for designing the aircraft

The aircraft designed by the Initiator from the A320neo is henceforth known as the ADI320neo. Table 5.2 compares the primary design parameters of the two aircraft, and reiterates the strength of the tool, established through past studies [19], [23], [15], [33]. The operative empty mass (OEM) is overpredicted slightly, while the harmonic fuel mass is underestimated by a similar amount. The maximum take-off mass (MTOM) shows good correlation as a side effect of this. The take-off wing loading and thrust loading also show close results compared to the reference, which are important parameters that guide the aircraft from the early sizing stages. The reference wing area also bears close similarity with the reference aircraft, as the MTOM and wing loading dictate this parameter. The tail area ratio is slightly overestimated by the Initiator, but requires a lot of scrutiny. The tail sizing methodology explained in chapter 4 involves numerous assumptions and simplifications with regards to the dynamic pressure ratio, lift slope, and maximum lift coefficient. Furthermore, it does not take into account aircraft family-based tail sizing, which could influence tail sizing significantly, as explored by Manzano [27].

Parameter	A320neo	ADI 320neo
OEM (t)	45	45.2
MTOM (t)	79.0	79.0
MZFM (t)	64.3	64.5
MLM (t)	67.4	68.5
Max. fuel mass (t)	21.0	21.1
Harmonic fuel mass (t)	14.7	14.5
Wing loading (N/m^2)	6321	6310
Thrust to weight ratio (-)	0.312	0.309
S (m^2)	122.6	122.8
S_{h}/S	0.25	0.26
L/D_{max}	-	17.6

Table 5.2: A320neo design parameters compared with the ADI320neo results from the Initiator

Figure 5.1 compares their payload-range diagrams, and illustrates the increasing discrepancy in range as the payload is reduced. The harmonic point is defined by the TLARs and hence is the same for both aircraft. The ferry mission represents the maximum range achieved with maximum fuel and zero payload, while the ”kink” mission, often termed the design point, is the mission run with maximum fuel

and the most payload within the MTOM cap. The result indicates that the ADI320neo overpredicts drag, which leads to higher fuel consumption; and is magnified as the range and fuel fraction rises. This is seen in the shortfall of range in the kink and ferry mission compared to the A320neo. However, priority is given for higher correlation at the harmonic point, as this is closer to typical operations and offers more relevant data, especially for LH2 aircraft. Kerosene aircraft have the luxury of installing fuel tanks whose volume is oversized for the design mission, as there is practically zero penalties and offers more operational flexibility. An LH2 aircraft cannot afford to have a tank oversized for it's design mission, as the tank increased mass would pose a large penalty. As a result of this, the payload range diagram for LH2 airplanes does not contain a kink- leading to the prioritization of higher accuracy at the harmonic point in this validation exercise.

Figure 5.2 shows the top view of the ADI320neo generated by the Initiator, illustrating the major components and their architecture. The purple section represents the cabin floor, with business and economy seats represented by blue and red. The cargo hold is also modelled, with a gap present for the pass-through wing and gear stowage. Although the selected variant has one auxiliary center fuel tank, this is not explicitly modelled, and merely accounted for as additional fuel volume in the wings.

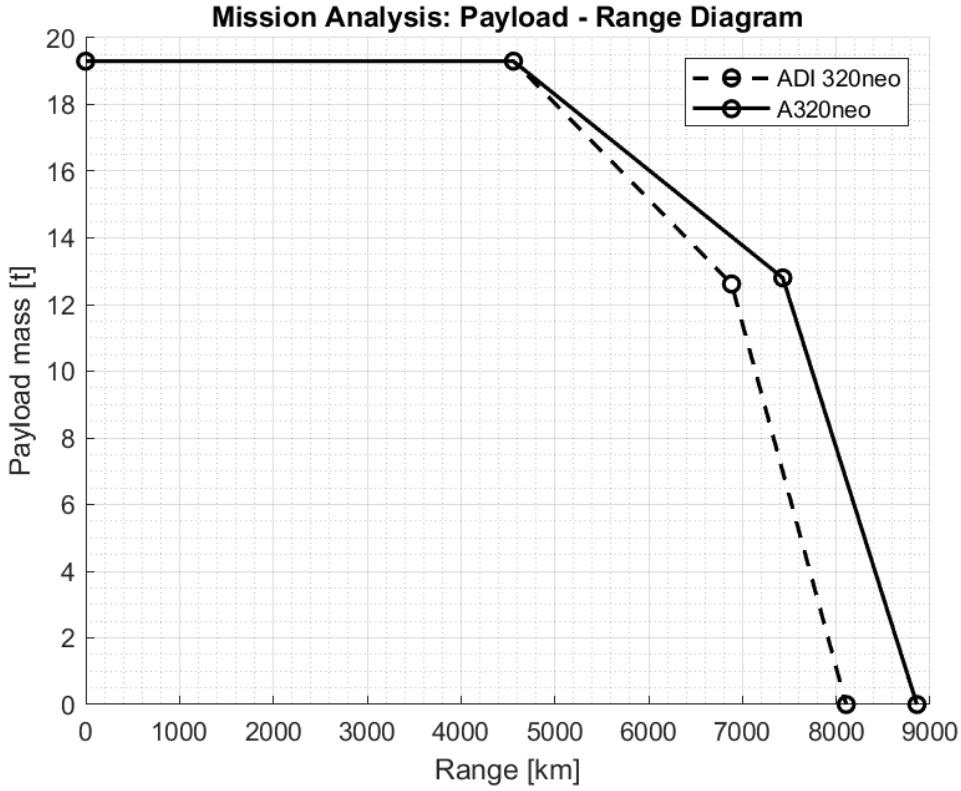

Figure 5.1: Payload-range diagram comparison of the Initiator's aircraft and the A320neo

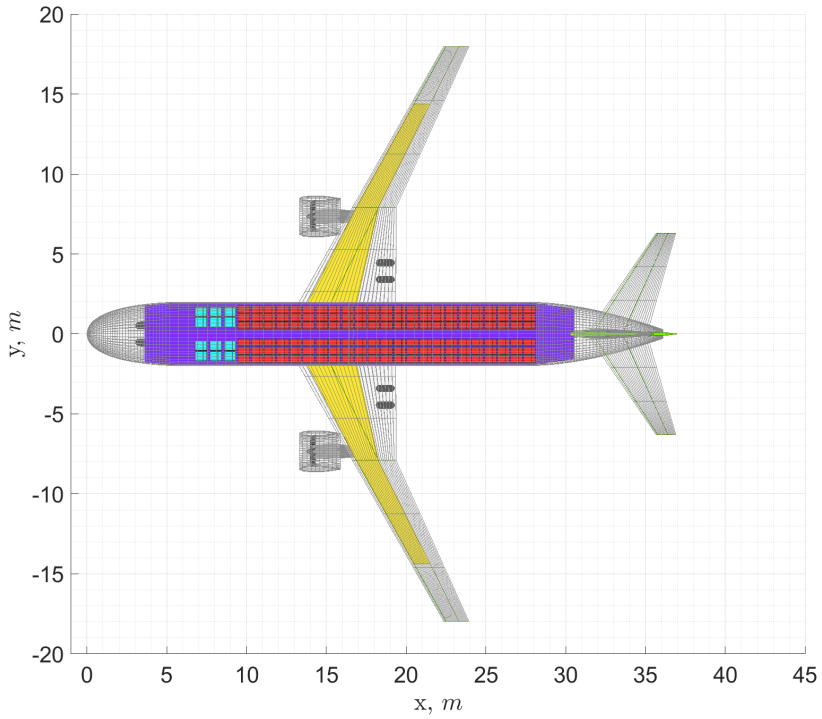

Figure 5.2: ADI320neo aircraft geometry, illustrating the fuel (yellow), cabin (purple), and other major components

5.3. Comparison with Similar LH2 concepts

Liquid hydrogen-based aircraft configurations are designed using the Initiator- which has been validated for kerosene aircraft- but not for LH2 designs. In order to build confidence with LH2 configurations and results, the preliminary designs are compared with proposals from the literature. While each configuration could be designed based on its literary counterpart's top level requirements, the differences in technology level assumptions, baseline aircraft, and fidelity levels, make for an imbalanced comparison. Hence, a decision is made to retain the same top-level requirements as presented, and analyze the relative change in design/performance parameters from each respective baseline aircraft. This change forms an indicator of the tank integration effects on the aircraft level, and is hence a useful parameter for judging the Initiator's LH2 aircraft design capabilities.

Tables 5.3 and 5.4 contrast the results by Silberhorn et al. [39] and the current study for aft tank and top tank layouts, respectively. The design range is significantly smaller in the current study, while the design payload is slightly larger, and the technology levels assumed are also very different. This immediately skews the comparison, and makes direct comparisons of parameters such as fuel mass or MTOM impractical. For the aft tank configuration, the relative change in operative empty mass; fuselage mass (m_{fuse}); and block energy consumption shows fairly good correlation, albeit slightly underestimating all three factors. The increased fuselage mass and OEM is primarily due to the extension needed to support the cryogenic tank, while the block energy consumption rises due to the increased weight and drag of the aircraft.

For the top tank configuration, the trends for relative change in OEM and energy consumption from baseline aircraft, diverge further between the two studies. The current study predicts a smaller increase in OEM and energy consumption compared to Silberhorn et al., despite having a larger maximum take-off mass and a lower aspect ratio wing. A detailed look at this configuration's results and its characteristics will be taken in the next chapter.

Parameter	Rear-integrated concept, Silberhorn et al. [39]	2SA-LH2-Aft
Design range (km)	6600	4560
Design payload (t)	17.5	19.3
OEM/MTOM (-)	0.65	0.67
Aspect ratio (-)	11.9	10.5
Change in OEM from baseline	+11%	+11%
Change in m_{fuse} from baseline	+28%	+23%
Change in design block energy from baseline	+6.9%	+6.1%

Table 5.3: Aft tank configuration design and performance comparison with the current study and literature

Parameter	Top-integrated concept, Silberhorn et al. [39]	2SA-LH2-Top
Design range (km)	6600	4560
Design payload (t)	17.5	19.3
OEM/MTOM (-)	0.64	0.65
Aspect ratio (-)	12.2	10.5
Change in OEM from baseline	+6.4%	+3.1%
Change in design block energy from baseline	+6.9%	+2.3%

Table 5.4: Top tank configuration design and performance comparison with the current study and literature

For the three-surface aircraft, the preliminary results are compared with the design proposed in the FlyZero project [3]. It is important to note that the foreplane is conceptualized as an active, controllable lifting surface which aids in trim drag reduction, whereas the current study employs a simpler, fixed foreplane, with flaps linked to the main wing. This difference in mechanism could be a large factor for the high discrepancy in relative change in energy consumption between the two studies, as seen in table 5.5.

Parameter	Narrowbody 3-surface concept [4]	3SA-LH2-Aft
Design range (km)	4445	4560
Design payload (t)	18.8	19.3
OEM/MTOM (-)	0.68	0.65
Aspect ratio (-)	13	10.5
Change in OEM from baseline	+15%	+4%
Change in l_{fuse} from baseline	+19%	+22%
Change in design block energy from baseline	-3.6%	+5.7%

Table 5.5: Three-surface configuration design and performance comparison with the current study and literature

The design range and payload are much closer here than the previous configurations' comparison, and the predicted MTOM and empty weight ratios remain similar between FlyZero and the current study. However, there is a large difference in the relative increase of empty weight between the two studies, alongside the aforementioned block energy consumption. Besides the use of the foreplane as an active control surface, the use of an NLF fuselage is the primary difference between the two concepts, and

could be a large contributing factor to the reduction in energy consumption compared to the baseline kerosene aircraft in the FlyZero study. Appendix B compares the geometry of the two aircraft, and highlights significant differences in foreplane size, tail size, and wing position. It is unknown what procedure was followed to enable the aft placement of the wing despite a small foreplane, or if relaxed stability requirements were utilized to size a small horizontal tailplane for the FlyZero concept.

Nonetheless, the methodology and modelling for the three-surface aircraft explained in chapter 4 are considered sufficiently accurate, albeit adopting a conservative approach for some key assumptions in the sizing/design process. The presented configurations are hence compared with similar concepts in literature, and will now taken forward for a balanced and fair assessment in chapter 6. The dual, forward-aft tank configuration remains very similar to the design presented by Onorato et al.[33] and hence, it was not deemed necessary to conduct another verification exercise for it.

6

Results and Discussions

6.1. Introduction to the Chapter

This chapter presents the results of the study, using the methodology described in chapter 4 and the calibrated parameters found in chapter 5. The studies and results for individual configurations are critically analyzed, and the best designs within each configuration are selected as a representative for a final, comprehensive comparison to identify the optimal configuration for the integration of hydrogen fuel. Section 6.2 investigates the design of the three-surface aircraft and its variations, while section 6.3 identifies the best top tank design, and section 6.4 does the same for the dual forward-aft tank configuration. The conventional aft tank configuration is treated as the baseline aircraft in all cases. Next, section 6.5 examines the effect of engine placement and operational limits on aircraft design and performance for all aft tank layouts. Finally, section 6.6 conducts the final comparison of the best of each configuration and draws key conclusions regarding the research questions.

All the results discussed henceforth are based on designs that used the following TLARs and configuration parameters (table 6.1), unless specified otherwise. The basic requirements themselves remain the same as for the kerosene aircraft, with additions specific to the use of hydrogen as a fuel.

Parameter	Value
Harmonic payload (t)	19.3
Number of passengers	150 (2 classes)
Mass per passenger (kg)	80
Harmonic Range (km)	4560
Cruise Mach number	0.78
Cruise altitude (m)	11278
Take-off distance (m)	2040
Approach speed (m/s)	67.7
$C_{L_{\text{max}}}$ take-off	2.45
$C_{L_{\text{max}}}$ landing	2.95
Wing aspect ratio	10.5
Diversion range (km)	370
Loiter endurance (min)	30
TSFC (kg/Ns)	0.496e-5
P_{vent} (kPa)	250

Table 6.1: Top-level aircraft requirements and performance parameters used as inputs for designing the aircraft

6.2. Three-Surface Aircraft

6.2.1. Design and Aerodynamics

As previously explained, the three-surface aircraft (3SA-LH2-Aft) employs a lifting foreplane to continuously provide a small portion of the total required lift. From a purely aerodynamic perspective, a single, high aspect ratio (AR) wing produces a moderate amount of drag to provide a given amount of lift. With the addition of a foreplane, the same lift is now split between an efficient high-AR wing and less efficient low-AR foreplane, which increases the combined induced drag. Furthermore, interaction effects between these lifting surfaces reduce the net aerodynamic efficiency; making the 3SA configuration an unsuitable choice from the perspective of aerodynamic point performance. As explained however, it has the potential to reduce overall aircraft drag through better landing gear integration and improve the mission-level performance by better tackling the large CG excursion.

The primary input design variables considered in this study are the foreplane area ratio (S_{FP}/S) and the foreplane incidence angle. The aspect ratio of the foreplane is fixed at 6, and the main wing's aspect ratio remains at 10.5, which is in line with the baseline kerosene aircraft. While increasing the foreplane's AR could improve performance, a larger value is not considered due to possible structural limitations and airbridge connection difficulties. It is also important to note that the effective aspect ratio of the foreplane is smaller than indicated from the planform, due to being partially buried in the fuselage- which is accounted for in the stability estimation model. To understand the effect of the foreplane area ratio, the two extreme values of 0.1 and 0.2 are compared. Figure 6.1 shows the top views of these two variants generated by the Initiator, and figure 6.2 shows the corresponding scissor plots of the two aircraft.

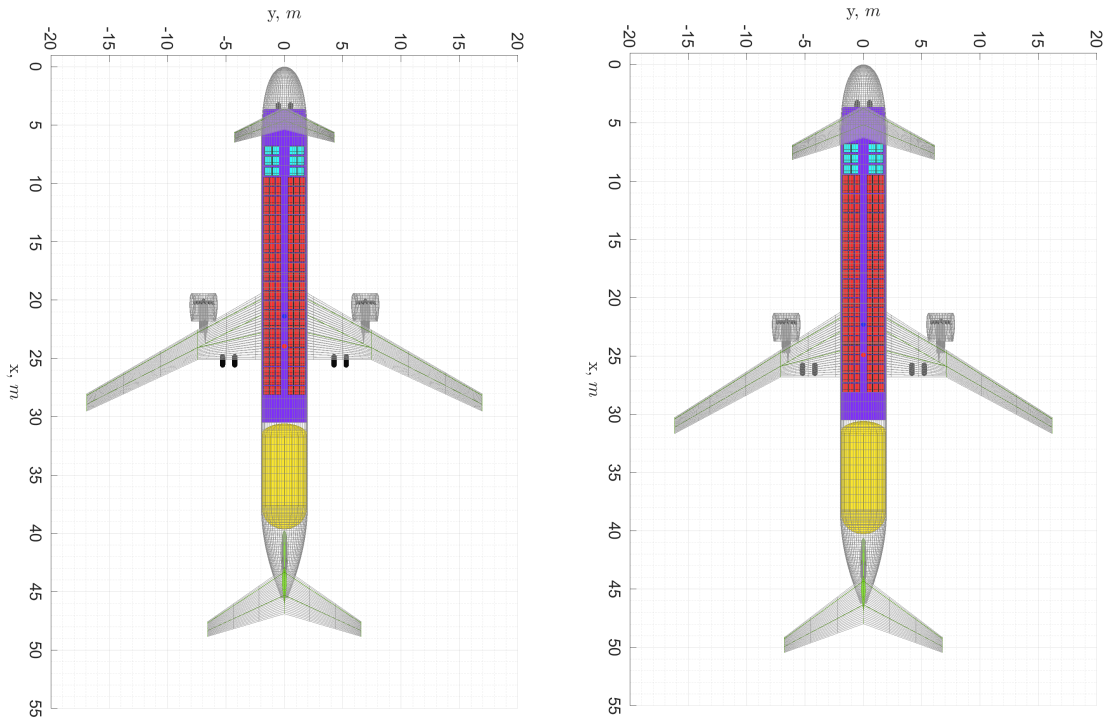

(a) Foreplane incidence = 2°, $S_{\text{FP}}/S = 0.1$ $L/D_{midcruise} = 16$

(b) Foreplane incidence = 2°, $S_{\text{FP}}/S = 0.2$ $L/D_{midcruise} = 15$

Figure 6.1: The three-surface aircraft viewed from above, showing the effect of foreplane size on wing apex positioning and tail sizing

The larger foreplane forces the stability limits further forward to maintain the same static margin of 5% MAC, while also relaxing the forward CG limit for equilibrium during landing. The resulting constraints push the main wing further aft for obtaining the minimum tail area -which critically- can make conventional main landing gear integration possible. Unfortunately, the larger foreplane and smaller wing also increase the net induced drag, as a larger share of the lift is now bourne by the less efficient

foreplane- which increases the fuel consumption. As a consequence of this, a longer fuel tank (and longer fuselage) is needed, which increases the empty weight of the aircraft in addition to exacerbating the CG excursion problem. Both these changes increase the drag on the aircraft, causing a snowball effect that yields a larger tail and worse performance for the aircraft with $S_{FP}/S = 0.2$. Another potential contributing factor to the relatively large difference in the lift-to-drag ratio between the designs is the trim drag in cruise. The main wing is positioned to minimize the tail area (and zero-lift drag as a result), which does not necessarily coincide with the position for minimum trim drag. This highlights the reason for conducting a foreplane incidence sweep, which is another parameter that can reduce the magnitude of the tail-off moment in cruise.

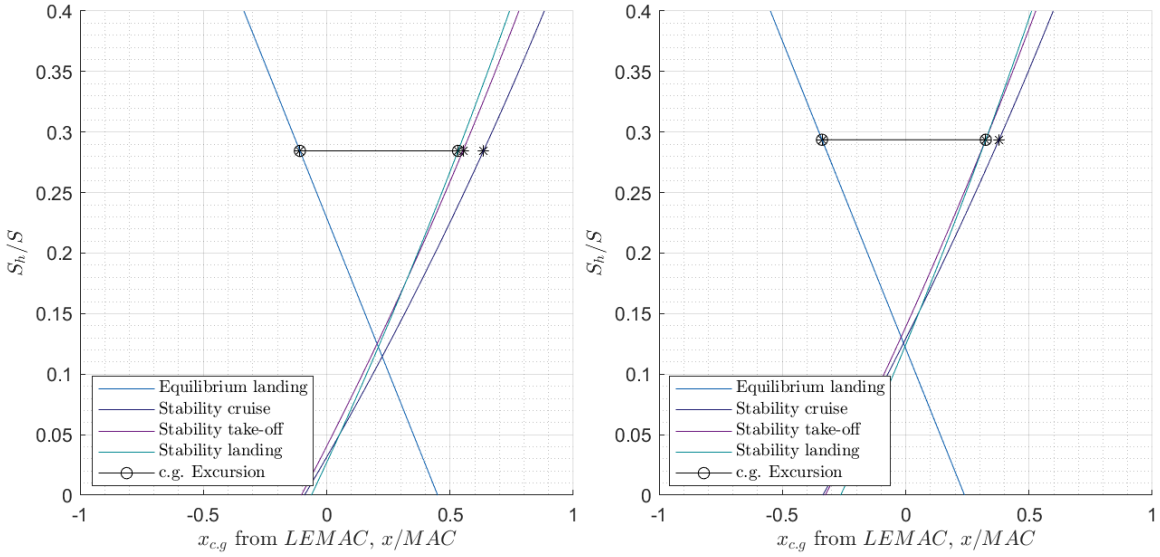

(a) $S_{FP}/S = 0.1$, resulting tail area ratio = 0.28
$\Delta(x/\bar{c})_{cg} = 0.64$

(b) $S_{FP}/S = 0.2$, resulting tail area ratio = 0.29
$\Delta(x/\bar{c})_{cg} = 0.66$

Figure 6.2: The scissor plots for tail sizing, showing the relative shift in the wing position and CG range through varying the foreplane size

6.2.2. Structural Implications

From a structural perspective, the presence of the foreplane changes the load distribution on the aircraft- reducing the lift near the middle of the fuselage and increasing the lift near the nose of the aircraft. Figure 6.3 shows the distribution of the bending moment across the fuselage for different foreplane incidence angles, obtained through a 1D beam model in the 1g flight condition. Each kink is a result of the lift transferred from the foreplane/wing/tail to the fuselage, which along with the weight distribution, produces the bending moment distribution. From the figure, it is clear that the foreplane incidence angle has a significant influence on fuselage bending loads. By increasing the incidence from 0° to 4°, the peak bending moment is reduced by nearly half due to the alleviation offered by the foreplane.

This change to bending loads is important because the sizing of the fuselage's primary structure is conducted based on critical load cases, involving pressurization loads, lateral loads, and longitudinal bending loads. The 2.5g pull-up manoeuvre in the MTOM condition is selected as the critical case for longitudinal loads, based on certification requirements. In this case, shifting from a foreplane incidence of 0° to 2° resulted in a fuselage mass reduction of 16%, a large improvement that was aided by improved aerodynamic efficiency.

Figure 6.4 shows operative empty mass of the 3SA configuration for different foreplane design combinations. The variation of OEM is primarily dictated by the changes in mass of the horizontal tail and fuselage, as the combined mass of the foreplane and wing remains relatively constant. For foreplane area ratios of 0.1 and 0.15, a reduction in OEM is observed moving from an incidence of 0° to 2°, which only continues reducing for the smallest foreplane at 4°. For the two larger area ratios, the OEM increases at the highest incidence angle as the fuselage mass rises, despite a reduction in the peak bending load. This is because the average bending load increases from the high foreplane lift, as

an extreme form of load alleviation. It is expected that this behaviour will also occur for the smallest foreplane case, but at a larger incidence angle, due to the lower level of lift it can offer in the current range. Nevertheless, all design variations of the three-surface aircraft have a lighter OEM than the conventional, 2-surface configuration- primarily due to large savings in fuselage weight.

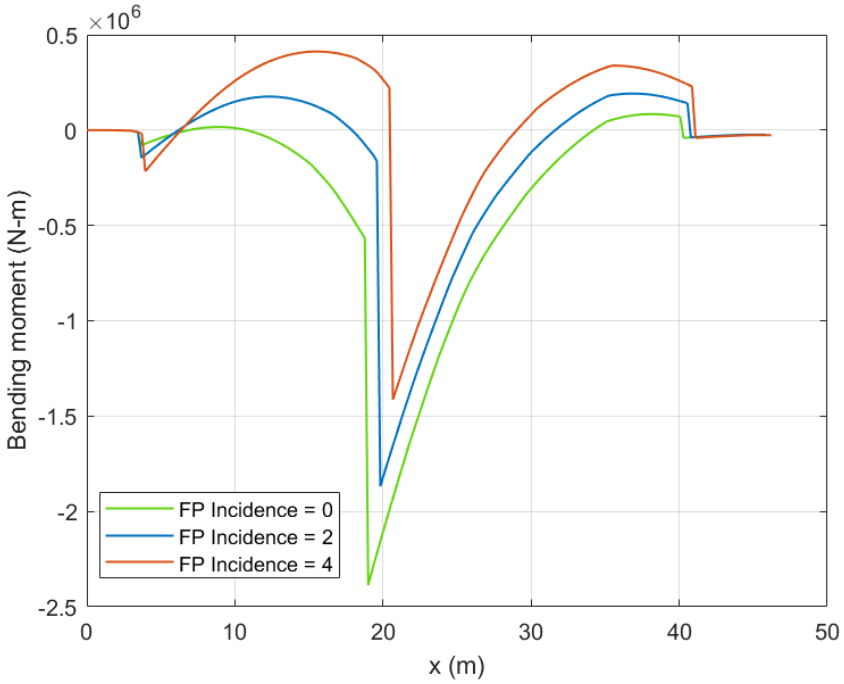

Figure 6.3: Fuselage bending moment distribution, $S_{FP}/S = 0.15$

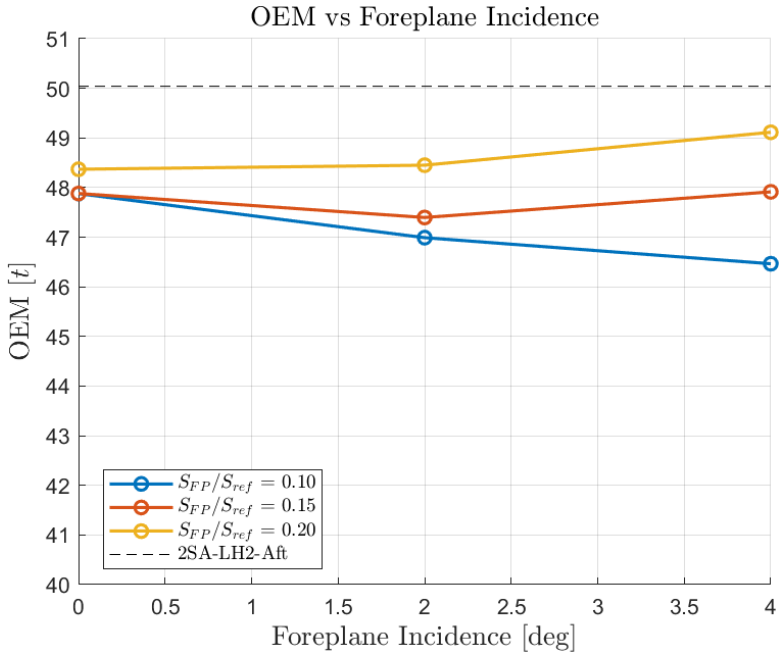

Figure 6.4: Operative empty weight as a function of the foreplance incidence angle

Despite the large reduction in OEM for the smallest foreplane when increasing the incidence angle,

other aspects of aircraft performance do not show similar improvements. Figure 6.5 shows a slight decrease in in the mid-cruise lift to drag ratio for all foreplane area ratios, as the incidence angle is increased. The mid-cruise point of the harmonic mission is often selected as a representative indicator of performance, as the evolution of weight and CG changes the performance over the mission. From the figure, it can be observed that L/D is much more sensitive to the foreplane area ratio than the foreplane's incidence angle, within the given ranges. This result appears to be consistent with the earlier discussion on higher net induced drag for larger foreplanes. The conventional, two-surface configuration could also be considered a special case of the 3SA configuration, with a foreplane area ratio of 0, and has the highest lift to drag ratio as well.

It is worth noting that the 3SA's zero lift drag and drag coefficient are 7.5% and 4% lower than the conventional, 2-surface configuration, as the lighter aircraft allows for a smaller reference area, and the tail can be sized smaller. Hence, the lower L/D ratio for the 3SA configuration is wholly due to its high induced drag.

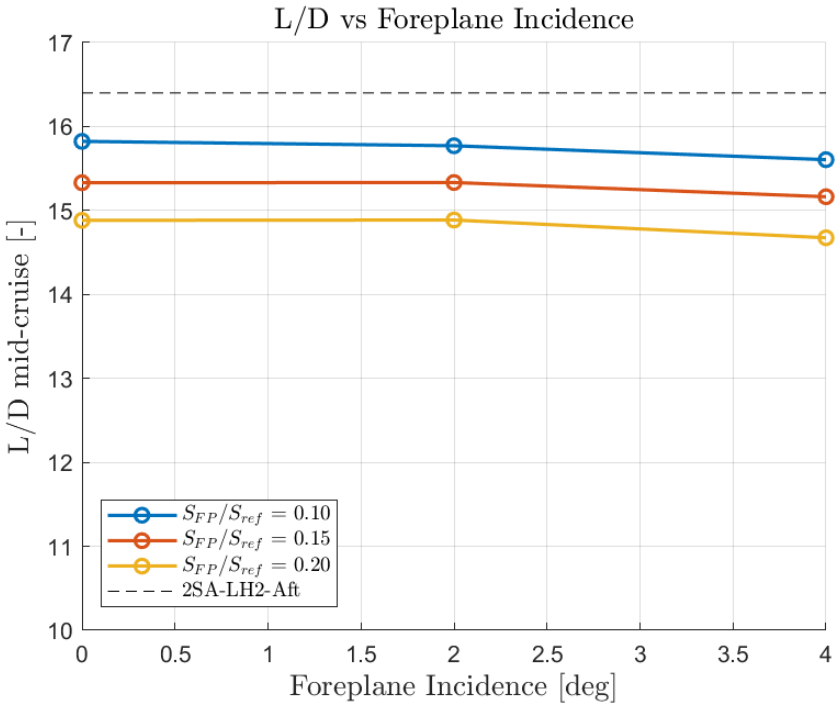

Figure 6.5: The L/D ratio of the aircraft mid-cruise, as a function of foreplane incidence angle

The current study considered the fuel consumption to be one of the most important figures of merit. This is one of the biggest drivers of operational costs, and minimizing this is obviously a key design objective. Figure 6.6 shows the variation of total harmonic fuel mass with the two foreplane design parameters. The results show that with foreplane area ratio of 0.1 and an incidence of 2°, the fuel consumption is a mere 0.6% lower than the baseline two-surface aircraft. For larger foreplane area ratios, the reduced glide ratio and increased OEM yields a higher fuel consumption, but with individual troughs at an incidence of 2°.

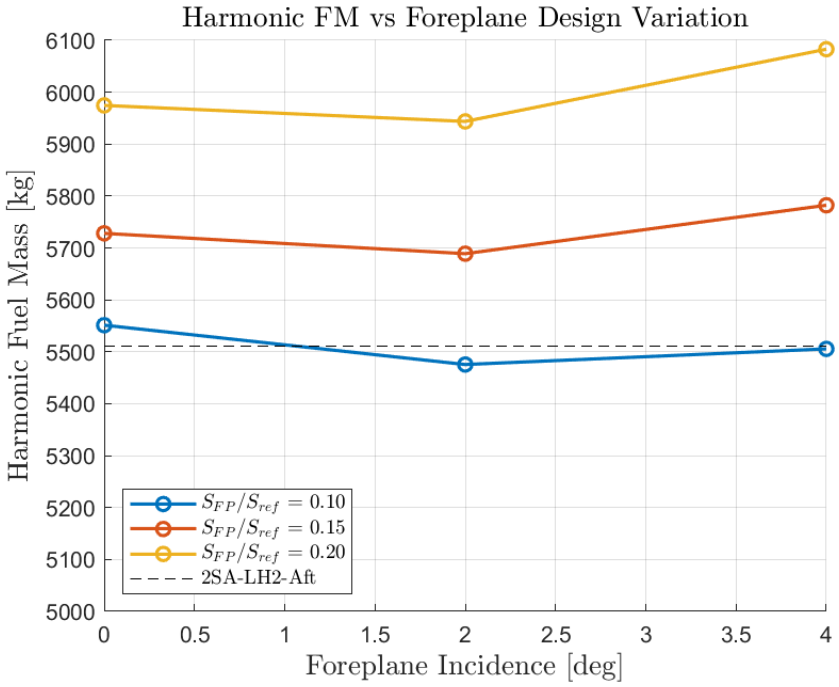

Figure 6.6: Fuel mass as a function of the foreplance incidence angle

Despite the smallest foreplane design displaying the lowest fuel consumption on paper, this design is not selected for the final comparison. One of the key goals of the 3SA configuration was simplify landing gear integration, and integration remains an arduous task with the smallest foreplane, as seen in figure 6.7 where the wheels are still halfway behind the trailing edge. The gear must connect with the rear spar of the wing for an efficient load path, or resort to fuselage mounted or wing podded gear configuration, explained in section 4.5. While some degree of rake on the main strut is often utilized as shown in figure 6.8, increasing this angle is not feasible without significant changes to make the struts stronger- which also would make it heavier. This means that all designs with unfavourable landing gear positions would have worse performance than indicated by the current preliminary design- as the drag and weight would increase regardless of the integration method selected. While it is not known how large of a penalty this would face, it is assumed to be larger than the alternative. Hence, the design with $S_{\text{FP}}/S = 0.15$ is selected to represent the three-surface configuration in the final comparison, as it offers conventional landing gear integration and moderate fuel consumption.

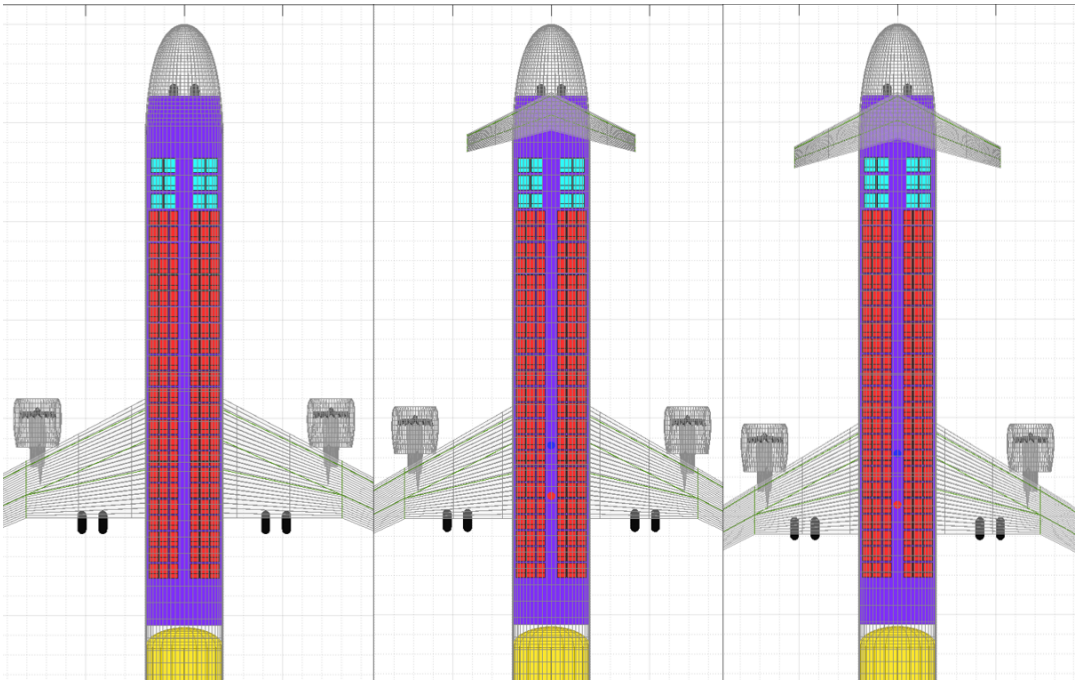

Figure 6.7: Main landing gear position relative to the wing, 2SA-LH2-Aft (left), $S_{FP}/S = 0.1$ (middle) vs $S_{\text{FP}}/S = 0.15$ (right)

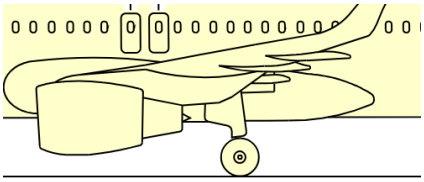

Figure 6.8: Landing gear strut with slight rake as seen on the A320neo [6]

6.2.3. Cruise Altitude Variation

Despite the three-surface configuration being substantially lighter than conventional configuration, as seen in figure 6.4, its lift to drag ratio and other performance parameters did not show similar improvements. Each aircraft has an optimal cruise altitude at which the ambient density enables minimal thrust requirement by matching the zero-lift drag and lift-induced drag. In order to investigate if the reason for the 3SA's poor L/D ratio and fuel consumption was even partly due to a suboptimal cruise altitude, a brief investigation is conducted into the effect of cruise altitude selection.

It is also worth noting that the altitude condition for minimum thrust required is not necessarily the condition that will result in minimum block fuel consumption. For instance, if the calculated altitude for minimum fuel consumption is very high, the fuel consumed to climb to that altitude may overshadow any savings made during the cruise itself. Thus, to simplify the investigation and avoid the complexity of mission trajectory optimization, a sweep of cruise altitudes is provided and an aircraft is designed for each case. Figure 6.9 shows the percentage change in OEM and fuel mass (FM) as the altitude is varied from the baseline value of 11,278m (37,000ft).

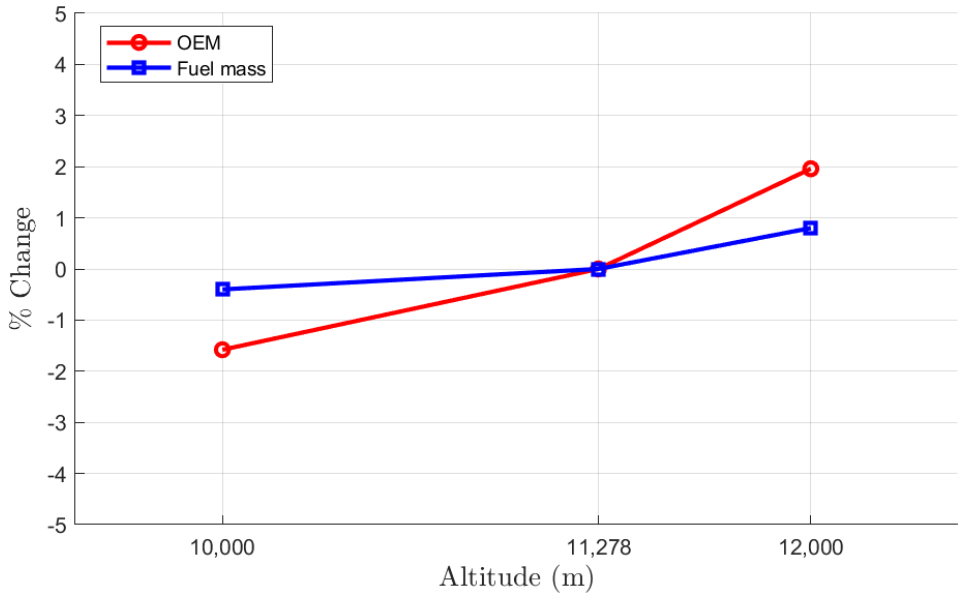

Figure 6.9: Effect of cruise altitude as a top-level requirement on design OEM and FM

The results indicate that there is minimal change in fuel mass (-0.4%) even for a large reduction in cruise altitude (-11%). Increasing the cruise altitude yields a stronger response, albeit still a small change in fuel mass. The operating empty mass appears to bear more sensitivity to the cruise altitude, and it was found that this was due to the sweep angle changing and affecting the wing mass as a result. The sweep angle changes because the cruise altitude changes the density, which changes the cruise lift coefficient- affecting the optimal sweep to avoid drag divergence at the given Mach number. Nonetheless, given these results for low fuel mass sensitivity to the cruise altitude, the altitude is kept constant for the 3SA, and consistent with all other configurations in the study.

6.3. Top Tank Configuration

The top tank configuration (2SA-LH2-Top) attempts to address the large CG excursion problem by placing the tank above the fuselage, close to the OEM CG. The minimized CG excursion allows for a smaller tail as well as a reduction in average trim drag, but potentially faces the penalty of increased fuselage drag. The x-position of the center of the tank is set to 45% of the fuselage length, close to the empty CG, which leaves the diameter of the tank as the main remaining design choice.

A shorter, wider tank is expected to offer higher gravimetric efficiency due to a smaller surface area to volume ratio while sacrificing aerodynamic performance. Alternatively, a slimmer, longer tank could mitigate the aerodynamic penalty at the cost of increased tank mass. Furthermore, the total vertical tail area is modelled as a function of the fuselage side area to ensure directional stability and control, and will have an impact on aircraft performance. Thus, to asses what design is most suitable at the aircraft-level, a design sweep of tank diameter ratio ($D_{\text{tank}}/D_{\text{fuse}}$) is conducted. The diameter of the isolated fuselage remains constant at 3.97m, in line with the reference aircraft. The lower limit of the sweep is set to 0.6 to ensure design convergence. Below this value, the tank's surface area grows drastically; necessitating very thick insulation which is no longer physically able to fit in the tank- making it an infeasible design.

In order to aid in the visualization of the trends in the results, the aircraft geometries are presented first in figure 6.10, displaying the effect of the diameter ratio on the tank length, with the fuselage directly beneath it. The figure also shows that the landing gear integration never becomes problematic, regardless of the diameter ratio. As previously explained, the tank fairing is not explicitly modelled and hence cannot be shown, but its effect on the drag and weight of the aircraft is accounted for in the sizing process.

The tail sizing trends are observed first. Figure 6.11 shows the variation of the horizontal and total

vertical tail area ratios with increasing tank diameter ratio, where the total vertical tail area is the sum of the central and secondary tails of the triple tail. The results show that the horizontal tail area remains practically constant, while the vertical tail size reduces with smaller tank diameters. This is because a slimmer tank has a larger planform area than a thicker tank of the same volume.

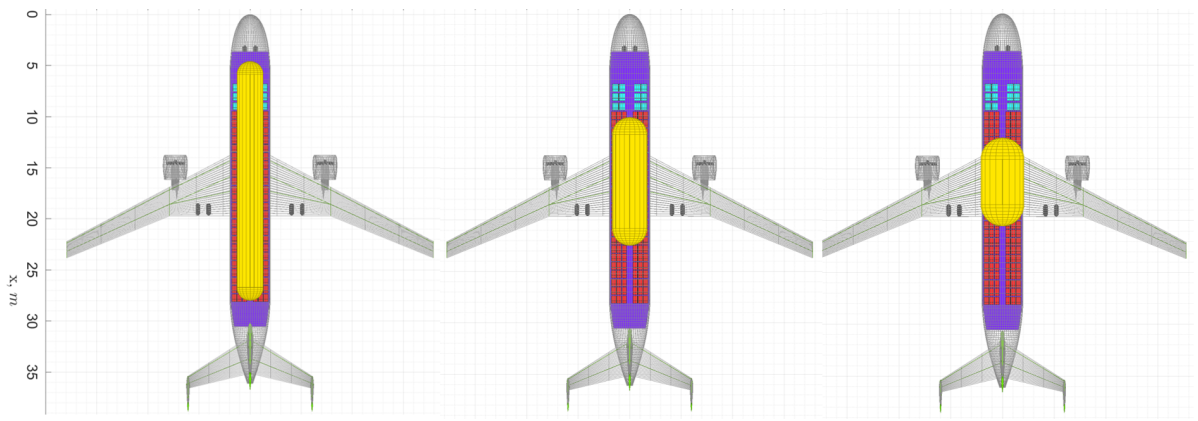

Figure 6.10: Some top tank configuration design variations. From left to right: D_{tank}/D_{fuse} = 0.65, D_{tank}/D_{fuse} = 0.85, and D_{tank}/D_{fuse} = 1.05

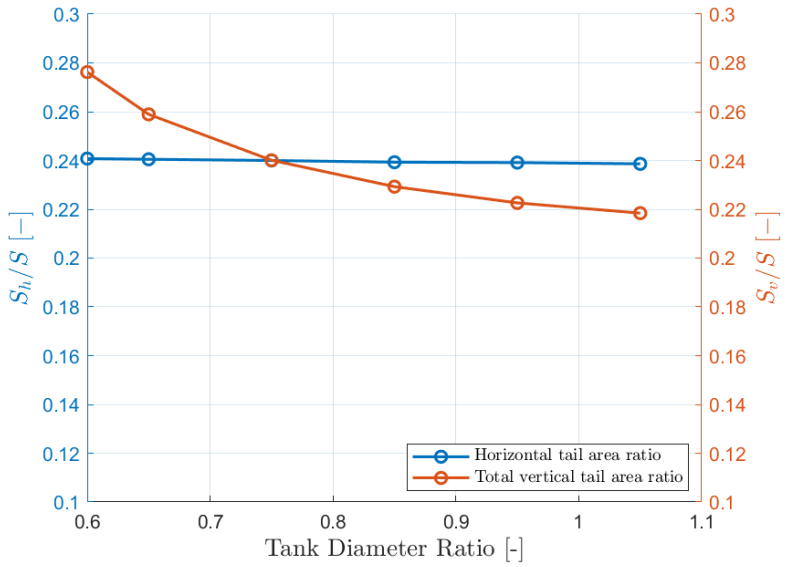

Figure 6.11: Effect of tank diameter ratio on horizontal and vertical tail design

Following logically, the trends in drag are now analyzed. Figure 6.12 presents the zero lift drag coefficient and total wetted area as a function of the tank diameter ratio. The change in wetted area is primarily driven by the tank/fairing area and vertical tail area, and a compounded effect is anticipated due to their linkage. The zero-lift drag coefficient is influenced by the wetted area ratio and the shape of the aircraft itself, and is seen to bear some sensitivity to the tank shape as a result. A low tank diameter ratio produces an effectively slender fuselage shape but with an increase in wetted area ratio; while a bulky tank trades some wetted area for increased pressure drag. The result indicates that C_{D_0} is lowest at a diameter ratio of 0.7, while the wetted area is minimized at a diameter ratio of 0.9.

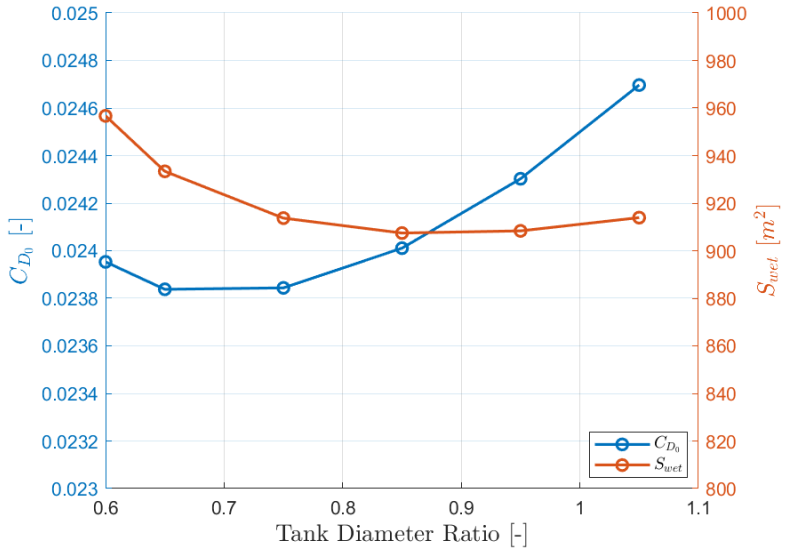

Figure 6.12: Effect of tank diameter ratio on zero-lift drag coefficient and total wetted area

The aircraft's performance is not solely governed by aerodynamics however, and hence the effect on weight is also an important consideration. As discussed, highly slender tanks are expected to have worse gravimetric efficiency and increase the empty weight- and this is exactly what is observed in figure 6.13. The two contours appear almost perfectly mirrored, indicating that the change in empty mass is primarily driven by tank mass and snowball effects. It can also be noted that the OEM plateaus as it approaches high tank diameter ratios, as the tank itself becomes closer to resembling a sphere- the shape with minimum surface area for a given volume.

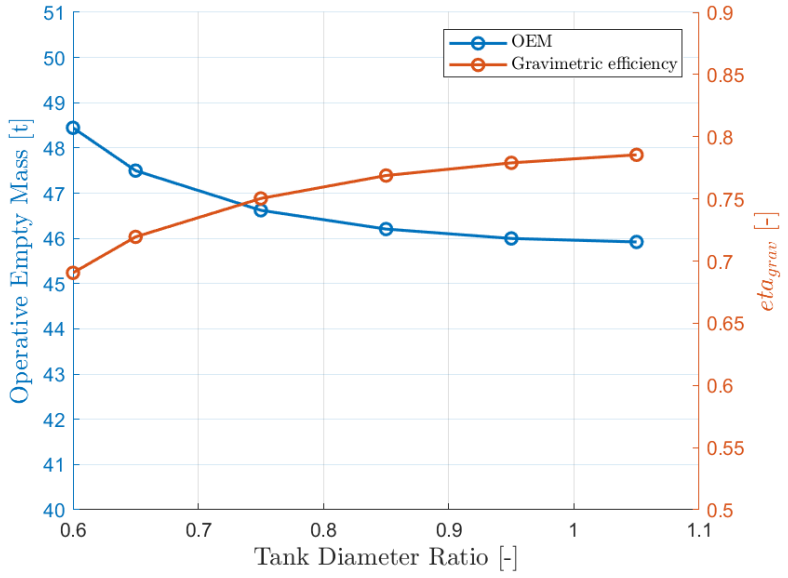

Figure 6.13: Effect of tank diameter ratio on OEM and tank gravimetric efficiency

These results have clearly established conflicting design objectives when it comes to selecting the best diameter ratio for improved aerodynamics or weight. As stated in the previous section, this study considers the block fuel consumption to be one of the most important figures of merit, and hence is studied now, alongside the mid-cruise lift to drag ratio. Figure 6.14 shows these results for aircraft designed with different tank diameter ratios. A diameter ratio of 0.8 is found to produce the minimum fuel consumption, which is significantly closer to the best design for drag and L/D (0.7) than the best design for weight (1.05); indicating that aerodynamic benefits dominate in this range. Nonetheless, the

design with minimum fuel consumption is selected to represent the top tank configuration in the final comparison.

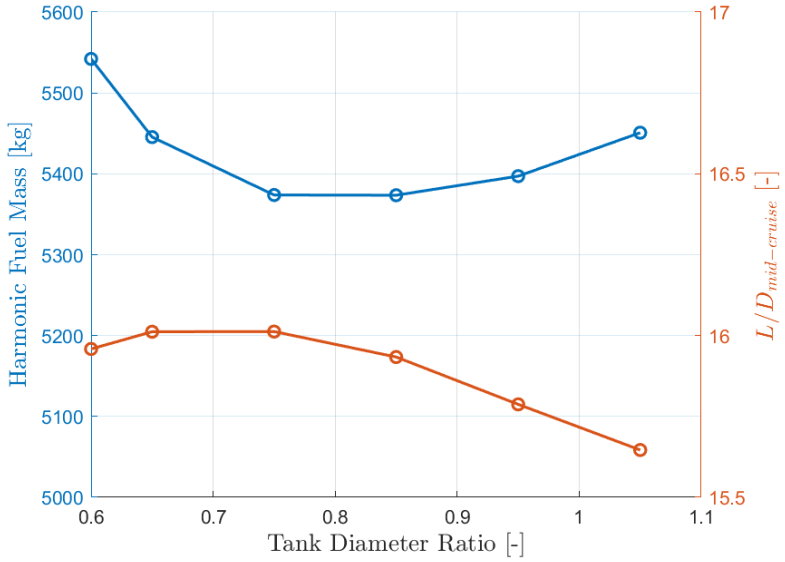

Figure 6.14: Effect of tank diameter ratio on fuel mass and mid-cruise glide ratio

6.4. Dual, Forward-Aft Tank Configuration

The aircraft configuration with dual, forward-aft tanks (2SA-LH2-FwdAft) is now investigated. Similar to the previous section, a primary input variable is selected and a design sweep is conducted to understand its effects on performance, and identify the optimal design. This concept splits the fuel into two separate tanks- one integral aft tank and one non-integral forward tank - to mitigate the CG excursion and its unfavourable effects. The aft tank is modelled in the same way as the other aft tank configurations, but the forward tank sits within the pressurized cabin, with a reduced radius and offset to one side. This is so that a cockpit-cabin connection is enabled, with the same width as the aisle in the cabin (0.6m).

The primary design variable selected is the fuel-split ratio between the forward and aft tank. If too much of the fuel is stored in the aft tank, the CG excursion increases, while increasing the fuel fraction of the forward tank increases weight due to its non-integral nature. Hence, a trade-off is expected in between these extremes. Again, to help visualize the effect of the fuel split on aircraft geometry, figure 6.15 is given below. Reducing the aft tank fuel fraction (AFF) results in non-insignificant increases to the overall aircraft length, as seen from the figure.

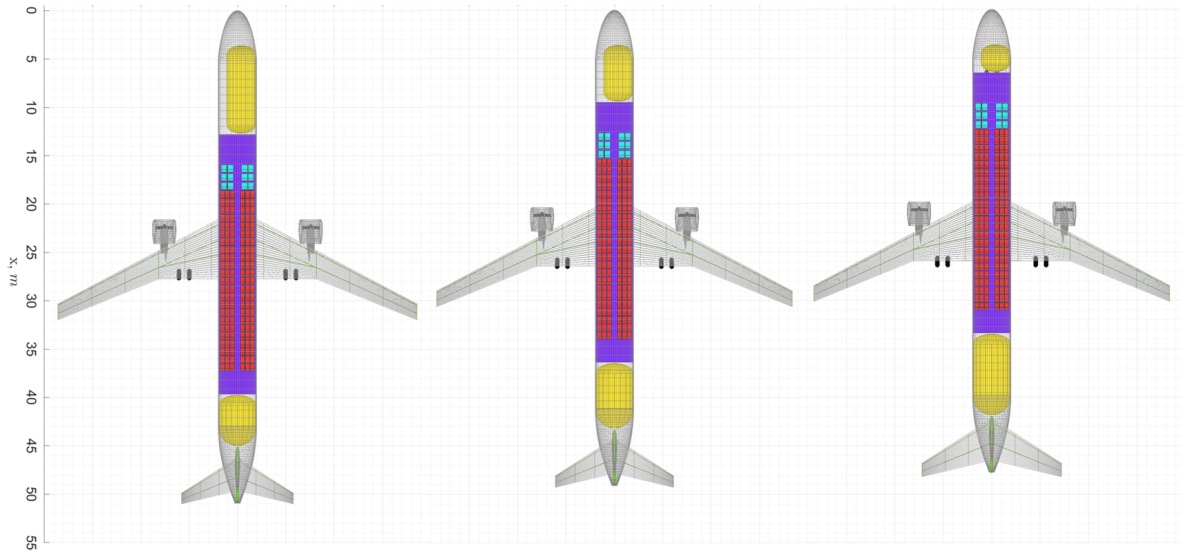

Figure 6.15: Some FwdAft tank configuration design variations. From left to right: aft tank fuel fraction (AFF) = 0.5, AFF = 0.7, and AFF = 0.9

The increased fuselage length also increases the moment arm for the horizontal tail, which can help counteract the rise in the CG excursion. Figure 6.16 shows the variation of the total CG excursion and the tail area ratio with different aft tank fuel fractions. The results show that an AFF of 0.6 can significantly reduce the overall CG excursion and the tail area ratio, and that these two parameters display high correlation with each other. Even though an AFF of 0.5 equally splits the fuel between the two tanks, their unequal diameters shifts the optimal condition to a slightly higher value. The total CG excursion cannot reach 0 at any point due to the loading variations of passengers and cargo, which always has a small contribution to the CG variance.

The effect of the fuel split ratio of individual tank performance and aircraft mass is investigated through figures 6.17 and 6.18. The results show that a high aft fuel fraction is favoured for the net gravimetric efficiency; which is logical given its higher diameter compared to the forward tank. The fuselage mass and length also reduce as AFF is increased, for the same reason. A large fuel fraction for the forward tank not only reduces the net gravimetric efficiency, but also causes a large increase in fuselage length to accommodate the thinner tank. The effect on OEM plateaus beyond AFF = 0.7 because at this point, the horizontal tail size and mass become larger and counteract the fuselage mass reductions.

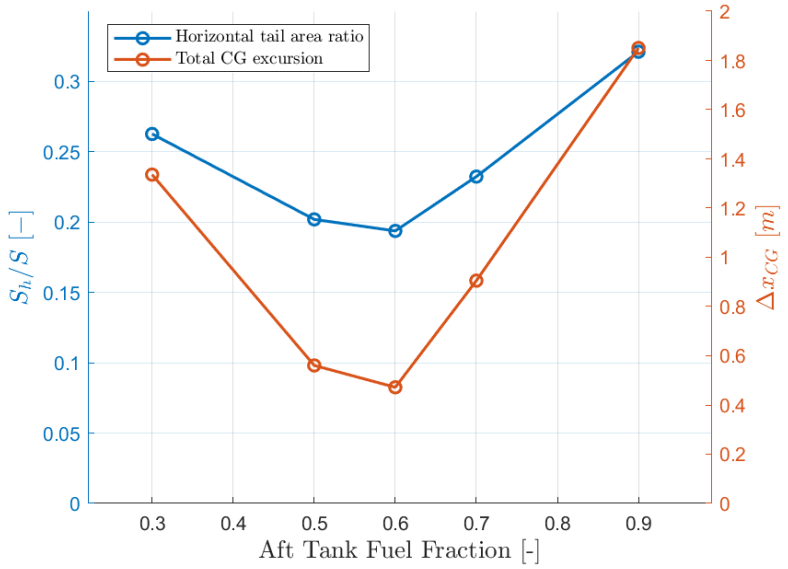

Figure 6.16: Effect of AFF on the magnitude of the total CG excursion and horizontal tail size

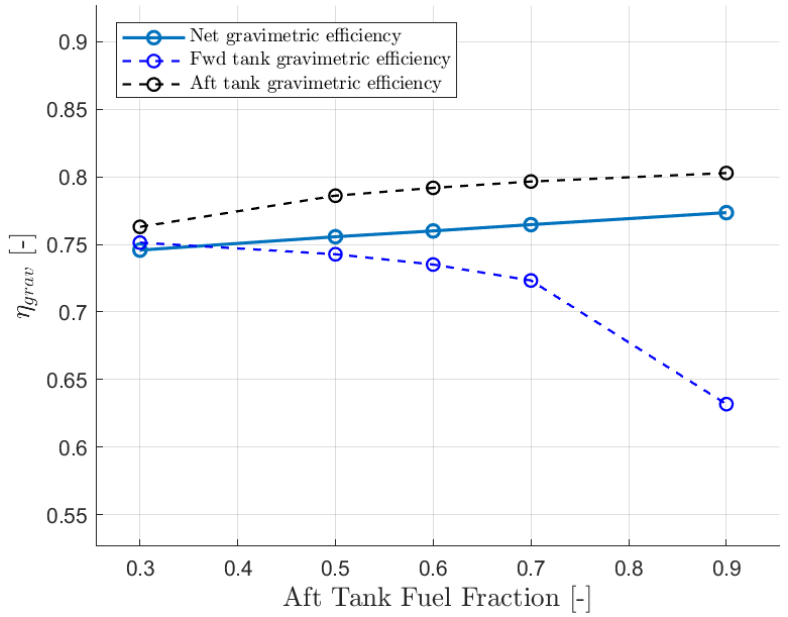

Figure 6.17: Effect of AFF on gravimetric efficiency

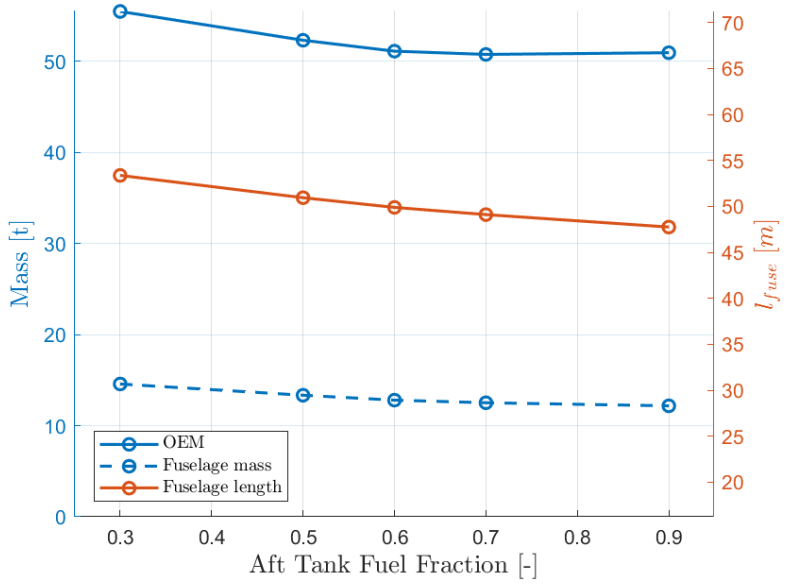

Figure 6.18: Effect of AFF on OEM, fuselage mass, and fuselage length

Finally, the trends in the mid-cruise L/D ratio and block fuel mass are considered. Based on the study so far, mass optimization has favoured a large AFF while the CG excursion favoured a more moderate AFF. In any case, it is clear that a high forward tank fuel fraction does not aid in improving any discipline. Figure 6.19 shows that the lowest fuel consumption and best mid-cruise glide ratio are coincident with the design for minimum CG excursion (AFF = 0.6), reiterating the importance of direct drag minimization over chasing performance increments by reducing weight; as the relative sensitivity of drag is higher in these studies. Thus, the same design is also selected to represent the dual forward-aft tank configuration in the final comparison.

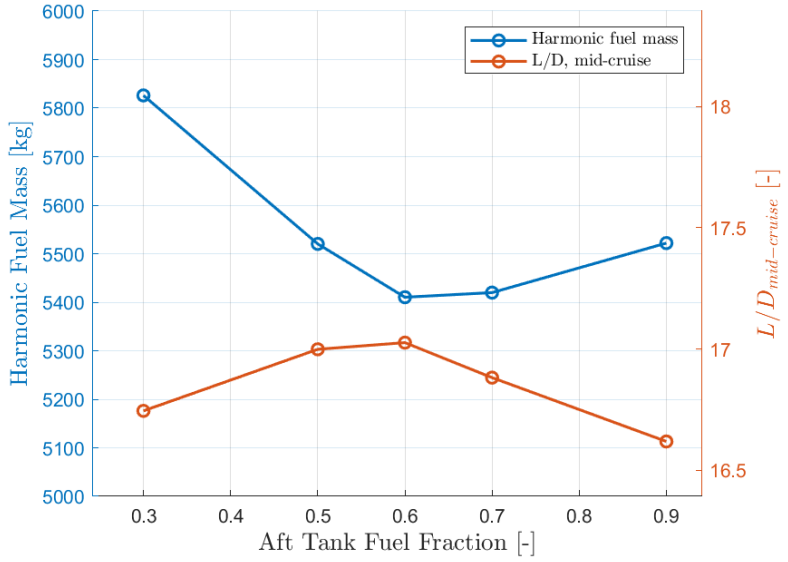

Figure 6.19: Effect of AFF on fuel mass and mid-cruise L/D

6.5. Effect of Engine Placement and Operational Limits

So far, LH2 configurations have attempted to improve aircraft performance by utilizing different tank layouts and adjusting certain parameters to optimize fuel consumption. In this section, the use of fuselage-mounted engines instead of wing-mounted engines is investigated, along with the effect of

employing operational limits in the design of the aircraft. These changes are only applied to configurations with the aft tank layout, as they are most impacted by the large CG excursion. No significant gains are expected with other tank layouts and are hence not considered in this section.

By placing the engines at the aft part of the fuselage, the OEM CG is brought closer to the fuel's CG, which means that the in-flight CG excursion would be reduced. However, this would also reduce the effective moment arm of the horizontal tail, which is undesirable. Furthermore, the overall CG range may expand due to the increased distance to the payload's CG, which also contributes to sizing a larger tail. In effect, a reduction in cruise trim drag would be traded for an increase in zero-lift drag, although a design exercise is required to determine which of these effects is dominant. The new position of the engines also triggers the use of a T-tail to avoid the hot exhausts and combat the moment arm reduction of the CG's new position. The engine pylons themselves are also now horizontal surfaces and would contribute to the stability, but keeping in line with a conservative approach; they are not accounted for in the sizing of the tail. The position of the engines is carefully selected to avoid keeping the tank or horizontal tail in the burst disc region, but unfortunately, this also increases the hazard of ingesting debris kicked up by the landing gear.

Operational limits are implemented as described in chapter 4. To summarize, the sizing of the tail and positioning of the landing gear is carried out solely on the basis of the flying CG limits of the harmonic mission. This narrower operating window enables higher efficiency and better landing gear integration at the cost of some operational flexibility. Figure 6.20 shows the loading diagrams for the two types of engine positions with operational limits activated. The results demonstrate that by placing the engines aft, a reduction in harmonic CG limits is possible despite an increase in the overall CG limits. The overall window expands because of the loading of the passengers and cargo, which is now further away from the OEM CG. The new mass distribution also aids in reducing the CG excursion for the ferry mission, but operational limits place this outside the flying limits; necessitating the use of ballast. Nevertheless, the harmonic mission performance is a strong point of interest and will be analyzed.

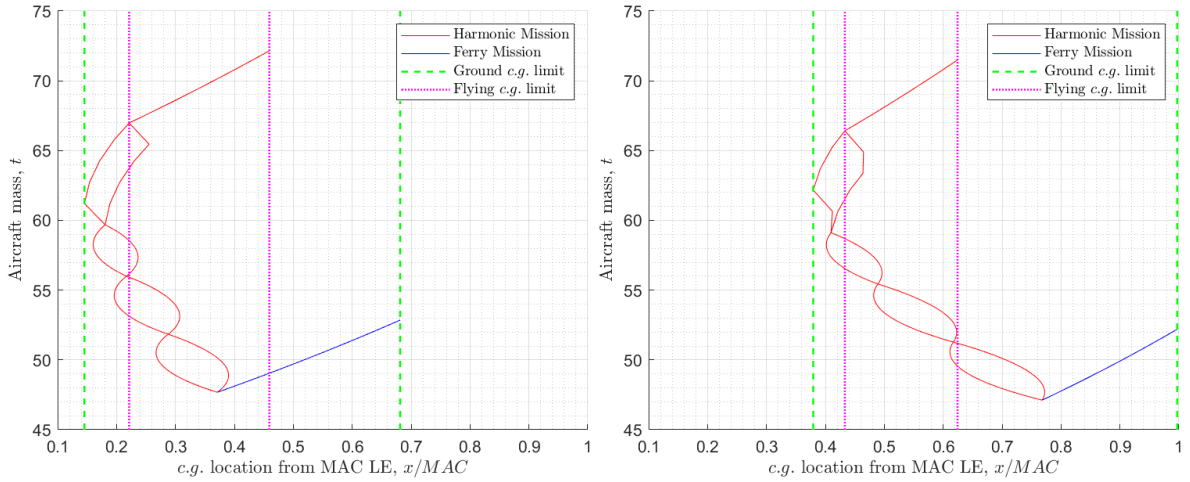

(a) Wing-mounted engines with operational limits $\Delta x_{\text{cg, flying}} = 0.25$ and $\Delta x_{\text{cg, ground}} = 0.54$

(b) Fuselage-mounted engines with operational limits $\Delta x_{\text{cg, flying}} = 0.19$ and $\Delta x_{\text{cg, ground}} = 0.62$

Figure 6.20: Loading diagram variation with engine placement, showing a larger reduction in flying CG limits for fuselage-mounted engines and operational limits active

Figure 6.21 shows the designed aircraft geometries for the two engine placement options and operational limits toggled on/off. Comparing the two wing-mounted engines, it can be seen that using operational limits in the design of the aircraft results in a smaller tail and a marginally shorter fuselage, due to a smaller tank. Crucially however, the main landing gear now sits directly under the wing's trailing edge- a marked improvement over the original case. This could allow for conventional landing gear integration, which further reduces drag and improves performance.

On the other hand, comparing wing- and fuselage- mounted engine configurations without operational limits, the landing gear position is revealed to become worse. However, this alone would not cause

a decrement in performance, assuming the baseline case already had a fuselage or pod mounted landing gear. A T-tail setup is used to avoid engine-tail exhaust/interaction effects, and there is a minimal reduction in the tail size is observed. When operational limits are applied to the design of this configuration, a drastic reduction in tail size is observed, due to the smaller CG excursion seen in the loading diagram. It is worth reiterating here that this tail is still oversized, as the stability estimation does not account for the contribution of engines and pylons to stability. With regards to the landing gear; its position is moved forward compared to the case without operational limits, but is still not close enough to the wing for conventional integration.

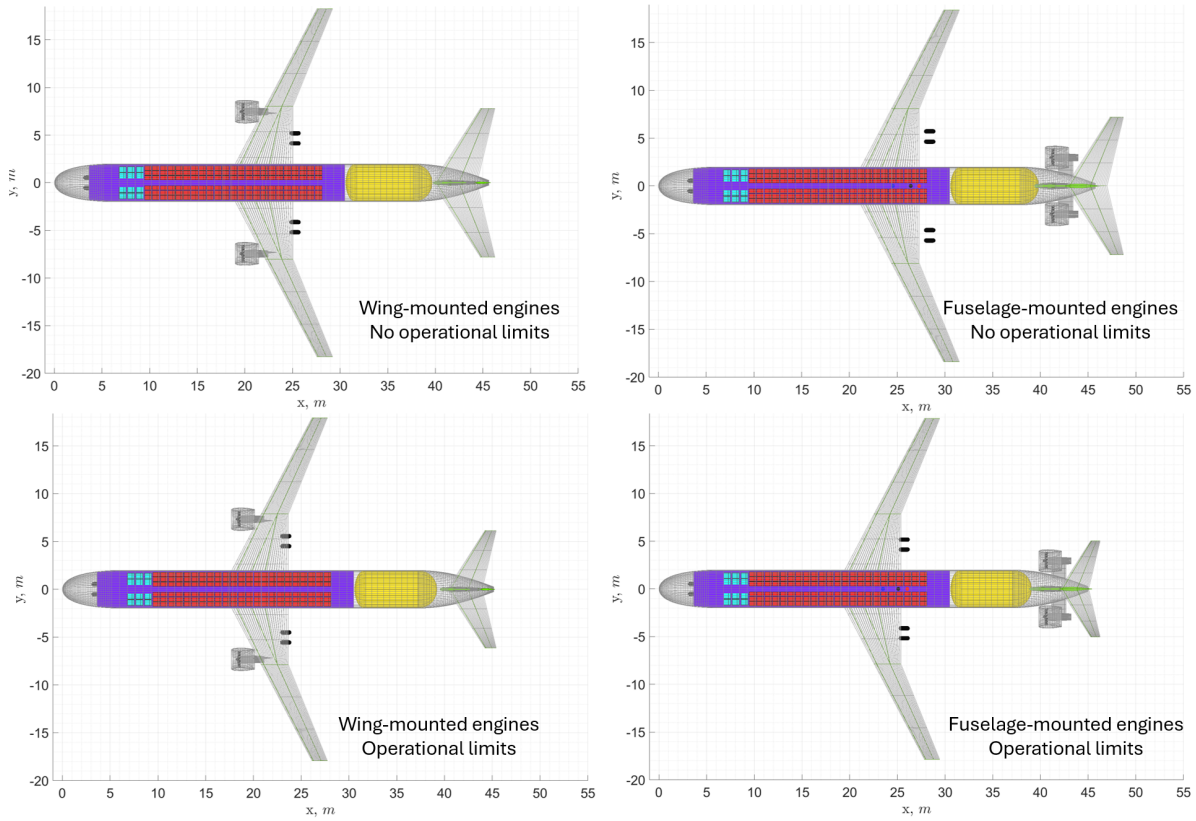

Figure 6.21: Aircraft geometries with the two engine location choices and operational limits activated/deactivated

The quantitative effect on tail area and drag is now studied. Figure 6.22 shows the relative change in the tail area ratio and zero-lift drag coefficient for each design combination of the 2SA-LH2-Aft aircraft, and demonstrates that fuselage-mounted engines in combination with operational limits more than halves the tail size and reduces the drag coefficient by almost 6%. Retaining wing-mounted engines and only applying operational limits reduces the drag by a smaller, yet substantial amount of 3.5%. Interestingly, the aircraft with fuselage-mounted engines and without operational limits still offers an improvement in performance over the baseline, despite contending with large CG limits. This is expected to be due to the smaller in-flight CG excursion (reduced trim drag as a result), and the shift to a T-tail.

This design also has a slightly higher mid cruise lift to drag ratio, and yet, comes with a block fuel consumption increase of 2%, as seen in figure 6.23. Since the engines are mounted aft, behind the tanks, there are two main factors that increase the weight of the aircraft: 1) increased fuselage stress, resulting in thicker stringers and panels, and 2) lack of wing load alleviation from the engines, requiring a stronger wing structure. The vertical tail also becomes heavier to support the T-tail. These factors cause the aircraft to become heavier and consume more fuel, in spite of the improved lift-to-drag ratio. For the remaining two design, operational limits are shown to reduce fuel mass by significant amounts; 6% for wing-mounted engines and close to 8% for fuselage-mounted engines- making them strong contenders for the best-performing liquid hydrogen aircraft. While the fuselage-mounted engines with operational limits has the best fuel mass on paper, it is important to remember that the drag penalty of

unconventional landing gear integration could push it behind the wing-mounted engine configuration.

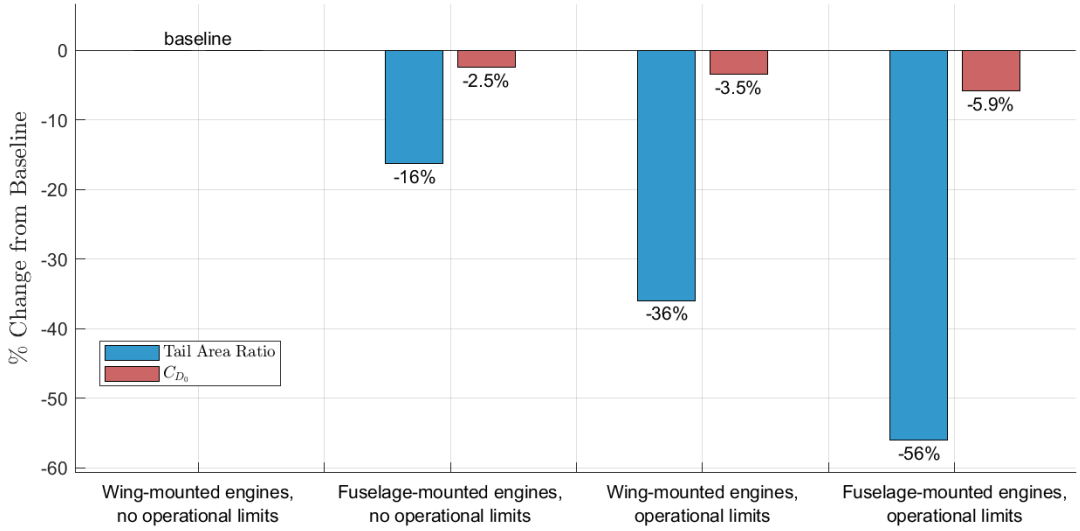

Figure 6.22: Relative change in tail area ratio and zero lift drag coefficient due to engine placement and operational limits

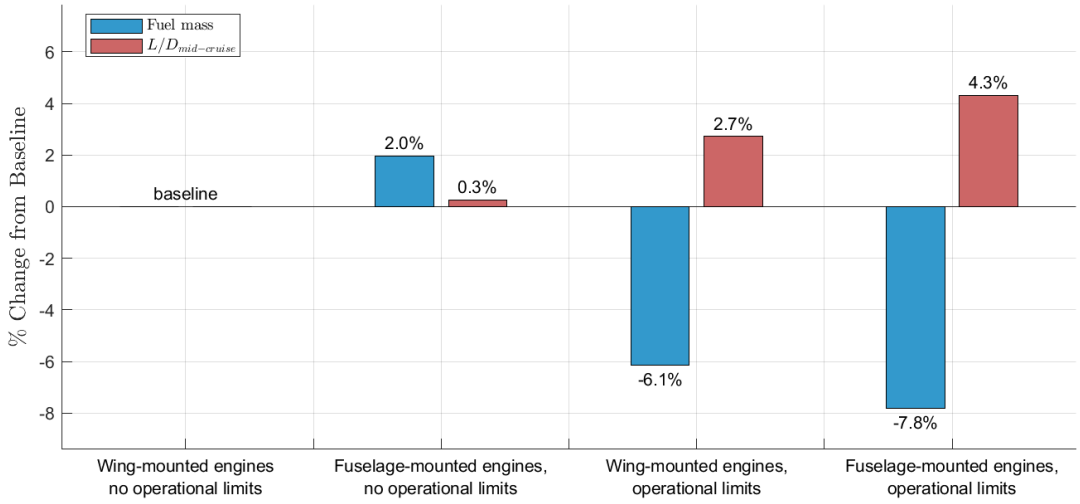

Figure 6.23: Relative change in block fuel mass and mid-cruise L/D due to engine placement and operational limits

The effects of engine placement and operational limits for the three-surface configuration follow similar trends as shown here, but with subdued improvements compared to its baseline configuration. The baseline configuration is taken as the optimized design from section 6.2, with the only other change made for fuselage-mounted engines being the shift from a high foreplane to a low foreplane. This was done to provide clean air for the engines by shifting the foreplane's wake further down. Although the Initiator does not directly simulate the effect of turbulent inflow, it was deemed a necessary design change to be representative of more detailed studies. It is also worth noting that operational limits did not unlock the option for conventional landing gear integration since the baseline 3SA configuration already was capable of this. Nevertheless, given these promising results -especially for the two-surface aircraft- designs with fuselage-mounted engines and/or operational limits will be included in the final comparison.

6.6. Final Comparison

Thus far, various aircraft configurations and design choices were investigated, and their respective top-performing designs were identified. Each of the selected aircraft will now be critically and com-

prehensively compared to answer the primary research question of what configuration is optimal for a medium-range, hydrogen-fuelled aircraft. The comparison will primarily consist of a quantitative analysis of various figures of merit, but will also include considerations on operations; developmental risk; and hazard analyses.

Table 6.2 shows numerous figures of merit obtained for the seven aircraft designs compared. The first three parameters convey input information while each following parameter is an output of the design from the Initiator that is deemed an important performance indicator. Keeping in line with previous discussion, the two-surface aft tank configuration (2SA-LH2-Aft) is treated as the baseline aircraft- a suitable role given its frequent appearance in the literature. The two variations of this configuration included are those designed with operational limits active (2SA-LH2-Aft (OL)) in addition to fuselage-mounted engines (2SA-LH2-Aft-FME(OL)) due to their promising performance characteristics. The optimized three-surface aircraft with and without operational limits (3SA-LH2-Aft and 3SA-LH2-Aft(OL)) are also selected for the same reasons, but the fuselage-mounted engines are ignored here due to unfavourable landing gear integration. Finally, the best-performing top tank (2SA-LH2-Top) and dual forward-aft tank configurations (2SA-LH2-FwdAft) round out the candidates. Each of the aircraft geometries are shown in figure 6.24 for reference.

Another figure of merit initially considered was the physics-limited minimum rotation speed on take-off. This was because the tail sizing procedure does not account for the take-off rotation constraint, and certain geometries feature landing gears that were placed towards the rear of the aircraft- triggering concerns that the actual design would not be able to meet the take-off distance requirement. However, a simplified take-off calculation found that the rotation speed was well below the stall speed for all designs, even for the most forward CG position- putting any concerns to rest.

6.6.1. Three-Surface Aircraft

Comparing the baseline two-surface aircraft to the baseline three-surface aircraft, several differences in the figures of merit immediately stand out. The 3SA has a significantly lighter fuselage due to the load alleviation from the foreplane, and is the primary reason behind the 5.4% reduction in empty mass. The tail area is reduced despite a slight increase in the CG excursion, as the larger moment arm of the T-tail and the addition of the foreplane improve the stability and control limits. The lighter overall aircraft also results in reduced reference area and wetted area; both of which aid in reducing the zero-lift drag as well.

In spite of all these improvements, the cruise lift-to-drag ratio drops by large amount- owing the rise in induced drag- and results in 3.5% higher energy consumption on the nominal harmonic mission. Thus, these results indicate that the penalties incurred by splitting lift between the wing and a foreplane outweigh the benefits of reduced weight and C_{D_0}. being the lighter aircraft, it also has a lower take-off thrust and better climb performance, but the reduced cruise efficiency hurts the overall fuel consumption. This indicates that the 3SA could be better suited for shorter missions with smaller cruise phases. One market-based advantage for the 3SA is that the presence of the foreplane allows the wingspan to drop below 36m, which is the ICAO type-III limit that most medium-range aircraft meet. In order for the conventional configuration to meet this requirement, it would have to incorporate folding wingtips or downgrade its aspect ratio, both of which would bring some detriment. Of course, the baseline's inability to have conventional landing gear integration must also be kept in mind, as this will bear a weight and drag penalty.

If the two configurations are levelled in terms of performance as a result of these changes, the conventional design would still be preferred for its proven design and reduced developmental risk. Simultaneously, the 3SA conceptualized in this study is built on conservative assumptions and methodologies, and hence represents a lower limit in terms of performance. A higher-fidelity study could perform twist-distribution optimization for the main wing and unlock more of its potential, providing significant gains in performance. This aspect is especially important for the 3SA because the foreplane considerably changes the nature of the flow upstream of the wing.

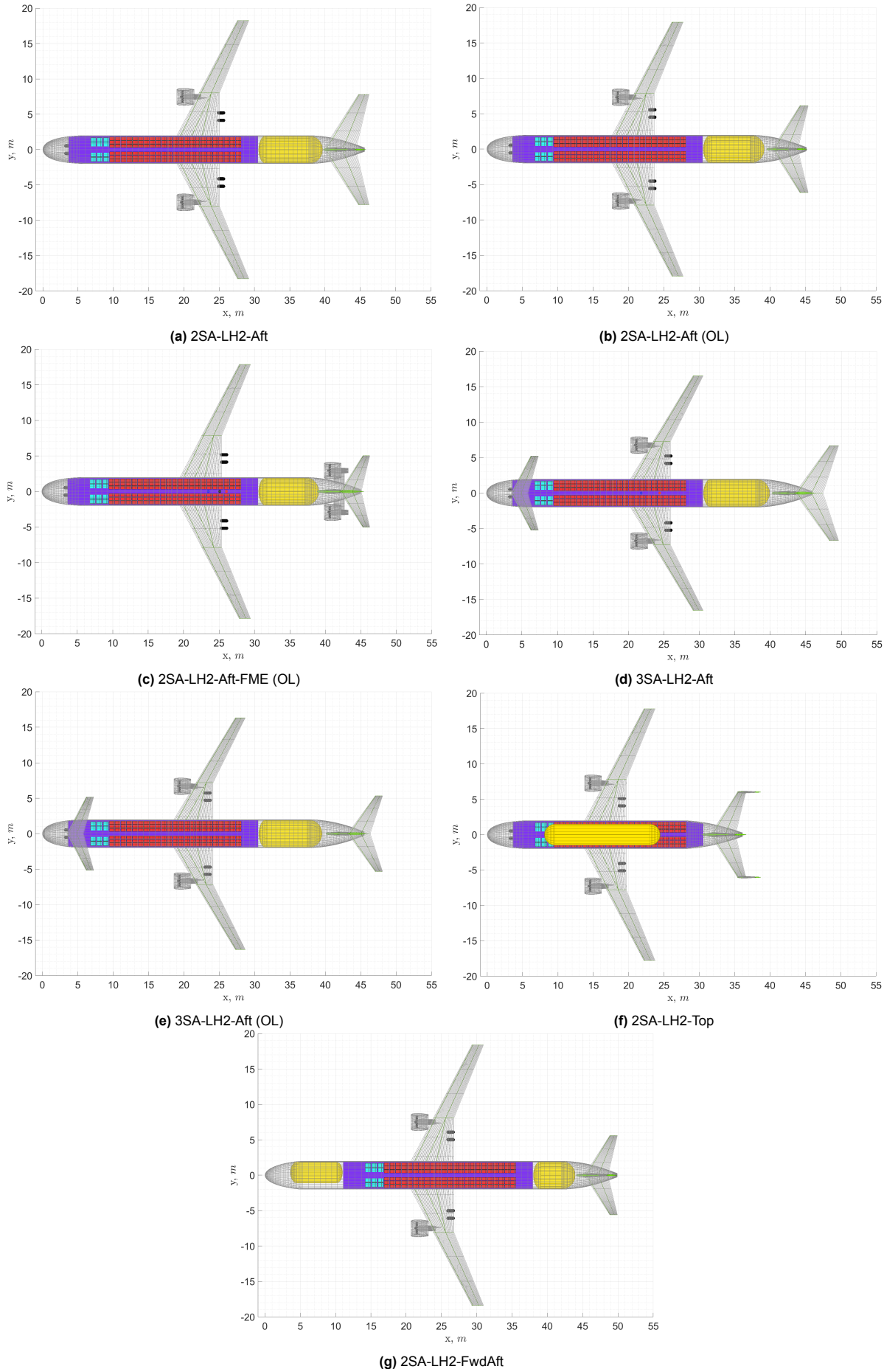

(a) 2SA-LH2-Aft

(b) 2SA-LH2-Aft (OL)

(c) 2SA-LH2-Aft-FME (OL)

(d) 3SA-LH2-Aft

(e) 3SA-LH2-Aft (OL)

(f) 2SA-LH2-Top

(g) 2SA-LH2-FwdAft

Figure 6.24: Comparison of the aircraft geometries

Parameter	2SA-LH2-Aft	2SA-LH2-Aft (OL)	2SA-LH2-Aft-FME (OL)	3SA-LH2-Aft	3SA-LH2-Aft(OL)	2SA-LH2-Top	2SA-LH2-FwdAft
Design specification	-	Operational limits active	Fuselage-mounted engines, operational limits	FPA = 0.15, FPI = 2°	FPA = 0.15, FPI = 2°, operational limits active	Tank diameter ratio = 0.75	Aft tank fuel fraction = 0.6
Tank structure	Integral	Integral	Integral	Integral	Integral	Non-integral	Non-integral and integral
Tail type	Standard	Standard	T-tail	T-tail	T-tail	Triple tail	Standard
η_{tank}	0.78	0.78	0.79	0.78	0.78	0.75	0.76
$\Delta x_{\text{CG, flying}}/MAC$	0.54	0.24	0.19	0.56	0.26	0.11	0.12
Landing gear position quality	×	✓	×	✓	✓	✓	✓
Ferry mission ballast (t)	-	2.6	3.8	-	2.8	-	-
S_{h}/S	0.38	0.24	0.17	0.29	0.19	0.24	0.19
Horizontal tail mass (t)	1.9	1.1	0.7	1.8	1.1	1.1	0.9
Fuselage mass (t)	11.6	11.1	11.5	8.6	9.8	10.2	12.8
Wing mass (t)	9.2	8.6	8.3	8.9	7.6	8.6	9.3
Aircraft length (m)	46	45	46	50	48	39	50
Take-off thrust (kN)	215	207	205	208	203	205	217
b (m)	36.5	35.8	35.7	33.0	32.6	35.6	36.7
S (m^2)	127	123	122	122	119	121	129
S_{wet} (m^2)	950	890	870	900	860	910	950
C_{D_0} (cts)	232	224	219	226	220	238	224
$C_{D_0}S$ (m^2)	2.95	2.75	2.66	2.76	2.62	2.88	2.89
$e_{\text{mid-cruise}}$	0.84	0.85	0.87	0.69	0.69	0.86	0.85
$L/D_{\text{mid-cruise}}$	16.5	16.9	17.2	15.3	15.7	16.0	17.0
FM, incl. reserves (t)	5.51	5.17	5.08	5.70	5.45	5.37	5.41
Nominal harmonic mission energy consumption (GJ)	539	506 (-6.1%)	496 (-8.0%)	558 (+3.5%)	536 (-0.56%)	526 (-2.4%)	530 (-1.7%)
OEM (t)	50.0	47.7 (-4.6%)	47.1 (-5.8%)	47.3 (-5.4%)	45.8 (-8.4%)	46.6 (-6.8%)	51.1 (+2.2%)
MTOM (t)	74.8	72.1 (-3.6%)	71.5 (-4.4%)	72.4 (-3.2%)	70.5 (-5.7%)	71.3 (-4.7%)	75.8 (+1.3%)

Table 6.2: Comparison of the selected aircraft

6.6.2. Top Tank configuration

Comparing the top tank configuration to the baseline, several changes are noted. Despite an increase in C_{D_0} due to higher fuselage drag, the net zero-lift drag ($C_{D_0}S$) reduces, as the reference area becomes smaller. Since the cruise speed and density are constant across all designs, $C_{D_0}S$ is considered a good point of comparison. It is also interesting to note that despite a reduction in tank gravimetric efficiency, the aircraft's total wetted area reduces compared to the aft tank layout. This is only possible through the assistance of the fairings to efficiently package the two cylinders (tank and fuselage) in a tandem manner. Figure 6.25 shows the large drop in total CG excursion by placing the tank on top of the fuselage instead of at the aft. The limits are now fully driven by the loading of passengers and cargo instead of fuel loading, as seen in the figure.

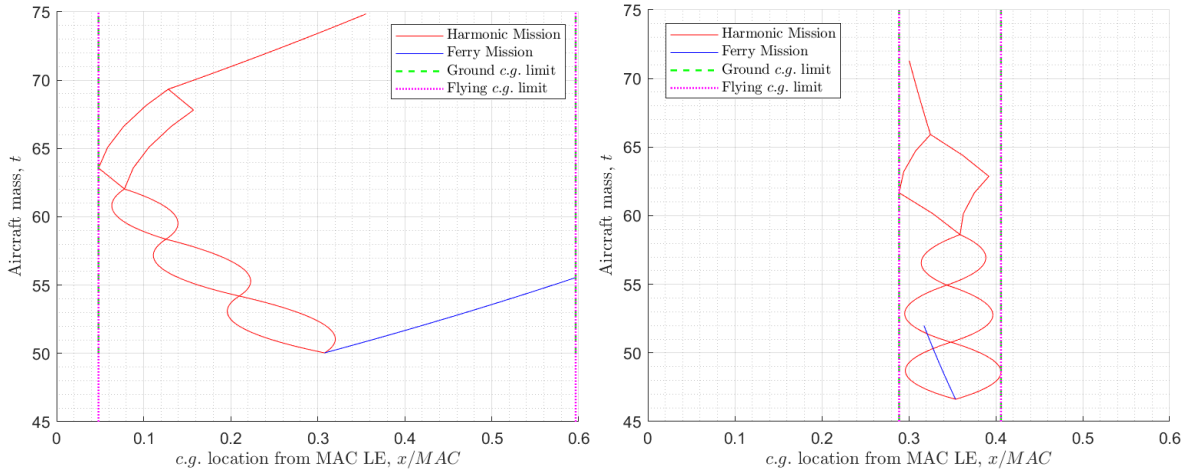

(a) 2SA-LH2-Aft, $\Delta(x/\bar{c})_{\text{cg}} = 0.54$ **(b)** 2SA-LH2-Top, $\Delta(x/\bar{c})_{\text{cg}} = 0.11$

Figure 6.25: Difference in loading diagrams due to tank placement

The placement of the tank improves fuselage mass, as extended stringers are no longer required, and the bending loads reduce over the shorter fuselage. The reduced CG excursion leads to a smaller, lighter horizontal tail, while the wing mass also reduces through snowball effects, resulting in a lighter overall structure (-6.8% OEM); even with the rise in η_{tank}. Thus, even though the mid cruise glide ratio is slightly smaller for the top tank configuration, it actually uses less thrust and hence burns less fuel- leading to a 2.4% reduction in nominal energy consumption.

Furthermore, the landing gear position is perfectly suited for conventional integration and the span of the aircraft is below 36m, allowing operations at Type-III airports without the need for folding wingtips or any other such technologies. Adding to this list of advantages is that compared to the baseline, this configuration has a smaller footprint on the ground and is not expected to need any special considerations with ground operations or hangar sizes. Given all these desirable characteristics and improvements, the top tank configuration is considered a great choice for a medium-rage hydrogen aircraft.

A hazard analysis of this configuration consists of various considerations and scenarios. Unlike the aft tank configuration, a tail-strike is no longer a major concern given the tank is unlikely to take damage from this. It is also better protected in the event of a belly landing, as the fuselage acts as a barrier against the ground. Of course, the struts will transfer the large transverse loads to the tank in such an event, but this is preferable to a direct impact to the tank. The separation of the tank from the fuselage and cabin is still beneficial, as the risk of mixing gases or contaminating the cabin is vastly reduced compared to the aft tank layout- which could also be critical in market acceptance of hydrogen. The biggest concern with the top tank layout is its exposure to engine fragments in case of a blade-out engine failure- which could trigger a catastrophic explosion of fuel if the tank is breached. This is also why some studies suggest splitting the tank and using a dry bay in the blade-out region, or reinforcing that section of the tank. Neither of these modifications is expected to have a major impact on the performance of the aircraft.

6.6.3. Dual, Forward-aft Tank Configuration

Like the top tank configuration, the FwdAft layout attempts to address the large CG excursion by placing the fuel's effective CG closer to the OEM and MTOM CG. As the fuselage length is increased by the lower diameter forward tank, the effective moment arm of the tail also increases, which helps reduce the tail size close to that of aircraft design with operational limits. While this is a very positive change, the extended fuselage length also increases the fuselage mass by a large amount, making it the heaviest fuselage of all configurations. The high length combined with an end-heavy mass distribution from the tanks and fuel does no favours for the fuselage stress, further contributing to the mass penalty. The overall weight of the aircraft is thus increased, driven primarily by the rise in fuselage weight, the lighter horizontal tail notwithstanding. Figure 6.26 provides a breakdown of the OEM of the two designs. The rise in systems mass is due to the heavier fuel tanks and systems of the dual tank configuration.

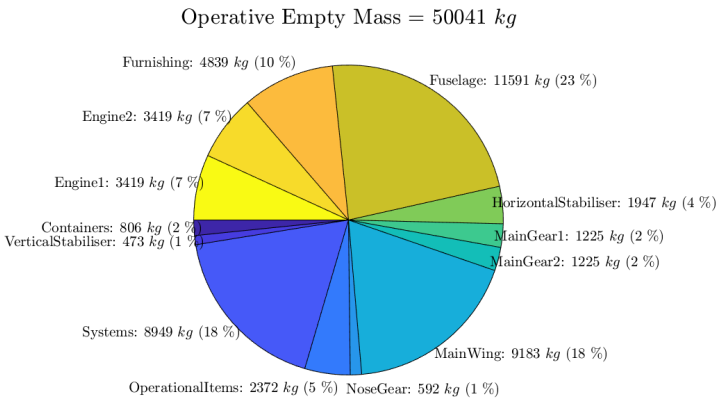

(a) 2SA-LH2-Aft

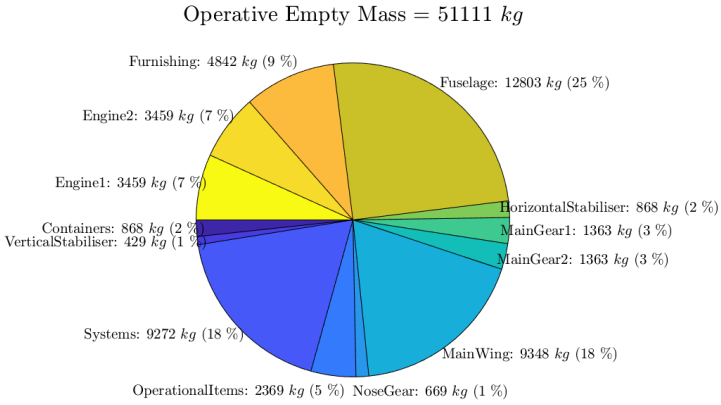

(b) 2SA-LH2-FwdAft

Figure 6.26: Operative empty mass breakdown comparison

The wetted area is on par with the baseline aircraft, but the more slender fuselage allows for a slight reduction in zero-lift drag; which -along with the reduction in average trim drag arising from a smaller in-flight CG shift- results in an improvement in $L/D_{\text{mid-cruise}}$. This aerodynamic improvement overcomes the increased weight, and the aircraft has a 1.7% reduction in nominal energy consumption; making it the only design that has a lower fuel mass in spite of higher OEM and MTOM.

Conventional landing gear integration seems possible, based on the position of the wheels and wing; and hence eliminates the need to consider the impact of additional fairing drag. The length of the aircraft being very high (50m) could pose constraints on ground operations at smaller airports, and the 36m span limit is also breached by this configuration. Thus, in terms of almost every figure of merit,

the FwdAft tank configuration falls short of the top tank configuration. Even if regulations allow for severing the cockpit-cabin connection and enable a full diameter integral tank, the slight performance benefits may not be worth it. This is because the cockpit would then need a separate ingress/egress door, toilet, and new operating procedures with no way of cabin access. In any case, the forward tank would still share the same atmosphere as the cabin and cockpit, which is a disadvantage from a safety perspective, as any leaks and gaseous mixing would form an explosive mixture inside the cabin. Given all these drawbacks, this configuration is expected to be the weakest in terms of market acceptance.

6.6.4. Engine Placement and Operational Limits

So far, various alternatives to the baseline aft tank layout were discussed and it was found that despite moderate changes in aerodynamic or structural disciplines; the net improvement in fuel consumption was always small- with just a 2.4% improvement in the best case. However, it is seen that by applying operational limits in the design of the aircraft, much larger reductions in fuel consumption are possible- a result that was not anticipated earlier.

With operational limits applied to the default, wing-mounted engines aircraft; the CG excursion is reduced by half and the tail area ratio by a third. The positive snowball effect reduces the size and mass of other components as well- leading to a 6.7% fall in zero lift drag and a 3.6% lighter MTOM. The net effect results in 6.1% lower energy consumption, all achieved simply through the application of operational limits. The smaller CG variation helped reduce weight, zero lift drag, and average trim drag. Furthermore, the landing gear position shifts to a much more favourable location, while the span also falls below the Type-III airport limit. By placing the engines behind the tank on the fuselage, an even greater improvement of 8% lower energy consumption is observed through further limiting the CG excursion. However, this configuration prevents the use of conventional landing gear integration, and would likely bear some drag penalty just as the baseline aircraft does. It may be worth noting that the Airbus ZEROe turbofan concept also features wing-mounted engines, an aft-tank layout, and no large horizontal tail. This could suggest that operational limits were applied in that case as well, to minimize the tail size.

The primary disadvantage of this configuration is the constraints it places on ground operations, and the large ballast mass it needs to fly safely for reduced payload missions. For the wing mounted engine configuration, a ballast of $2.6t$ is needed at the front of the cabin for flying the ferry mission, as the CG is pushed far aft by the fuel. Additionally, a part of the fuel must be left inside the tank to keep the CG within the forward limit at the end of the mission- further reducing the ferry range. The ballast is conceptualized in the form of a water tank that could be filled or emptied based on the requirement, and partially embedded into the hold. The required ballast mass would reduce as the payload increased- favouring high load factor missions. For the fuselage-mounted engine configuration, the effect is worsened, necessitating $3.8t$ of ballast for its ferry mission. Considering the 3SA with active operational limits, similar trends and improvements are obtained, but on a smaller scale. Even though this results in the lightest aircraft in the lineup, the fuel mass only becomes marginally lower than the baseline, due to reasons relating to induced drag discussed previously.

From a safety perspective, all these designs have the same tank layout and are on equal footing there. The base of the tailcone may have to be strengthened to bear the impact of a tail strike, which is a major concern for these configurations. Since the tank is behind the aft bulkead, the cabin's atmosphere is isolated from the tank's environment- but the fuel lines passing to the wing-mounted engines still need to go through a part of the fuselage. Fuselage mounted engines have an advantage here, as no part of the tank or fuel system comes near the cabin region. This engine configuration however, would be prone to ingesting debris kicked up by the main landing gear given its position; leading to engine failure. Moving the engines further forward would reduce this risk but introduce the risk of blade-out failure striking the tank. Therefore, wing-mounted engines may be preferred solely in terms of reliability, as engines are typically the most expensive component of the aircraft.

6.6.5. Final Recommendation

Through these results and analyses, knowledge is gained regarding aircraft performance, landing gear integration, operational constraints, and safety factors. A recommendation is now made as to what configuration is optimal for liquid hydrogen aircraft.

- The two-surface aft tank configuration with operational limits and wing-mounted engines is seen as a very strong candidate. Not only does it reduce block energy consumption more than other major configurations, but also reduces the wingspan to meet Type-III airport requirements, and crucially- enables simple landing gear integration that was not previously possible. The fuselage-mounted engine configuration is not capable of this, and offers only 2% better fuel consumption; which would reduce when landing gear fairing drag is accounted for. Furthermore, the required ballast mass and operational constraints for off-design payloads increases compared to the wing-mounted engine configuration. For this reason, 2SA-LH2-Aft (OL) is selected as the best configuration, especially for routes with high traffic and load factors.
- For airlines or networks that demand more operational flexibility, the top tank configuration (2SA-LH2-Top) is seen as the best candidate. It offers a moderate improvement over the baseline aircraft without resorting to operational limits, and also features a small footprint compared to other concepts. Off-design missions in and out of smaller airports can be flown easily, without consideration for ballast, tail support jacks, order of loading, or general airport compatibility. In addition, this configuration offers good safety characteristics, which may be key to market acceptance and early adoption for liquid hydrogen aircraft.

Each of the seven designs performed well in specific areas, but these two configurations are proposed as the most optimal integration of hydrogen fuel; considering all aspects including fuel economy, safety, and operability.

7

Conclusion

7.1. Conclusion

Shifting to carbon-free fuels in aviation is seen as a key step towards meeting climate goals, and liquid hydrogen is seen as a good solution to this. LH2's low volumetric energy density and special storage requirements necessitate a large tank on the aircraft, which has a major impact on the performance of the aircraft. This triggers the question of what aircraft configuration is optimal for integrating hydrogen fuel in the medium-range category.

Several aircraft configurations were conceptualized and put through a qualitative downselection process to arrive at four specific configurations of interest: 1) the conventional two-surface aft tank aircraft, 2) the three-surface aft tank aircraft, 3) the top-tank aircraft, and 4) the dual, forward-aft tank aircraft. Methodologies are developed and modifications are made to effectively size and analyze these configurations through TU Delft's aircraft design tool; the Initiator. The option to design an aircraft with operational limits is also implemented, intended for use on aft tank layouts due to their high variation of the center of gravity.

A validation exercise is conducted for the Initiator, taking the A320neo as the reference aircraft and designing an aircraft using the same TLARs. A similar process is carried out for hydrogen configurations from literature, and the performance of the tool was found to be acceptable. The aft tank two-surface aircraft is treated as the baseline configuration, while other configurations are optimized to obtain the best design from each concept for the final comparison. The main problems faced by the baseline aircraft are:

- The high CG range leading to very large tail sizes and high drag as a result
- Large in-flight CG excursion leading to high average trim drag
- Unfavourable main landing gear position relative to the wing

The primary design variables for the three-surface aircraft are taken as the foreplane area ratio and foreplane incidence angle. The results show that increasing the area ratio increases fuel burn, as a larger share of the lift is borne by the low aspect ratio forplane; increasing the total induced drag. However, the results also showed that by correctly tuning the lift on the foreplane, the bending stresses in the fuselage could be reduced; leading to lower a lower fuselage mass and OEM. Furthermore, the 3SA was found to provide better landing gear positions relative to the wing, and would enable conventional landing gear integration- a key objective of this configuration. The baseline aircraft on the other hand, is incapable of this and must incorporate fuselage-mounted or wing podded-landing gears; both of which increase weight and drag.

The primary design variable with the top tank configuration is selected as the tank diameter ratio, and effectively controls the slenderness of the tank. This design tackles the large CG excursion by simply placing the tank in a non-integral manner above the fuselage instead of behind the cabin. The fuel's CG is now much closer to the payload and OEM CG, and hence reducing the CG range. This comes

at a cost of slightly higher zero-lift drag, as the tank sits above the fuselage- but also results in a large reduction of weight. The optimal diameter ratio is found to be 0.75, and was a trade between improving aerodynamics or tank gravimetric efficiency.

For the forward-aft tank configuration, the chief design variable was the fraction of total fuel designed for the aft tank. The forward tank is offset to one side and has a reduced diameter to enable a cockpit-cabin connection. As a result, this tank is non-integral and is less efficient than the aft tank. However, it is beneficial to store some fuel here, as it helps reduce the net CG excursion. The findings indicate that an aft fuel fraction of 0.6 produced the minimum fuel consumption, primarily as a trade between fuselage weight and tail drag.

The effects of engine placement and operational limits are investigated together for aft tank layouts. Engines mounted to the fuselage, behind the tank were thought to have the potential to reduce average trim drag by bringing the OEM CG closer to the fuel tank- and hence reducing the in-flight CG excursion. However, penalties arose in the form of increase wing and fuselage mass due to the new weight distribution, and increased the overall fuel consumption. By incorporating operational limits, the tail sizing and landing gear position would be set purely based on the harmonic mission instead of the entire CG envelope. The results discovered that the baseline aircraft's harmonic fuel consumption could be reduced by 6% (with wing-mounted engines) or 8% (with fuselage-mounted engines) simply by activating operational limits. This was because the smaller CG excursion enabled the use of a much smaller horizontal tail which reduced drag, and caused a snowball effect with tank, fuselage, and wing mass. Furthermore, the main landing gear's position relative to the wing improved to the point where conventional integration was made possible for the wing-mounted engines; a very positive outcome. Regrettably, these performance benefits come at the cost of reduced operational flexibility. Off design-payload missions necessitated the use of heavy ballast mass at the front of the aircraft to stay within safe CG limits, while ground operations now needed special considerations for tail support sticks or specific loading patterns.

The final comparison consists of seven different designs: four from the main configurations (individually optimized designs), and three from the application of operational limits to aft tank layouts. The results show that among all design without operational limits, the top-tank configuration produces the lowest energy consumption (2.4% reduction over the baseline); while the forward-aft layout has the second lowest despite being the heaviest design. The 3SA design results in the lightest OEM and MTOM, as well as the lowest zero-lift drag; but the high induced drag renders the configuration with the worst fuel economy.

The application of operational limits is found to provide much larger improvements in aircraft performance than any changes in tank layout or configuration. Nominal mission harmonic energy consumption is reduced by at least 6% compared to the baseline. Further benefits are seen in terms of improved landing gear integration, and wingspan reduction to meet ICAO Type-III aiport limits; increasing viability. Considering all these factors, the two-surface aircraft with operational limits is proposed as the best design for hydrogen aircraft- especially for routes with high traffic and load factors. For airlines or networks that demand more operational flexibility, the top tank configuration is proposed as the optimal design. Its configuration offers a more moderate improvement in energy consumption over the baseline, but comes with a high standard of safety and does not need pay any regard to ballast or ground operating constraints. These two aircraft configurations are judged to be the optimal integration of hydrogen fuel in the medium-range category, and the choice between the two is driven by market-specific requirements.

7.2. Recommendations for Future Work

In this section, numerous recommendations are made for future studies on hydrogen aircraft concepts and design investigations.

- The three-surface aircraft configuration in this study has worse fuel consumption despite large reductions in weight and zero-lift drag than the baseline aircraft. This is believed to be due to high levels of induced drag. While a part of this increase in induced drag may be unavoidable, the performance could still be significantly improved if the design tool incorporated wing twist optimization. The presence of the foreplane impacts the nature of the flow upstream of the main

wing, and if the wing twist is tailored to this condition, lower induced drag is anticipated. A similar effect is also applicable to the horizontal tail, and a simple incidence optimizer to ensure no unnecessary lift/downforce is being inadvertently produced by it would be a valuable addition.

- The conceptual model of the 3SA in literature uses the foreplane as an active trim-drag reducing surface, whereas the current study assumes a fixed foreplane with flaps linked to the main wing. Switching to the latter model requires significant changes to the design tool, but could prove to unlock a lot of the configuration's potential. Another valuable change in its design for future studies would be to allow the main wing to utilize the maximum span- and increase its aspect ratio as a result. Currently, the aspect ratio of the main wing is kept consistent with the baseline aircraft, and the full span is not used.
- The modelling of fuselage drag, vertical tail area, and tank support mass in the top tank configuration relies heavily on assumptions from the designer, increasing uncertainty. Higher fidelity modules for these components would be very helpful in providing more accurate estimations for aircraft performance. Furthermore, the mission analysis module does not account for the vertical CG excursion and its impact on trim drag, which should also be implemented.
- The weight and drag impact of using fuselage-mounted or wing-podded landing gears though concentrated, higher fidelity studies would be very beneficial in the design of hydrogen aircraft. The knowledge of aspects would benefit and help guide the design of aft-tank layouts by a great amount.
- The current study proposes a design with operational limits as one of the best solutions for hydrogen aircraft. Simple calculations were conducted and large ballast masses were obtained for reduced payload missions. The structural impact of this has not been analyzed, and there is a risk that the ferry mission's weight distribution becomes the critical case for fuselage structural sizing - increasing the mass of the aircraft. This would also reduce the performance of the harmonic mission and hence must be investigated further.

References

[1] E. J. Adler and J. R. R. A. Martins. “Blended Wing Body Configuration for Hydrogen-Powered Aviation”. In: *Journal of Aircraft* 61.3 (2024), pp. 887–901. DOI: 10.2514/1.C037582.

[2] E. J. Adler and J. R. R. A. Martins. “Hydrogen-powered aircraft: Fundamental concepts, key technologies, and environmental impacts”. In: *Progress in Aerospace Sciences* 141 (2023), p. 100922. DOI: https://doi.org/10.1016/j.paerosci.2023.100922.

[3] Aerospace Technology Institute. *FlyZero*. Accessed: 2025-01-27. 2022. URL: https://www.ati.org.uk/flyzero/.

[4] Aerospace Technology Institute. *Zero-Carbon Emission Aircraft Concepts*. Accessed: 2025-01-27. 2022. URL: https://www.ati.org.uk/flyzero-reports/?category=97.

[5] Air Transport Action Group. *The Future of Aviation: Benefits Beyond Borders to 2050*. Technical Report. Air Transport Action Group, 2021. URL: https://aviationbenefits.org/media/167187/w2050_full.pdf.

[6] Airbus. *A320: AIRCRAFT CHARACTERISTICS, AIRPORT AND MAINTENANCE PLANNING*. Accessed: 2025-05-24. May 2017. URL: https://aircraft.airbus.com/sites/g/files/jlcbta126/files/2025-01/AC_A320_0624.pdf.

[7] Airbus. *A330-700L: AIRCRAFT CHARACTERISTICS, AIRPORT AND MAINTENANCE PLANNING*. Accessed: 2025-05-24. Dec. 2022. URL: https://aircraft.airbus.com/sites/g/files/jlcbta126/files/2023-02/Airbus-Commercial-Aircraft-AC-A330-700L.pdf.

[8] Airbus. *A330: AIRCRAFT CHARACTERISTICS, AIRPORT AND MAINTENANCE PLANNING*. Accessed: 2025-05-24. Dec. 2023. URL: https://aircraft.airbus.com/sites/g/files/jlcbta126/files/2023-08/ac_a330_jul2023_0.pdf.

[9] Airbus. *Airbus ZEROe - how to store liquid hydrogen for zero emission flight*. Accessed: 2025-01-24. 2025. URL: https://www.airbus.com/en/newsroom/news/2021-12-how-to-store-liquid-hydrogen-for-zero-emission-flight.

[10] Airbus. *ZEROe: Towards the world’s first hydrogen-powered commercial aircraft*. Accessed: 2025-01-24. 2023. URL: https://www.airbus.com/en/innovation/energy-transition/hydrogen/zeroe.

[11] Airbus Deutschland. *Liquid Hydrogen Fuelled Aircraft - System Analysis*. Tech. rep. Final technical report, Project no.: GRD1-1999-10014, 2003.

[12] *Aircraft Design Initiator*. Accessed: 2025-07-27. URL: http://fppwiki.lr.tudelft.nl/index.php/Synthesis/Initiator.

[13] *Some Unconventional Aero Gas Turbines Using Hydrogen Fuel*. Turbo Expo: Power for Land, Sea, and Air, Volume 2. 2002, pp. 683–690. DOI: 10.1115/GT2002-30412. URL: https://doi.org/10.1115/GT2002-30412.

[14] G. D. Brewer. *Hydrogen Aircraft Technology*. 1st. Routledge, 1991. DOI: 10.1201/9780203751480. URL: https://doi.org/10.1201/9780203751480.

[15] M. Brown and R. Vos. “Conceptual design and evaluation of blended-wing body aircraft”. In: *AIAA Aerospace Sciences Meeting*. 2018, p. 0522. URL: https://arc.aiaa.org/doi/pdf/10.2514/6.2018-0522.

[16] Clean Sky 2 Joint Undertaking and FCH2 Joint Undertaking. *Hydrogen-Powered Aviation: A Fact-Based Study of Hydrogen Technology, Economics, and Climate Impact by 2050*. Technical Report. Clean Sky 2 / FCH2, 2020. URL: https://www.cleansky.eu/sites/default/files/inline-files/20200507_Hydrogen-Powered-Aviation-report.pdf.

[17] DLR. *EXACT: Project Overview*. Accessed: 2025-01-14. 2024. URL: https://exact-dlr.de/project-overview/.

[18] R. Elmendorp. “Synthesis of novel aircraft concepts for future air travel”. Master’s thesis. PhD thesis. Delft University of Technology, 2014.

[19] R. Elmendorp, R. Vos, and G. La Rocca. “A conceptual design and analysis method for conventional and unconventional airplanes”. In: *29th Congress of the International Council of the Aeronautical Sciences*. Vol. 1. ICAS. 2014. URL: https://repository.tudelft.nl/file/File_57085ee5-7e20-4a04-bcb5-441970698316.

[20] R. D. Finck. *Stability and Control DATCOM (Data Compendium)*. Tech. rep. United States Air Force, 1978. URL: https://apps.dtic.mil/sti/html/tr/ADB072483/.

[21] G. Gardiner. *Collins Aerospace to lead COCOLIH2T project*. Accessed: 2025-01-27. Mar. 2023. URL: https://www.compositesworld.com/news/collins-aerospace-to-lead-cocolih2t-project-.

[22] A. Gomez and H. Smith. “Liquid hydrogen fuel tanks for commercial aviation: Structural sizing and stress analysis”. In: *Aerospace Science and Technology* 95 (2019), p. 105438. DOI: 10.1016/j.ast.2019.105438.

[23] M. Hoogreef et al. “Conceptual assessment of hybrid electric aircraft with distributed propulsion and boosted turbofans”. In: *AIAA Scitech 2019 Forum*. 2019, p. 1807. URL: https://arc.aiaa.org/doi/pdf/10.2514/6.2019-1807.

[24] *JetZero - The Next Generation*. Accessed: 2025-01-24. 2025. URL: https://www.jetzero.aero/why-jetzero/.

[25] S. Karpuk, Y. Ma, and A. Elham. “Design Investigation of Potential Long-Range Hydrogen Combustion Blended Wing Body Aircraft with Future Technologies”. In: *Aerospace* 10.6 (2023), p. 566. URL: https://www.mdpi.com/2226-4310/10/6/566.

[26] T. W. Lukaczyk et al. “SUAVE: an open-source environment for multi-fidelity conceptual vehicle design”. In: *AIAA/ISSMO Multidisciplinary Analysis and Optimization Conference*. 2015, p. 3087.

[27] Á. G. Manzano. “Systematic Tailplane Design for an Aircraft Family Concept”. MA thesis. Delft University of Technology, 2024. URL: https://repository.tudelft.nl/file/File_01814914-c650-46fb-a584-52c55d34a068?preview=1.

[28] M. G. Millis et al. *Hydrogen fuel system design trades for high-altitude long-endurance remotely-operated aircraft*. Tech. rep. NASA, 2009.

[29] S. K. Mital et al. “Review of current state of the art and key design issues with potential solutions for liquid hydrogen cryogenic storage tank structures for aircraft applications”. In: *NASA Technical Report* (2006). NASA report.

[30] P. Mokotoff et al. “FAST: A Future Aircraft Sizing Tool for Conventional and Electrified Aircraft Design”. In: *AIAA SciTech 2025 Forum*. 2025, p. 2374.

[31] T. Montellano, A. Heidebrecht, and M. Hoogreef. “Structural Analysis of a Novel Integral Tank Concept for Hydrogen Storage Onboard Commercial Aircraft”. In: *AIAA SCITECH 2025 Forum*. 2025, p. 1244. URL: https://repository.tudelft.nl/record/uuid:e739bd62-a414-4c9e-a461-e61bc739d706.

[32] G. Onorato. “Fuel Tank Integration for Hydrogen Airliners”. MA thesis. Delft University of Technology, 2021. URL: https://resolver.tudelft.nl/uuid:5700b748-82c6-49c9-b94a-ad97c798e119.

[33] G. Onorato, P. Proesmans, and M. F. M. Hoogreef. “Assessment of hydrogen transport aircraft: Effects of fuel tank integration”. In: *CEAS Aeronautical Journal* 13.4 (2022), pp. 813–845. URL: https://link.springer.com/article/10.1007/s13272-022-00601-6.

[34] M. Prewitz, J. Schwärzer, and A. Bardenhagen. “Potential analysis of hydrogen storage systems in aircraft design”. In: *International Journal of Hydrogen Energy* 48.65 (2023), pp. 25538–25548. DOI: https://doi.org/10.1016/j.ijhydene.2023.03.266.

[35] P. Proesmans and R. Vos. “Hydrogen, medium-range airplane design optimization for minimal global warming impact”. In: *CEAS Aeronautical Journal* (2024), pp. 1–26. URL: https://link.springer.com/article/10.1007/s13272-024-00734-w.

[36] U. C. J. Rischmüller et al. “Conceptual design of a hydrogen-hybrid dual-fuel regional aircraft retrofit”. In: *Aerospace* 11.2 (2024), p. 123.

[37] A. Rolt et al. *Technology and Scenario Evaluation Studies and Benchmarking Report ENABLEH2*. Tech. rep. ENABLEH2, 2023. URL: https://cordis.europa.eu/project/id/769241/reporting.

[38] San Diego Air and Space Museum. *TU-104 with Podded Main Landing Gear - Archival Photo*. Accessed: 2025-07-01. 2015. URL: https://www.flickr.com/photos/sdasmarchives/50982959321.

[39] D. Silberhorn et al. “Assessment of hydrogen fuel tank integration at aircraft level”. In: *Proceedings of the Deutscher Luft- und Raumfahrtkongress*. 2019, pp. 1–14. URL: https://core.ac.uk/download/pdf/237080603.pdf.

[40] S. Tiwari, M. J. Pekris, and J. J. Doherty. “A review of liquid hydrogen aircraft and propulsion technologies”. In: *International Journal of Hydrogen Energy* 57 (2024), pp. 1174–1196. URL: https://doi.org/10.1016/j.ijhydene.2023.12.263.

[41] F. M. Troeltsch et al. “Hydrogen powered long haul aircraft with minimized climate impact”. In: *AIAA Aviation Forum*. 2020, p. 2660.

[42] Universal Hydrogen. *Universal Hydrogen*. Accessed: 2025-01-24. 2025. URL: https://en.wikipedia.org/wiki/Universal_Hydrogen.

[43] Vecteezy. *Indian Air Force Boeing C-17A Globemaster III Photo*. Accessed: 2025-07-01. 2022. URL: https://www.vecteezy.com/photo/34773077-indian-air-force-boeing-c-17a-globemaster-iii-military-transport-plane.

[44] V. F. Wilod Versprille. “Aerodynamic shape optimization of a liquid-hydrogen-powered blended-wing-body”. In: *trabajo de fin de máster, Universidad Técnica de Delft* (2022). URL: https://repository.tudelft.nl/file/File_aa0dc697-cfd2-4e60-a100-cf4ef5ef33b1?preview=1.

[45] D. Verstraete et al. “Hydrogen fuel tanks for subsonic transport aircraft”. In: *International Journal of Hydrogen Energy* 35.20 (2010). Hyceltec 2009 Conference, pp. 11085–11098. ISSN: 0360-3199. DOI: 10.1016/j.ijhydene.2010.06.060.

[46] E. Waddington, J. M. Merret, and P. J. Ansell. “Impact of liquid-hydrogen fuel-cell electric propulsion on aircraft configuration and integration”. In: *Journal of Aircraft* 60.5 (2023), pp. 1588–1600. DOI: https://doi.org/10.2514/1.C037237.

[47] *Which aircraft models need a tripod jack for tail support at airport?* Accessed: 2025-07-01. 2015. URL: https://aviation.stackexchange.com/questions/24569/which-aircraft-models-need-a-tripod-jack-for-tail-support-at-airport.

[48] C. Winnefeld et al. “Modelling and designing cryogenic hydrogen tanks for future aircraft applications”. In: *Energies* 11.1 (2018). ISSN: 1996-1073. DOI: 10.3390/en11010105.

[49] ZeroAvia. *ZeroAvia - Hydrogen-electric aviation*. Accessed: 2025-01-24. 2025. URL: https://zeroavia.com/.

A

Input File Example

```
<?xml version="1.0" encoding="utf-8"?>
<initiator xmlns:xsi="http://www.w3.org/2001/XMLSchema-instance"
    xsi:noNamespaceSchemaLocation="initiator.xsd">
  <aircraft>
    <name>A320-NEO-LH2-TopTank</name>
    <description>Airbus A320-NEO LH2 with over-cabin tank</description>
    <missions default="Harmonic">
      <mission name="Harmonic">
        <requirement>
          <name>Pax</name>
          <value>150</value>
        </requirement>
        <requirement>
          <name>PayloadMass</name>
          <value>19300</value>
        </requirement>
        <requirement>
          <name>CruiseMach</name>
          <value>0.78</value>
        </requirement>
        <requirement>
          <name>Altitude</name>
          <value>11278</value>
        </requirement>
        <requirement>
          <name>Range</name>
          <value>4560</value>
        </requirement>
        <requirement>
          <name>TakeOffDistance</name>
          <value>2040</value>
        </requirement>
        <requirement>
          <name>ApproachSpeed</name>
          <value>67.7</value>
        </requirement>
        <requirement>
          <name>NumberOfFlights</name>
          <value>100000</value>
        </requirement>
        <requirement>
          <name>AirworthinessRegulations</name>
          <value>FAR-25</value>
        </requirement>
        <requirement>
          <name>TimeToClimb</name>
          <!-- Time to climb to a specified altitude -->
          <value mapType="vector">10;4000</value>
          <!-- Time [minutes] ; Altitude [meter]     -->
```

```
        </requirement>
        <requirement>
          <name>LoiterTime</name>
          <value>30</value>
        </requirement>
        <requirement>
          <name>DivRange</name>
          <value>370</value>
        </requirement>
        <requirement>
          <name>AirportClassification</name>
          <value>FAA-IV</value>
        </requirement>
      </mission>
    </missions>
    <performance>
      <parameter>
        <name>LDmax</name>
        <value>18</value>
      </parameter>
      <parameter>
        <name>SFC</name>
        <value>0.175</value>
      </parameter>
      <parameter>
        <name>FuelType</name>
        <value>LH2</value>
      </parameter>
      <parameter>
        <name>CLmaxLanding</name>
        <value>2.95</value>
      </parameter>
      <parameter>
        <name>CLmaxTakeOff</name>
        <value>2.45</value>
      </parameter>
      <parameter>
        <name>CLmaxClean</name>
        <value>1.3</value>
      </parameter>
    </performance>
    <configuration>
      <parameter>
        <name>WingAspectRatio</name>
        <value>10.5</value>
      </parameter>
      <parameter>
        <name>WingLocation</name>
        <value>Low</value>
      </parameter>
      <parameter>
        <name>HasKink</name>
        <value>1</value>
      </parameter>
      <parameter>
        <name>TEinboardSweep</name>
        <value>0</value>
      </parameter>
      <parameter>
        <name>TailType</name>
        <value>TripleTail</value>
      </parameter>
      <parameter>
        <name>RootAirfoil</name>
        <value>SC20414</value>
      </parameter>
      <parameter>
        <name>KinkAirfoil</name>
        <value>SC20412</value>
      </parameter>
      <parameter>
```

```
        <name>KinkTwist</name>
        <!-- twist angle at kink, code will consider wing incidence-->
        <value>-3</value>
      </parameter>
      <parameter>
        <name>TipAirfoil</name>
        <value>SC20410</value>
      </parameter>
      <parameter>
        <name>TipTwist</name>
        <!-- twist angle at tip, code will consider wing incidence and possible kink twist-->
        <value>-1.2</value>
      </parameter>
      <parameter>
        <name>SupercriticalAirfoil</name>
        <value>1.1</value>
      </parameter>
      <parameter>
        <name>Freight</name>
        <value>false</value>
      </parameter>
      <parameter>
        <name>FuselageTank</name>
        <value>false</value>
      </parameter>
      <parameter>
        <name>CompositeStructures</name>
        <!-- Fuselage,Wing,Empennage-->
        <value mapType="vector">0;0;0</value>
      </parameter>
      <parameter>
        <name>TankLayout</name>
        <value>top</value>
      </parameter>
      <parameter>
        <name>SphericalTank</name>
        <value>false</value>
      </parameter>
      <parameter>
        <name>IntegralTank</name>
        <value>true</value>
      </parameter>
    </configuration>
    <parts mainPart="Fuselage">
      <fuselage name="Fuselage" type="Conventional">
        <paxDivision mapType="vector">1</paxDivision>
        <!-- should sum to 1 -->
        <!-- Based on A320 Europe, Lufthansa (SeatGuru) -->
        <!-- http://www.seatguru.com/airlines/Lufthansa/Lufthansa_Airbus_A320-200_NEK.php -->
        <!-- Dimensions: Seat width, arm rest width, seat pitch, seatbackspace, legspace (
            last 2 unused) -->
        <cabins>
          <cabin name="Cabin1">
            <class>
              <name>FC</name>
              <seatingArr mapType="vector">2;2</seatingArr>
              <seatingDim mapType="vector">0.57;0.078;0.914;0.8;0.3</seatingDim>
            </class>
            <class>
              <name>EC</name>
              <seatingArr mapType="vector">3;3</seatingArr>
              <seatingDim mapType="vector">0.46;0.048;0.813;0.8;0.3</seatingDim>
            </class>
            <classDistribution mapType="vector">0.08;0;0;0.92</classDistribution>
          </cabin>
        </cabins>
      </fuselage>
      <wing name="Main␣Wing" type="MainWing"/>
      <wing name="Horizontal␣Stabiliser" type="HorizontalTail"/>
      <wing name="CentralVT" type="VerticalTail"/>
          <wing name="SideVT1" type="VerticalTail"/>
```

```
190           <wing name="SideVT2" type="VerticalTail"/>
191       <engine name="Engine-1" type="TurboFan" distributed="false">
192         <location>Main Wing</location>
193         <!-- engine x location, fraction of fuselage length for fuselage mounted; spanwise
                fraction for wing/tail mounted, negative for other wing; -->
194         <!-- offset from wing in x fraction of engine length;offset in z  fraction of engine
                diameter-->
195         <LocationFracs mapType="vector">0;0.4;-0.8;-0.6</LocationFracs>
196         <bypassRatio>11</bypassRatio>
197         <motor name="Turbine-1" type="Turbine"/>
198         <fan name="Fan-1" type="Fan"/>
199       </engine>
200       <engine name="Engine-2" type="TurboFan" distributed="false">
201         <location>Main Wing</location>
202         <LocationFracs mapType="vector">0;-0.4;-0.8;-0.6</LocationFracs>
203         <bypassRatio>11</bypassRatio>
204         <motor name="Turbine-2" type="Turbine"/>
205         <fan name="Fan-2" type="Fan"/>
206       </engine>
207           <tank name="TopTank" type="top">
208         <location>Fuselage</location>
209       </tank>
210           <!-- <The aft and fwd tanks are there only to ensure the code runs smoothly, do no
                  exist on aircraft. This is similar to fwd tank in aft only configuration> -->
211       <tank name="AftTank" type="aft">
212         <location>Fuselage</location>
213       </tank>
214       <tank name="FwdTank" type="fwd">
215         <location>Fuselage</location>
216       </tank>
217     </parts>
218   </aircraft>
219   <runList>DesignConvergence,PlotTool</runList>
220   <settings>
221     <include source="defaultSettings.xml" priority="101"/>
222     <include source="LH2Settings.xml" priority="100"/>
223     <setting>
224       <name>LuggageMass</name>
225       <value>20</value>
226     </setting>
227     <setting>
228       <name>UseFemWingWeight</name>
229       <value>true</value>
230     </setting>
231     <setting>
232       <name>FemWingWeightCorrectionFactor</name>
233       <value>1.32</value>
234     </setting>
235     <setting>
236       <name>FuselageWeightEstimationCorrectionFactor</name>
237       <value>1.32</value>
238     </setting>
239     <setting>
240       <name>FlapLiftMomentCorrectionFactor</name>
241       <value>0.87</value>
242     </setting>
243     <setting>
244       <name>SparPositions</name>
245       <value mapType="vector">0.10;0.6</value>
246     </setting>
247     <setting>
248       <name>UseAuxiliarySparForFuelTank</name>
249       <value>false</value>
250     </setting>
251     <setting>
252       <name>TailControl</name>
253       <value>full moving</value>
254     </setting>
255     <setting>
256       <name>MainWingKinkLocation</name>
257       <value>0.44</value>
```

```
    </setting>
    <setting>
      <name>UsableFuelVolume</name>
      <!-- Fraction of fuel tank volume usable for fuel storage -->
      <value>1.0</value>
    </setting>
    <setting>
      <name>ventingPressure</name>
      <value>250000</value>
    </setting>
      <setting>
      <name>TankDiameterRatio</name>
      <value>0.6</value>
    </setting>
  </settings>
  <moduleInputs>
    <input module="PlotTool">
      <plotModules>Geometry,DesignConvergence</plotModules>
    </input>
  </moduleInputs>
</initiator>
```

B

Aircraft Geometries

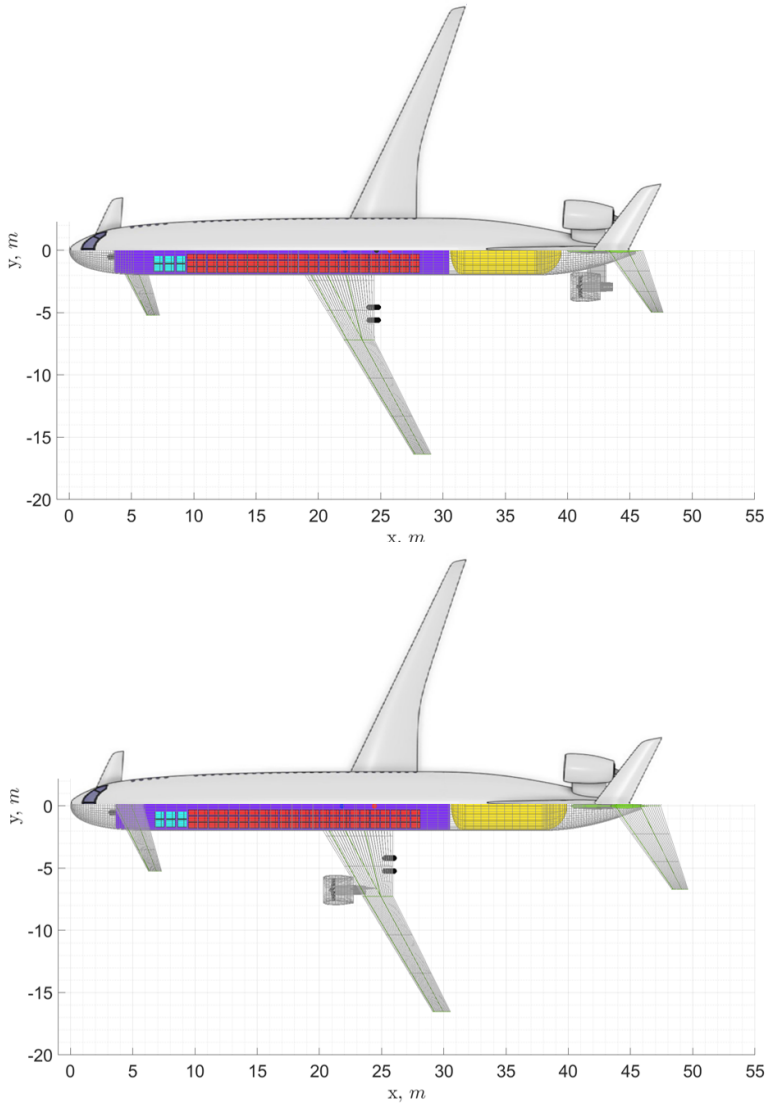

Figure B.1: The geometry of the 3SA-LH2-Aft-FME (OL) and 3SA-LH2-Aft designs compared to the FlyZero 3SA concept [4]